6-2010

Impact Characteristics of Nano composites

Ammar Mohamed Al Omari

جامعة الإمارات العربية المتحدة
UNITED ARAB EMIRATES UNIVERSITY

United Arab Emirates University
Deanship of Graduate Study

IMPACT CHARACTERESTICS OF POLEMERIC NANOCOMPOSITES

By

Ammar Mohamed Al Omari

Supervised by

Prof. Yousef Haik

Mechanical Engineering Department
Faculty of Engineering, UAEU

Dr. Saud Aldajah

Mechanical Engineering Department
Faculty of Engineering, UAEU

A Thesis submitted to the Deanship of Graduate Study at the United Arab Emirates University in partial fulfillment of the requirements for the degree of Master of Science in

Mechanical Engineering

June, 2010

Impact Characteristics of Nanocomposites

A Thesis submitted to the
Deanship of Graduate Studies
United Arab Emirates University

In partial fulfillment of the requirements for
M.Sc. Degree in Mechanical Engineering

Examination Committee

Prof. Yousef Haik, Chair
Mechanical Engineering Department
Faculty of Engineering, UAE University
Al Ain, UAE

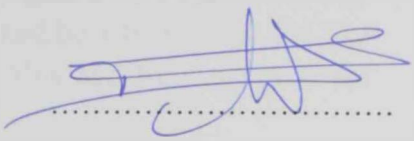

Dr. Saud Aldajah
Mechanical Engineering Department
Faculty of Engineering, UAE University
Al Ain, UAE

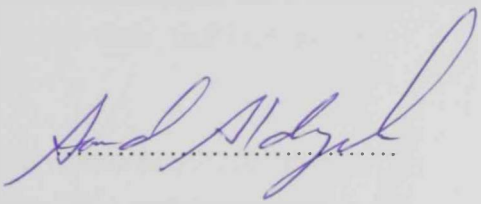

Dr. Ahmed Alawar, Internal Examiner
Mechanical Engineering Department
Faculty of Engineering, UAE University
Al Ain, UAE

Dr.Khalid Al Zebdah, External Examiner
Mechanical & Industrial Engineering Department
Faculty of Engineering, Sultan Qaboos University University
Muscat, Oman

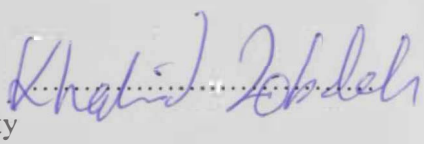

United Arab Emirates University
June 2010

ACKNOWLEDGMENTS

I would like to express my sincere thanks to all of the people who have assisted me in my efforts towards receiving a master degree at UAE University.

I am grateful to Prof. Yousef Haik, my advisor, in his support and for giving me the opportunity to perform this work. I wish to thank him for his confidence in me which was reflected in his flexibility, his willingness to let me decide the direction of this research, and to pursue it in a manner that I felt most suitable. I would also like to express my gratitude towards my co-advisor, Dr. Saud Aldajah. I appreciate the time he invested in advising me and for his openness, honesty, and sincerity.

I owe thanks to all of the people at the Mechanical Engineering Department who have always been willing to provide assistance, give advice, and be a friend. I would like to thank Abdulsattar NourAldain, Alaa Haik, Hussain Abu Alila and Muthana Aziz for their help.

I wish to thank the engineers in the Nondestructive Testing Department at Abu Dhabi Aircraft Technologies Corporation for allowing me to use their facilities to test samples. Their expert opinion and advice is greatly appreciated.

I would not be truly thankful if I did not express gratitude towards my parents who raised me in an environment where I could realize and pursue my life's ambitions.

Above all, my deepest gratitude and appreciation goes to my wife. She is my inspiration and guiding light in everything I do. The many personal sacrifices she has made for me to accomplish this work is greatly appreciated. She has been there through it all, the good and the bad. I will be eternally thankful for her understanding and support.

ABSTRACT

Nanocomposite materials have seen a significant increase in use and have created a revolution in high-performance structures. They exploit the properties of different materials which create structures that are stronger, stiffer, impact resistant and more durable against environmental factors. They can be tailored to have better electric, magnetic, optical properties, and be chemically, thermally and explosion resistant depending on the application. The current research study investigates the impact characteristics of polymeric based nanocomposites strengthened with various types of nano and micro fillers. An in-house designed impact testing machine was utilized to typify the impact characteristics of different nanocomposite materials through a dead weight drop mechanism. In order to fully understand the role of nano and micro fillers in enhancing the mechanical properties of composite materials, a number of samples were prepared and tested. The samples included layered woven Kevlar with Carbon Nanotubes, Nanoclay, Aluminum Oxide and Silicon Carbide particles. Different weight percentages of fillers were prepared in order to optimize the impact behavior of the composite material. Three-point bending test, nano-indentation, microhardness DSC and TGA were utilized to study the impact of the above mentioned nano and micro fillers on the thermal, flexure and mechanical behavior of the composites. The results showed that the nanoclay fillers were the best to enhance the impact and mechanical properties of the composite materials with 4.3 weight % of nanoclays being the optimum percentage.

Table of Contents

Chapter, **Page**

Chapter 3: Results & Discussion

Chapter 4: Finite Element Analysis

List of Figures

List of Tables

Chapter 1

INTRODUCTION

CHAPTER 1

INTRODUCTION

In this chapter, an overview describes the objective of this research study is introduced. Literature review summarizes the impact resistance of composites, the need, the potential of Nanocomposites and the research done on the impact of Nanocomposites.

1.1 OVERVIEW

The objective of this research is to determine the effect of adding different types of fillers on the low-speed impact (<10 m/sec) resistance of laminated polymeric based woven Kevlar composite. The primary interest of this study is to improve the composite impact resistance and energy absorption without a significant increase in weight or volume. By performing drop weight tests on various configurations of nano enhanced Kevlar laminates specimens, the increase in energy absorption due to the nanoadditives components will be determined and the changes of failure modes will be noticed. The approach used to determine the energy absorption change due to the various nano components added will be to compare the penetration resistance and the number of damaged layers in the different nanocomposite to that of the control Kevlar composite. Also, inspection and analysis of the impacted specimens will be made to gain an understanding of the characteristics of an effective low-speed impact resistant of nanocomposites. Mechanical and thermal analysis characterization of nanoclay/vinylester composite will be done to determine the effect of nanoclay on enhancing the Vinylester matrix.

Composites are artificially produced multiphase materials having a desirable combination of the best properties of the constituent phases. Usually, one phase (the matrix) is continuous and completely surrounds the other (the dispersed phase). In general, composites were classified as particle-reinforced, fiber-reinforced, and structural [1], as shown in Fig. 1.1.

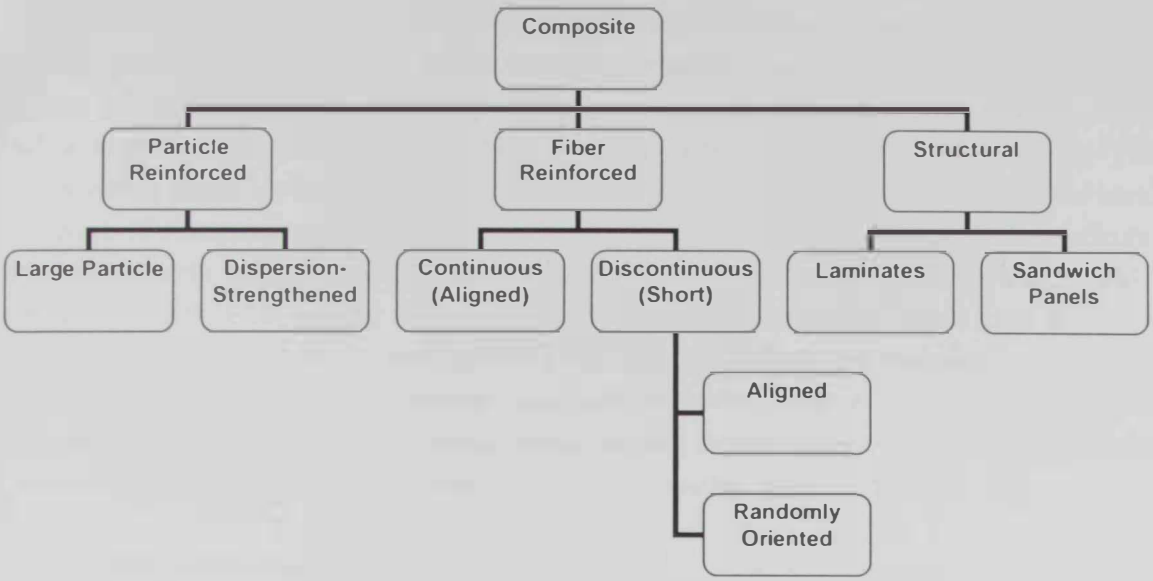

Fig. 1.1 Classification scheme for the various composite types.

Composite materials played an important role in many applications. Due to their high energy absorption capacity, light weight and high ductility, composites are logical choices in impact applications.

The last three decades have witnessed a steady increase in the use of lightweight polymeric composites for structural applications. In addition to their excellent quasi-static mechanical properties such as high specific stiffness and strength, it has become essential for these composite structures to perform well under various types of impact loading. For example, in the aerospace industry, the residual compressive strength of an impact damaged composite structure has become the design-limiting factor. Major aspects of current damage-tolerant design philosophies in other industrial sectors are similar to that of the aerospace industry [2].

Impact testing is normally performed with a swinging or a dropping weight. The object of these tests is to measure the amount of energy transferred or "lost" from the striking body to the sample. For bodies without flaws or notches, the transferred energy consists of energy to initiate crack and energy to propagate a crack. In recent years the drop-weight method has become the preferred technique for impact testing of composites because a greater range of testing parameters is possible and the results are more readily analyzed. Also, the drop weight test allows for a greater variety of specimen geometries, which is an advantage over the Charpy and Izod impact tests [2]. Impact events can be categorized into four velocity ranges; low, high, ballistic, and hypervelocity. Low velocity impact may include situations such as a dropped tool (< 30m/sec) whereas high

velocity impact might include a bird colliding with an airplane (30 - 250 m/sec). Ballistic impact events include situations such as a projectile fired from a gun at speeds in excess of 250 m/sec. Finally, orbital debris traveling in outer-space at velocities up to 15,000 m/sec is considered to be hypervelocity impact events [3]. Impact resistance is the ability of a material to absorb and dissipate energies under impact or shock loading. The response to impact loads ranges from localized damage to total disintegration. Even local damage of composites can be serious since it can lead to delamination and other effects, such as matrix cracking. During impact loading fracture modes may be significantly different than static tensile failure. This is particularly true for strain rate sensitive materials. Kevlar, which is a commercial name of aramid fiber, showed high performance in impact resistance tests. Kevlar composites have been extensively utilized as lightweight armor structures in applications ranging from military helmets to large scale vehicle systems such as aircraft, spacecraft, land vehicles, and naval vessels [4].

The reinforcement of polymers using fillers, whether inorganic or organic, is common in modern plastics. Polymer nanocomposites, or the more inclusive term, polymer nanostructured materials, represent a radical alternative to these polymer composites. In contrast to polymer systems where reinforcement is on the order of microns, polymer nanocomposites are exemplified by discrete constituents on the order of a few nanometers [5]. Nanophase composites show a great promise for light-weight, high-strength, high-toughness materials and in applications such as impact-resistant body armor [6].

1.2 IMPACT RESISTANCE OF COMPOSITES

Impact behavior of composites studies are of enormous complexity. A single impact event can produce several different damage modes simultaneously. These damage modes are affected by the properties of both the impactor and the laminate. The multitude of impactor and laminate variable combinations coupled with the complexity of the impact behavior has led to the vast amount of research devoted to the analysis and improvement of fiber reinforced polymer impact performance [7]. Due to the wide range of polymeric composites types and shapes and due to the variation in impact testing methods and impact speeds, many previous researches performed to characterize the impact parameters such as energy absorption, compression after impact strength, resistance to penetration, delamination and other failure modes.

Kevlar reinforced composite, combination of Kevlar with other types of fiber-reinforced composite was examined by many researches. Gustin et al. [8] studied Impact, compression after impact, and tensile stiffness properties of carbon fiber and Kevlar combination sandwich composites. Different samples consisted of impact-side face sheets

having different combinations of carbon fiber/Kevlar and carbon fiber/hybrid. The focus of his work was to determine if any improvement in impact properties existed as a result of replacing the impact-side face sheet layers of carbon fiber with Kevlar or hybrid. Zhu et al investigated experimentally the penetration of laminated Kevlar-29/polyester plates by conical nosed projectiles and proposed a range of models for the various energy-absorbing mechanisms such as the indentation of projectile tip, the bulging of the back surface of the laminate, fiber failure, delamination and friction to estimate the target resistance to the projectile motion [9].

Finite element analysis played an important role in investigating impact and failure of composites, tell now, there is no model can simulate all failure possibilities of composite material. Different model with different simplification found in literature, some models study the delamination between composite layers, some of them study the matrix fiber delamination. Fiber fracture had been considered in some models besides the matrix cracking. T. He et al built finite element model to examine the penetration and perforation of Kevlar and glass fiber-reinforced plastic laminates struck by rigid projectiles with different nose shapes within a wide range of impact conditions [10]. H.E. Johnson and his team built numerical model to simulate woven vinylester composite plates. He used a simple, gradually damaging three-dimensional material model and the results were compared with full-scale tests. The model was based on damage mechanics principles using cyclic test data to obtain modulus reduction with damage. Delamination was modeled with a mixed-mode traction separation law using cohesive elements [11]. Many damage mechanics models are available in literature, some providing good delamination predictions. The damage mechanics and fracture methods for predicting delamination under impact was studied in [12].

The drop-weight technique has been adopted in the recent composite impact tests because of the variety of specimen geometries. Response of E-glass reinforced vinylester and urethane panels of varying structures subjected to shock loading and drop weight impact loading had been studied by M. Hebert [13]. Drop weight impact performance was measured by energy absorbed by the samples, depth of penetration, and extent of internal damage. The drop weight technique used to study the progressive damage behaviors of plain-weave hybrid S2 glass-IM7 graphite fibers/toughened epoxy impacted at different velocities. Good agreement between experimental and FE results had been achieved when comparing dynamic force, strain histories and damage patterns from experimental measurements and FE simulations [14].

A combined experimental and 3-D dynamic nonlinear finite element approach was adopted to study composite beams made of S2 glass-reinforced toughened epoxy subject to drop-weight or ballistic impact by [15].

1.3 NANOCOMPOSITES

A nanocomposite material has had the attention, imagination, and close scrutiny of scientists and engineers in recent years. This scrutiny results from the simple premise that using building blocks with dimensions in the nano size range makes it possible to design and create new materials with unprecedented flexibility and improvements in their physical properties. This ability to tailor composites by using nano size building blocks of heterogeneous chemical species has been demonstrated in several interdisciplinary fields. The most convincing examples of such designs are naturally occurring structures such as bone, which is a hierarchical nanocomposite built from ceramic tablets and organic binders. Because the constituents of a nanocomposite have different structures and compositions and hence properties, they serve various functions. Thus, the materials built from them can be multifunctional [6]. It has been shown that the nano materials enhance the mechanical properties of polymeric based composites [16-26]. Polymer nanocomposites are composites with a polymer matrix and filler with at least one dimension less than 100 nm [27]. The fillers can be plate-like (clays), high aspect ratio nanotubes, and lower aspect ratio or equiaxed nanoparticles. While some nanofilled composites (carbon black and fumed silica-filled polymers) have been used for over a century, in recent years the dedicated research and development of nanofilled polymers has greatly increased. This is due to our increased ability to synthesize and manipulate a broad range of nanofillers and significant investment by government and industry in this field [27].

Current interest in nanocomposites has been generated and maintained because nanoparticle and carbon nanotube-filled polymers exhibit unique combinations of properties not achievable with traditional composites. For example, the inclusion of equiaxed nanoparticles in thermoplastics, and particularly semicrystalline thermoplastics, increases the yield stress, the tensile strength, and Young modulus compared to pure polymer. Other examples include scratch-resistant transparent amorphous thermoplastic coatings. These combinations of properties can be achieved because of the small size of the fillers, the large surface area the fillers provide, and in many cases the unique properties of the fillers themselves. Unlike micron-filled composites, these novel fillers often alter the properties of the entire polymer matrix while, at the same time, imparting new functionality because of their chemical composition and nanoscale size [27]. The most commonly used clay in the synthesis of polymer nanocomposites is montmorillonite (MMT) which is the major constituent of bentonite. It is well known that filler anisotropy, i.e. large length to diameter ratio (aspect ratio), is especially favorable in matrix reinforcement. The nanocomposites containing organoclay have been further employed as the matrix material to produce hybrid nanoclay/fibre reinforced polymer composites that possess improve the mechanical and fracture properties [28, 29].

The era of polymer nanocomposites received an impetus after the work of a researcher from Toyota in 1987 [30]. Toyota discovered the possibility of synthesizing polymer nanocomposites based on nylon-6/organophilic montmorillonite clay that showed dramatic improvements in mechanical and physical properties and heat distortion temperature at very low content of layered silicate. Since the first discovery by Toyota researchers on the reinforcing effect of relatively cheap nanoclay on the polymeric material [31] Many researchers [32-47] have focused on it: Weiping et al. [47] reported that nanoclay could increase the fracture toughness of epoxy by 2.2 and 5.8 times. Lei et al. [48] studied the dependences of Young's modulus and fracture toughness on clay concentration using the tensile and 3-point bending methods. Qi et al [49] investigated the effect of several nanoclay additives, which were mixed with DGEBA epoxy resin using a mechanical stirrer, on tensile modulus, tensile strength and fracture toughness of the nanocomposite. Ho et al [50] increased the tensile strength and Vickers' hardness value of the epoxy using nanoclay mixed by mechanical stirring method. Due to unique structure of montmorillonite, the mineral platelet thickness is only one nanometer, although its dimensions in length and width can be measured in hundreds of nanometers, with a majority of platelets in 200–400 nm range after purification. Due to very small size and thickness of the platelets, a single gram of clay contains over a million individual platelets. The term polymer layered silicate nanocomposites describes a class where the reinforcing phase, in the shape of platelets, has only nano level dimensions. There is substantial improvement in mechanical and physical properties of nanocomposites and this too at a very low silicate content (3–6 wt %) [23]. Improved mechanical and thermal properties are of interest for under-the-hood applications in the automotive industry [30]. Subramaniyan et al [51] studied the improvement fracture on vinylester / MMT nano clay composites. The same investigators reported that when the nano-clay particles were used to enhance the polymer matrix material in a conventional glass fiber-reinforced composite, the interlaminar fracture toughness of the composite was less than that of the composite without the nano-clay particles. Alignment of the nano-clay particles along the fiber axis was suggested as a possible reason for this result.

Today, efforts are being made globally for using nanoclays in almost all types of polymer matrices. In addition to organically modified natural montmorillonite, synthetic layered silicates such as laponite, hectorite and saponite have been used as rheological modifiers in paints, inks, greases and cosmetics. Organoclays obtained by interaction of these layered silicates with ammonium or phosphonium salts act as thixotropic agent in the above applications. One of the major obstacles in using nanofillers specially nanotubes as polymer filler is the cost; however, advances in the synthesis of CNTs continue to rapidly improve both their quantity and quality, though growing structurally

perfect nanotubes at large scales is not yet at hand. However, it is only a matter of time before CNTs are mass produced at low cost [17].

1.4 IMPACT CHARCTERISTICS OF NANOCOMPOSITES

Experimental evidence showed that some nanocomposites with certain matrices and filler materials may achieve significant and simultaneous improvements in stiffness, fracture toughness, impact energy absorption and vibration damping, and these characteristics could be of particular importance in automobile or airplane structures [52]. In the last few years, polymeric based nanocomposites started to be a part of the favorable material for impact resistance. Due to the high strength–weight ratio of these materials, intensive research to invest this material in aerospace application besides armoring. Some of the reported research work is based on experimental work and the other based on computer simulation. It has been found that impact response of composite materials is a very complex process, which involves stress wave transfer, damage creation and propagation, heat and sound transfer, phase change, etc. In order to understand the impact response and damage mechanism so that impact tolerant structures can be designed, multiscale modeling from atomistic to structural level is mandatory. Because of the highly coupled, multidamage mode, and multiscale nature of the problem, closed-form solutions are improbable. The combination of physics based theoretical models and advanced numerical simulation, is a promising alternative approach [53]. Babur Deliktas et al, presented the nonlocal computational aspects for the micromechanical based perforation and penetration problem of Metal–Matrix Composites due to high impact loading, with the overall characteristic response of the impacted plate due to bending, dishing and a cone shaped macrocrack in the material [54]. A.M. Dongare [55] proposed an angular dependent-embedded atom method framework for metal–matrix ceramic particle reinforced nanocomposites, which was based on the combination of thoroughly tested potentials developed for pure components and, therefore, provided an attractive alternative to the design of new alloy potentials with original functional forms. By in appropriating the current local thermo-viscoplasticity and rate-dependent damage or fracture theories, Abu Al-Rub et al [56], predicted the ballistic limit velocity in high speed impacts of heterogeneous ductile targets such that an incorporation of an explicit length scale parameter through the nonlocal theory was imperative. Using a multi-objective optimization approach, Taha and his colleagues found that optimal distribution of carbon nanotubes in carbon composite interface enables producing blast resistant carbon composites [57]. In another research, ballistic impact damage simulation of 3D woven composite using the unit cell approach was conducted by [58]. Bhuiyan et al [59] infused carbon nanofibers (CNF) into closed cell foams and altered the foaming process, resulting in smaller cell sizes and increased cell wall thickness, and when used in sandwich constructions, improved the damage tolerance in

low-velocity impact scenario and also reduced the damage size. Computer simulation was introduced by Al-Ostaz et al [60] to characterize the low-cost fire resistant exfoliated graphite nanoplatelet reinforced glass/carbon polymeric based composites under low-velocity impact. Quasi-isotropic composite laminates of plain and interleaved composite laminates clamped all around were impact tested to assess the improvement in impact resistance of composite laminates that have been interleaved by electrospun Nylon 6 nanofabric. Based on this preliminary study, results showed that; polymer nanofabric interleaving marginally increased the laminate thickness, by about 2.0%. Polymer nanofabric interleaving increased the threshold impact force by about 60%, reduced the rate of impact damage growth rate to one-half with impact height. The concept has merit for more detailed study for optimizing and for multi-functionalizing fiber reinforced composite laminates [61]. Experimental study had been used for characterizing the dynamic modulus, loss factor, Tg, creep and stress relaxation properties of graphite platelet and nanoclay reinforced composites by [62]. Low-velocity impact tests were performed in a drop-weight instrumented impact test. It is observed the energy absorption of pure vinylester almost doubled when reinforced with 2.5 wt. percentage Cloisite 30B nanoclay and exfoliated graphite nano platelets [63,64]. Ballistic impact energy absorption behaviors of Polycarbonate (PC), PMMA and PMMA/PC composites were examined by Song [65]. Failure behavior of PMMA changes as the impact velocity and thickness increases. The hybrid system of PMMA with a thin layer of PC exhibited synergistic effect by showing superior performance over monolithic PC or PMMA. PMMA/ nano silicate samples exhibited similar behavior to the monolithic PMMA. The influence of nanoclay on the impact damage resistance of carbon fiber–epoxy composites had been investigated by Iqbal et al [66] using the low-velocity impact and compression after impact (CAI) tests. The CFRPs containing organoclay brought about significant improvement in impact damage resistance and damage tolerance in the form of smaller damage area, higher residual strength and higher threshold energy level. The presence of nanoclay in the epoxy matrix induced the transition of failure mechanisms of CFRP laminates during the CAI test, from the brittle buckling mode to more ductile, multi-layer delamination mode. Addition of 3 wt% clay was shown to be an optimal content for the highest damage resistance. Avila et al investigated the influence of exfoliated nano-structures on sandwich composites under impact loadings. A set of sandwich composites plates made of fiberglass/nano-modified epoxy face sheets and polystyrene foams was prepared. The epoxy system was bisphenol a resin and an amine hardener. The fiber volume fraction used was around 65%, while the southern nanoclay content varied from 0 wt. % to 10 wt. %. The sandwich panels were submitted to low-velocity impact tests with energies from 5 J to 75 J. Two sets of experiments were performed; high velocity + low mass and low velocity + high mass. Damage caused by the two groups of experiments and peak forces measured were dissimilar. The results show that the addition of 5 wt. % of nanoclay lead to more efficient energy absorption. The failure modes were also

analyzed and they seem to be affected by the nanoclay addition to face sheets [67]. High impact polystyrene (HIPS)/organoclay nanocomposites via in situ polymerization were synthesized and their rheological properties were investigated, two types of organoclays were used: a commercially available organoclay, Cloisite 10A (C10A), and a laboratory-prepared organoclay [68].

1.5 MATERIALS USED

1.5.1 Woven Kevlar

Kevlar is an aramid fiber, a term invented as an abbreviation for aromatic polyamide developed in 1965 by DuPont Company. The chemical composition of Kevlar is poly para-phenyleneterephthalamide, and it is more properly known as a para-aramid. Aramids belong to the family of nylons. Common nylons, such as nylon 6,6, do not have very good structural properties, so the para-aramid distinction is important. The aramid ring gives Kevlar thermal stability, while the para structure gives it high strength and modulus [69]. Kevlar aramid has a high tensile strength, higher tensile modulus and lower density than fiber glass but it is more expensive than glass fiber [70]. Aramid fibers provide the highest tensile strength-to-weight ratio among reinforcing fibers. They provide good impact strength. Like carbon fibers, they provide a negative coefficient of thermal expansion. The disadvantage of aramid fibers is that they are difficult to cut and machine. Aramid fibers are produced by extruding an acidic solution (a proprietary polycondensation product of terephthaloyol chloride and *p*-phenylenediamine) through a spinneret. The filaments are drawn through several orifices. During the drawing operation, aramid molecules become highly oriented in the longitudinal direction [71].

Woven roving fabric laminates have proved to have superior impact energy absorbing properties to those of laminates made of unidirectional prepregs [72,73]. Woven fabrics are used in a number of engineering applications across various industries, including such products as automobile airbags; flexible structures like boat sails and parachutes; reinforcement in composites; architectural expressions in building roof structures; protective vests for military, police, and other security circles; and protective layers around the body in planes. Woven fabrics consist of yarns woven in the fill and the warp directions. The yarn is crimped, or curved, as it is woven up and down over the cross yarns. The nonlinear mechanical behavior of the fabric arises from different sources: the nonlinear response of the individual yarns, the exchange of crimp between the fill and the warp yarns as they are stretched, and the contact and friction between the yarns in cross directions and between the yarns in the same direction. In general, the fabric exhibits a significant stiffness only along the yarn directions under tension. The tensile response in the fill and warp directions may be coupled due to the crimp exchange

mentioned above. Under in-plane shear deformation, the fill and warp direction yarns rotate with respect to each other. The resistance increases with shear deformation as lateral contact is formed between the yarns in each direction. The fabrics typically have negligible stiffness in bending and in-plane compression [74].

1.5.2 Vinylesters

Vinylesters are formed by the chemical reaction of an unsaturated organic acid with an epoxide-terminated molecule. In vinylester molecules, there are fewer unsaturated sites for cross-linking than in polyesters or epoxies and, therefore, a cured vinylester provides increased ductility and toughness.
They offer good chemical and corrosion resistance and are used for FRP pipes and tanks in the chemical industry. They are cheaper than epoxies and are used in the automotive and other high-volume applications where cost is critical in making material selection [71].

1.5.3 Carbon Nanotubes

There are excellent reviews and publications on the mechanical and the physical properties of carbon nanotubes [75, 76 & 77].

In this section, only a brief summary of the classification of carbon nanotubes will be presented. Carbon nanotubes have attracted much attention in the past several years because of their unique potential uses for structural, electrical, and mechanical properties. Nanotubes have high Young's modulus and tensile strength, and they can be metallic, semiconducting, or semimetallic, depending on the helicity and diameter [78]. Classifications of carbon nanotubes can be grouped as single-wall (SWNT), multiwall (MWNT), and the newly established small-diameter (SDNT) material, based on the number of walls present in the carbon nanotubes. By definition, SWNTs are single walled carbon nanotubes about 1 nm in diameter with micrometer-scale lengths; MWNTs are multiwalled carbon nanotubes with an inner diameter of about 2 to 10 nm, an outer diameter of 20 to 70 nm, and a length of about 50 μm ; and SDNTs have diameters of less than 3.5 nm and have lengths from several hundred nanometers to several micrometers. These SDNTs generally have one to three walls [5].

1.5.4 Multiwall carbon nanotubes (MWCNT)

Multiwall carbon nanotubes have an interior diameter of 2 to 10 nm, an exterior diameter of 20 to 75 nm, and a length of 50 μm. Multiwall carbon nanotubes are produced by chemical vapor deposition (CVD) synthesis of xylene-ferrocene composition at a relatively low temperature of 725°C, and with high purity > 95

percentage. Multiwall carbon nanotubes are nanoscale carbon fibers with a high degree of graphitization. Multiwall carbon nanotubes are technically neither fullerenes nor molecular. They are attractive materials intermediate between SWNT and CNF with properties vastly superior to graphite and carbon black [5].

1.5.5 Silicon Carbide

Properties: Silicon Carbide is highly dispersed, amorphous, very pure silica that is produced by high-temperature hydrolysis of silicon tetrachloride in an oxyhydrogen gas flame. It is a black, fluffy powder consisting of spherically shaped primary particles. The primary particles are spherical and free of pores. The primary particles in the flame interact to develop aggregates, which join together reversibly to form agglomerates [5].

1.5.6 Aluminum Oxide

Properties: Aluminum Oxide has an average primary particle size of about 13 nm and a specific surface of about 100 m^2/g. The aluminumoxides produced through precipitation of aluminum hydroxide from aluminate solution followed by calcinations consist of particles in the order of magnitude of micrometers. High surface aluminum oxide gels, in contrast to Aluminum Oxide, have a high proportion of internal surface [5].

1.5.7 Montmorillonite nanoclays

Nanoclay is the most widely investigated nanoparticle in a variety of different polymer matrices for a spectrum of applications [79]. The origin of bentonite (natural clay) is most commonly formed by the in-situ alteration of volcanic ash. Another, less common, origin is the hydrothermal alteration of volcanic rocks. Bentonite contains montmorillonite but also can contain glass, mixedlayer clays, illite, kaolinite, quartz, zeolite, and carbonates. Clay soil has particle size of less than 2 μm. The expanding clays are phyllosilicates, smectite, and montmorillonite, and the nonexpanding clays are talc, kaolin, and mica. The starting material of Southern Clay Products' (SCP, located in Gonzales, Texas) commercial clay products is from volcanic eruptions in the Pacific Ocean and the western United States during the Cretaceous period (85 to 125 million years ago) [5].

1.6 Study Objective

The primary objective of this research is to investigate the impact penetration resistance of woven Kevlar laminated composites under low speed impact by adding different additives to the matrix phase. Fillers in different characteristics are used:

1) Ceramic particles (Aluminum Oxide (Al_2O_3) and Silicon Carbide (SiC)).
2) Nanoclay.
3) Nanotubes (Multi Wall Carbon Nanotubes (MWCNT's)).

The variation of additives percentage usually lead to different characteristics of the resulting composite, increase in energy absorption by high percentage of fillers may accompany tendency to delamination, for this purpose, different percentages of each additive will be utilized. The results will be compared to control specimen composed from Kevlar plies only.

The laminated composites are prepared manually of fifteen plies of woven Kevlar49 arranged in symmetrical 0/45 alternation. Painting the matrix mix over each ply using painting brushes, then rolling each ply using metallic roller to insure saturation of resin and complete bonding between layers, after that composite hot pressing technique is performed, this insure plies perfect bonding, unify the thickness and to fast cure the sample.

Drop-Weight apparatus is used to determine the minimum energy to completely penetrate the control sample (Kevlar laminates in vinylester resin only. The nano enhanced composites then will be impacted by the same amount of energy to record the response of each composite under the same amount of energy. The research is divided into experimental and FEM simulation. Finite Element simulation saves time, money and sometimes give better understanding than experimental approach , Finite element approach is used to model the impact response, deformation and composite failure. The boundary conditions of the problem mimic the exact drop weight test conditions and the impact nose is modeled as a rigid body. Commercial FE software ABAQUS/Explicit is utilized.

1.7 Scope of Study

Composite materials are a logical choice in impact resistance applications due to its high energy absorption capacity, light weight and high ductility. The applications vary between bullet proof vest, airplanes wings, sport car bodies and many other applications. This research include experimental and finite element analysis of low speed impact of woven Kevlar layers, Kevlar is an aramid fiber usually used in impact applications, the

Kevlar composite matrix will be enhanced with different types of additives. The first chapter discusses the literature review of applications of composites and nano composites in impact resistance. The second chapter explains the experimental setup and procedures of this research. The third chapter summarizes the results of this research with discussion. The finite element chapter which is chapter four presents simulation model for impacted composites. The last two chapters discuss the conclusion and recommendations.

1.8 Summary of Achievements

The effect of adding small amounts of various fillers on the impact resistance of Kevlar/ Vinylester composites have been studied. It was demonstrated that the amount of each different additive exerts significant influence over the energy absorption capability of polymer based composites. The different fillers contribute to the enhancement of the energy absorption and failure modes of composites, the silicon carbide gave considerable enhancement in energy absorption capacity, nanoclay with 4.3 wt % enhanced both the absorption energy and the delamination resistance. Deep investigation on the nanoclay/vinylester composites was performed, The results from three point bending test, micro hardness test and nano indentation test were consistent and showed that 2 wt % of nanoclay will give the stiffest and hard composite. The enhancement in mechanical properties of the nanoclay composites did not accompany considerable changes in the thermal properties.

Chapter 2

EXPERIMENTAL PROCEDURE

CHAPTER 2

EXPERIMENTAL PROCEDURE

This chapter concentrates on the experimental procedures for this research study, it starts with the fabrications of control samples and samples with additives, then it discusses few techniques used in this research; the hot pressing technique, sonication and composite machining. This chapter also describes the various tests used to examine the composite samples like three point bending, microhardness, nano indentation, thermal analysis and the drop weight impact test. Then detailed description of the test procedures is presented.

2.1 SPECIEMEN FABRICATION

2.1.1 Control Specimens

The control specimen was manufactured from fifteen woven Kevlar49 layers (17 x 17 cm size, thickness 0.125 mm) arranged symmetrically in $0^{o}/45^{o}$ orientations, see Fig 2.1. The Kevlar plies were bonded together with vinylester resin. K-12 hardener with 0.5 wt% was added to insure and accelerate the vinylester curing. The fiber fraction was 27 wt %. The percentage of vinylester was determined by the minimum amount of resin required to insure complete saturation of Kevlar layers by resin, this will validate the assumption of perfect bonding between the composite layers when it is needed to simplify the finite element simulation. The fiber and matrix percentages will be known after the complete curing of the composite. The total weight of Kevlar layers was measured and recorded before composite preparation. The total weight of the composite after resin curing was measured and the weight of matrix phase is the difference between the composite and the weight of fiber according to the equation,

$$m_{composite} = m_{fiber} + m_{matrix} \quad [1]$$

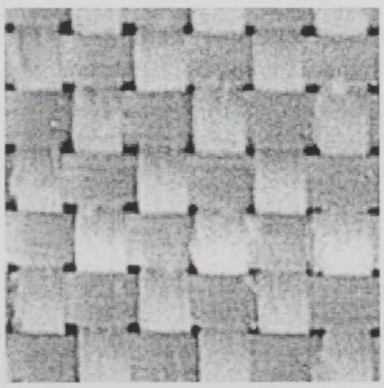

Fig. 2.1 Single Woven Kevlar Layer

There are four basic steps involved in any composites part fabrication: wetting/ impregnation, lay-up, consolidation, and solidification. All composites manufacturing processes involve the same four steps, although they are accomplished in different ways [70]. In the impregnation step, fibers and resins were mixed together to form a lamina. In a wet lay-up process, each fabric layer was wetted with resin using a squeezing roller or painting brush for proper impregnation. The purpose of this step was to make sure that the resin flows entirely around all fibers. Viscosity, surface tension, and capillary action were the main parameters affecting the impregnation process. The purpose of the lay-up step was to achieve the desired fiber architecture as dictated by the design. Performance of a composite structure relies heavily on fiber orientation and lay-up sequence. In the Lay-up step, composite laminates were formed by placing fiber resin mixtures or prepregs (pre-impregnated) at desired angles. The desired composite thickness was built up by placing various layers of the fiber and resin mixture. In lay-up process, layers were laid at a specific fiber orientation, either manually or by machine. The consolidation step involves creating intimate contact between each layer of lamina. This step ensures that all the entrapped air was removed between layers during processing. Consolidation is a very important step in obtaining a good quality part. Poorly consolidated parts will have voids and dry spots. Consolidation of continuous fiber composites involves two important processes: resin flow through porous media and elastic fiber deformation [80, 81 & 82]. During the consolidation process, applied pressure is shared by both resin and fiber structure. Initially, however, the applied pressure is carried solely by the resin (zero fiber elastic deformation). Fibers go through elastic deformation when the compressive pressure increases and resins flow out toward the boundary. There are various consolidation models that ignore the fiber deformation and consider only resin flow [83]. The final step was solidification, the lower the solidification time, the higher the production rate achievable by the process. In thermoset composites, the rate of solidification depends on the resin formulation and cure kinetics. Heat was supplied during processing to expedite the cure rate of the resin. In thermoset resins usually the higher the cure temperature, the faster the cross-linking process. In thermoplastics, there is no chemical change during solidification and therefore solidification requires the least amount of time. In thermoplastics processing, the rate of solidification depends on the cooling rate of the process. In thermoset composites, the temperature is raised to obtain faster solidification; whereas in thermoplastics processing, the temperature is lowered to obtain a rigid part [71]. Regular painting brush was utilized to distribute the resin evenly over the first Kevlar ply. the second ply was placed in 45° angel over the first ply (0° angel). Consolidating metallic roller (Fig. 2.2) was scrolled over the second ply to force the resin to penetrate the second ply, eliminate air bubbles inside resin and to eliminate cavities between the two Kevlar layers. After that resin was brushed again over the second play and the third Kevlar ply was laid down in 0° orientation (the same orientation of the first Kevlar ply). The same scenario was adapted to prepare the rest of Kevlar

layers, scrolling by the metallic roller, brushing the resin, placing the new Kevlar layer. After that, the specimen was placed inside the hot press machine, the two pressing plates were sprayed by mold release agent and heated up to 175°C, then the laminated composite was compressed by force equal 450 kg distributed over 30 x 30 cm area for 15 minutes. (section 2.2.3).

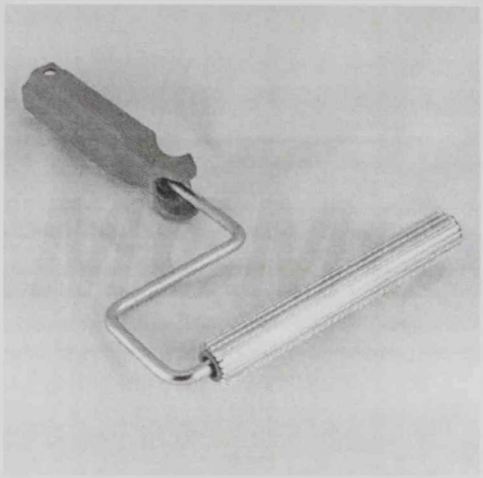

Fig. 2.2 Consolidating metallic roller

The first composite (15 layers of Kevlar + vinylester) was prepared by adding 56 g of Vinylester to 117 g (15 layers) of Kevlar. The resin percentage was 32 wt % of the composite and the Kevlar fibers were 68 wt %. The second composite (15 layers of Kevlar + vinylester) was prepared by adding 29 g of Vinylester to 78 g (15 layers) of Kevlar. The resin percentage was 27 wt % of the composite and the Kevlar fibers were 73 wt %.

2.1.2 Nano Composite Specimens

The introduction of inorganic nano particles as additives into polymer systems has resulted in polymer nanocomposites (PNs) exhibiting multifunctional, high-performance polymer characteristics beyond what traditional filled polymeric materials possess. The development of these new materials enables the circumvention of classic material performance trade-offs by accessing new properties and exploiting unique synergies between materials, that only occur when the length scale of morphology and the fundamental physics associated with a property coincide, i.e., on the nano scale level. Multifunctional features attributable to polymer nanocomposites consist of improved thermal resistance and/or flame resistance, moisture resistance, decreased permeability,

charge dissipation, and chemical resistance. Through control/alteration of the additives at the nano scale level, one is able to maximize property enhancement of selected polymer systems to meet or exceed the requirements of current military, aerospace, and commercial applications. The technical approach involves the incorporation of nano particles into selected polymer matrix systems whereby nano particles may be surface-treated to provide hydrophobic characteristics and enhanced inclusion into the hydrophobic polymer matrix [5].

2.1.2.1 Multiwall Carbon Nanotubes (MWCNT's)

Multiwall Carbon Nanotubes (MWCNT's) obtained from Nanolab (Newton, Massachusetts, USA) were added in two different percentages to the vinylester to manufacture two different sets of samples, this allowed us to investigate if this enhance the matrix properties, hence the mechanical properties of the composite or not. The diameter of each single CNT range was 10 – 30 nm, with CNT length 5 – 20 μm.

Firstly, 8g of CNT's were mixed with methanol, then a sonication process was applied for five minutes at the maximum frequency (80 % Duty cycle, see section 2.2.4). After that the beaker that contains the CNT's /Methanol mix was immersed in a hot oil bath (this will insure uniform heat distribution around the beaker) to evaporate the methanol. Continues heating at 200°C for 45 minutes was performed to get rid of methanol. The first composite (15 layers of Kevlar + vinylester + CNT's) was prepared by adding 2.5 g of CNT's to 250 g of vinylester, this will produce matrix contains 1 wt % of CNT's (1% of resin). The same procedures of preparing the control sample were followed. Painting brush was utilized to distribute the matrix mix evenly over the first Kevlar ply; the second ply was placed in 45° angel over the first ply (0° angel). Consolidating metallic roller was scrolled over the second play; the third Kevlar ply was laid down in 0° orientation (the same orientation of the first Kevlar ply). The same scenario was adapted to prepare the rest of Kevlar layers. After that, the specimen was placed inside the hot press machine at the same conditions of the control sample, the two pressing plates were sprayed by mold release agent and heated to 175°C, then the laminated composite was compressed by force equal 450 kg distributed over 30 x 30 cm area for 15 minutes. This will produce a plate like composite, the weight of the final plate was recorded to evaluate the fiber/matrix fractions, the resin was 31.8 wt % of the composite and the Kevlar fibers were 68.2 wt %. The plate then was cut to 5 cm X 5 cm samples.

The second composite was prepared by adding 5 g of CNT's to 250 g of vinylester, this will produce matrix contains 2 wt % of CNT's (2% of resin). The weight of the final plate was recorded to evaluate the fiber/matrix fractions, the resin was 40.2 wt % of the composite and the Kevlar fibers were 59.8 wt %. The same sequence of

procedures of the previous sample was done. This plate then was cut to 5 cm X 5 cm samples.

2.1.2.2 Aluminom Oxide (Al_2O_3)

Aluminum Oxide (Al_2O_3) with 50 μm particle size from FLUKA(St. Gallen, Switzerland) Company (usually used for chromatography) were added in two different percentages to the vinylester to manufacture two different sets of samples, the Al_2O_3 is a very hard material, and usually it is used in polishing and abrasive applications.

The first composite (15 layers of Kevlar + vinylester + Al_2O_3) was prepared by adding 5.55 g of Al_2O_3 to 143.71 g of vinylester, this will produce matrix contains 3.7% wt of Al_2O_3 (3.7 % of resin).

The same procedures of preparing the control sample were followed. Painting brush was utilized to distribute the matrix mix over [0/45] woven Kevlar plies. Consolidating metallic roller was scrolled over. The same scenario was adapted to prepare all of Kevlar layers. After that, the specimen was placed inside the hot press machine at the same conditions of the control sample. The weight of the final plate was recorded to evaluate the fiber/matrix fractions, the mix was 35 wt % of the composite and the Kevlar fibers were 65 wt %. This means that the Al_2O_3 represent 1.31 wt% of the composite. The plate then was cut to 5 cm X 5 cm samples.

The second Al_2O_3 composite was prepared by adding 26.68 g of Al_2O_3 to 172.4 g of vinylester, this will produce matrix contains 15.5 % wt of Al_2O_3 (15.52 % of resin). The weight of the final plate was recorded to evaluate the fiber/matrix fractions, the resin was 42 wt % of the composite and the Kevlar fibers were 58 wt %. This means that the Al_2O_3 represent 5.6 wt% of the composite. The same sequence of procedures of the previous sample was done. This plate then was cut to 5 cm X 5 cm samples.

2.1.2.3 Nano Clay (NC)

Nano clay Montmorillonite clay, Nanomer I.34TCN (Sigma-Aldrich, Missouri, USA) contains 25-30 wt. % methyl dihydroxyethyl hydrogenated tallow ammonium were added in two different percentages to the vinylester to manufacture two different sets of samples. Nanoclays have become an attractive materials because of their potential use in wide range of applications such as in polymer nanocomposites [84].

The first composite (15 layers of Kevlar + vinylester + NC) was prepared by adding 25 g of NC to 223.9 g of vinylester, this will produce matrix contains 11.2 % wt of NC (11.2 % of resin).

The same procedure of preparing the previous samples wase followed. The weight of the final plate after curing was recorded to evaluate the fiber/matrix fractions, the mix was 43 wt % of the composite and the Kevlar fibers were 57 wt %. This means that the NC represent 4.3 wt% of the composite. The plate then was cut to 5 cm X 5 cm samples.

The second NC composite was prepared by adding 37.5 g of NC to 211.4 g of vinylester, this will produce matrix contains 17.7 % wt of NC (17.7 % of resin). The weight of the final plate was recorded to evaluate the fiber/matrix fractions, the matrix mix was 62 wt % of the composite and the Kevlar fibers were 38 wt %. This means that the NC represent 9.4 wt% of the composite. The same sequence of procedure of the previous sample was done. This plate then was cut to 5 cm X 5 cm samples.

2.1.2.4 Silicon Carbide (SiC)

Black Silicon carbide from PANADYNE Company (Warminster, Pennsylvania) with 1200 Grit number (15.3 μm particle size) were used to enhance the vinylester matrix.

The first composite (15 layers of Kevlar + vinylester + SiC) was prepared by adding 5.7 g of SiC to 193.3 g of vinylester, this will produce matrix contains 2.95 % wt of Sic (2.95 % of resin). The same procedures of preparing the previous samples were followed. The weight of the final plate after curing was recorded to evaluate the fiber/matrix fractions, the mix was 29 wt % of the composite and the Kevlar fibers were 71 wt %. This means that the SiC represent 0.82 wt% of the composite. The plate then was cut to 5 cm X 5 cm samples.

The second SiC composite was prepared by adding 28.57 g of SiC to 220.3 g of vinylester, this will produce matrix contains 12.97 % wt of SiC (12.97 % of resin). The weight of the final plate was recorded to evaluate the fiber/matrix fractions, the resin was 36.3 wt % of the composite and the Kevlar fibers were 63.7 wt %. This means that the SiC represent 4.15 wt% of the composite. The same sequence of procedures of the previous sample was done. This plate then was cut to 5 cm X 5 cm samples.

2.1.3 Composite Hot Press Technique

This process is also called compression molding or the matched die technique. In this process, prepregs are stacked together and then placed between heated molds. This process is primarily used for making simple shapes such as flat laminates. This process is used for making parts with constant thickness. The fiber volume fraction is usually greater than 60%. [71].

The following manufacturing steps are commonly followed during the hot press technique:

1. The temperature is set on the temperature gauge and the heater is switched on.
2. The mold is cleaned and release agent is applied.
3. The prepreg is cut to the desired shape, size, and orientation.
4. The prepregs are laid on top of each other.
5. The laminate is then placed between two heated platens.
6. The bottom platen is raised against the top platen.
7. The desired pressure is applied.
8. The temperature is raised.
9. The laminate is processed for approximately 4 to 10 min.
10. The mold is cooled at the desired cooling rate, typically at 2 to 10°C/min.
11. The pressure is released by moving the bottom platen downward.
12. The mold is opened and the part is removed. [71].

Advantages of the Hot Press Technique:

This process is very suitable for performing research and development work and for making flat test samples. The following are some of the advantages of the hot press technique:

1. Composites with high fiber volume fraction are achieved.
2. Parts from small to big sizes can be manufactured by this technique.
3. The parts are recyclable.

Limitations of the Hot Press Technique:

1. The process is limited to making simple parts such as flat plates.
2. The process has not gained much commercial importance.
3. Thick structures are difficult to be produced by this technique.

2.1.4 Sonication

Most of the polymer/CNT composite studies to date carried out in solution have employed sonication for the CNT's to insure better mixing with polymers. However, sonication introduces defects, including buckling, bending, and dislocations in the carbon structure. Prolonged sonication increases disorder, reduces nanotube length, and ultimately leads to the formation of amorphous carbon [85]. In addition, high shear mixing, in the presence of selected polymers, has also been used to unentangle ropes, yielding homogeneous dispersion. If the sonication is carried out in the presence of

polymer, then it is also important to understand the effect of sonication on polymer molecular weight [86].

Firstly, CNT's were added and mixed with methanol, and then a sonication process was applied for five minutes at the maximum frequency (10 unit) of Branson Sonifier 450 device. After that the CNT's /Methanol mix was immersed in hot oil bath to evaporate the methanol. Continues heating at 200°C for 45 minutes was performed to get rid of methanol.

2.1.5 Composite Machining

There are several types of machining operations, such as cutting, drilling, routing, trimming, sanding, milling, etc., performed to achieve various objectives. The majority of these machining processes are similar to metal machining.

Machining of composites is done to create holes, slots, and other features that are not possible to obtain during manufacturing of the part, also to create the desired tolerance in the component. Some times machining is performed to prepare the surface for bonding, coating, and painting purposes. To make prototype parts from a big blank or sheet of material, a machining operation is performed. This process is very economical. During cutting of aramid composites, aramid fibers absorb a significant amount of energy due to their ductile nature and the cut surface is not smooth. To obtain high quality edges and to avoid fuzzing in aramid composites, the cutting process must proceed in such a way that the fibers are being preloaded by tensile stress and then cut in a shearing action. For a rotating tool, this means that fibers must be pulled from the outside diameter toward the center. A sharp cutting edge and a comparatively high cutting speed are desirable to avoid receding of fibers into the matrix [87]. Rotating cutting tool with high speed (usually used for cutting wood) was used to prepare samples, the edge of the samples were grinded using ordinary silicon carbide papers.

There were few Challenges during Machining of Composites, it creates discontinuity in the fiber and thus affects the performance of the part, the temperature during cutting should not exceed the cure temperature of the resin for thermoset composites to avoid material disintegration. Aramid fibers are tough and absorb the cutting energy. Fiber kinking or burr surfaces are obtained during cutting of aramid composites. Machining of composites sometimes causes delaminations at the cut edges of continuous composites. The lay-up sequence and fiber orientations have a significant effect on the amount of delamination [88].

The samples prepared in this study had 17 cm x 17 cm dimensions see Fig 2.3, small squares with 5 cm x 5 cm was needed to fit the specimen chamber of the drop weight apparatus. Cutting process was performed for sampling the test specimens, high speed rotating saw was utilized. Each 17 x 17 (star shape) sample was enough to produce five or six samples with 5 x 5 cm dimension.

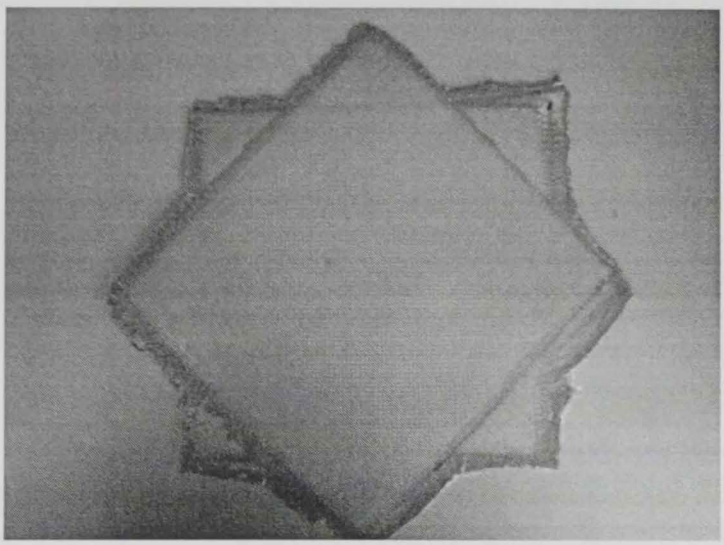

Fig. 2.3 15 plies wove Kevlar in [0/45] orientation

2.2 VINYLESTER/NANO CLAY COMPOSITES

A study of the Mechanical and Thermal properties of Montmorillonite nano clay addition to vinylester resin was performed; five different percentages of nano clay in vinylester were prepared by hand mixing (0%, 2%, 4.3 %, 7% and 9.4%). The same percentages of hardener were used (0.5 % wt), and the samples cured at room temperature for complete four days, after that the samples were heated at 120° C, for 60 minutes.

2.2.1 Mechanical Properties Analysis

2.2.1.1 Three Point Bending Test

The aim was to study the enhancement made by the addition of the Nanoclay on the stiffness of the vinylester. Set of three point bending tests according to ASTM D790 [89] standard recorded the load deflection curves of different weight percentages of nanoclay/ vinylester composites see Fig. 2-4. Two samples were prepared for each one of the different five NC percentages. The modulus of elasticity then calculated.

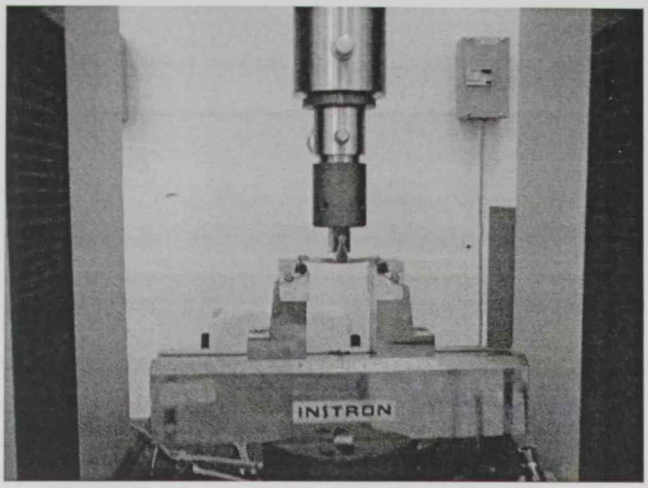

Fig. 2.4 Three Point Bend Test [89]

The flexural modulus is the ratio of stress to strain in flexural deformation, or the tendency for a material to bend. It is determined from the slope of a stress-strain curve produced by a flexural test [89].

Flexural modulus (E_{bend}) was calculated by the following formula:

$$E_{bend} = \frac{L^3 * m}{4 * b^3 * d}$$

E_{bend} = flexural Modulus of elasticity, (MPa).

L = Support span, (mm).

b = Width of test beam, (mm).

d = Depth of tested beam, (mm).

m = The gradient (i.e., slope) of the initial straight-line portion of the load deflection curve, (P/D), (N/mm).

2.2.1.2 Micro Hardness Test

Hardness tests are no longer limited to metals, and the currently available tools and procedures cover a vast range of materials including polymers, elastomers, thin films, semiconductors, and ceramics. Hardness measurements as applied to specific classes of materials convey different fundamental aspects of the material. Thus, for metals, hardness is directly proportional to the uniaxial yield stress at the strain imposed by the indentation. This statement, however, may not apply in the case of polymers, since their yield stress is ill defined. Yet hardness measurement may be a useful characterization technique for different properties of polymers, such as storage and loss modulus. Similarly, the measured hardness of ceramics and glasses may relate to their fracture toughness, and there appears to be some correlation between micro hardness and compressive strength [90].

The term micro hardness test usually refers to static indentations made with loads not exceeding 1 kgf. The indenter is either the Vickers diamond pyramid or the Knoop elongated diamond pyramid. The procedure for testing is very similar to that of the standard Vickers hardness test, except that it is done on a microscopic scale with higher precision instruments [91]. The Vickers test is often easier to use than other hardness tests since the required calculations are independent of the size of the indenter, and the indenter can be used for all materials irrespective of hardness. The basic principle, as with all common measures of hardness, is to observe the questioned material's ability to resist plastic deformation from a standard source.
The Vickers micro hardness test is exactly the same geometry and calculation method as the standard Vickers test, the only exception is that the applied force is in the range 0.001 to 1 kgf.

Vickers hardness number (HV), is an expression of hardness obtained by dividing the force applied to a Vickers indenter by the surface area of the permanent impression made by the indenter [92].
The Vickers hardness, kgf/mm^2 is determined as follows:

$$HV = 1.8544 \times P/d^2$$

Where:

P = force, kgf.
d = length of long diagonal, mm [92].

Micro Hardness Tests were performed for the different Nanoclay/ Vinylester composites, the Vickers micro hardness test was utilized, different trials were measured for every sample. The whole readings were taken along centerlines at the mid width of the sample on both faces. The regions of porosities were avoided and the average of readings was calculated.

2.2.1.3 Nano Indentation

Nanoindetation tests were performed on Nano Test Materials testing platform (Micro Materials Ltd, Wrexham, UK) that is equipped with a three sided pyramid diamond indenter tip (Berkovich type). Five indents were performed for each Vinylester/Nanoclay samples. The distance between indentations was 50 μm to avoid interaction. The hardness (H) and the elastic modulus (E) were calculated from the load–displacement data. As the indenter was allowed to penetrate into the specimen, both elastic and plastic deformation occurred and only the elastic portion of the displacement was recovered during unloading. The slope S at the maximum load point $\frac{dP}{dh}$ is the experimentally measured stiffness of the upper portion of the unloading data (Oliver-Pharr method [93]) which can be used to calculate the reduced modulus of elasticity using the equation

$$E_r = \frac{S\sqrt{\pi}}{2\beta\sqrt{A_p}} \qquad \text{.....(1)}$$

Where A_p is the area of the indentation at the contact depth, β is a constant that depends on the geometry of the indenter ($\beta = 1.034$ for a Berkovich indenter). The reduced modulus E_r is a combination of the sample material and indenter elastic deformations [94, 95]. The effects of non-rigid indenters on the load- displacement behavior is taken into considerations by defining the reduced modulus through the equation:

$$\frac{1}{E_r} = \frac{1-\nu_s^2}{E_s} + \frac{1-\nu_i^2}{E_i} \qquad \text{.....(2)}$$

where E_s and ν_s are the Young's modulus and Poisson's ratio for the sample . Poisson's ratio is taken to be 0.35 for Vinylester, Ei and ν_i are the same parameters for the indenter and for a diamond indenter E_i is 1140 GPa and ν_i is 0.07.

2.2.2 Thermal Analysis

2.2.2.1 Thermal Gravimetric Analysis (TGA)

TGA Q50 Device from TA Instruments (New Castle, Delaware) was utilized to study the thermal weight-change of the Nanoclay/ Vinylester samples. The aim of this study was to investigate if the addition of the nanoclay to enhance the mechanical properties was at the expense of the thermal properties (decomposition temperature) or not. The Thermo gravimetric analyzer measures the amount and rate of weight change in a material, either as a function of increasing temperature, or isothermally as a function of time, in a controlled atmosphere. It can be used to characterize any material that exhibits a weight change and to detect phase changes due to decomposition, oxidation, or dehydration. This information helps us identify the percentage weight change and correlate chemical structure, processing, and end-use performance [96].

The TGA measurements were performed under nitrogen atmosphere with balance purge flow 40 mL/min and sample purge flow 60 mL/min. About 10 mg of the composites samples were used each time. The measurements were done with a heating rate of 20°C/min in the temperature range (0-600 °C).

2.2.2.2 Differential scanning calorimetry (DSC)

Differential Scanning Calorimetry or (DSC) is a thermo analytical technique in which the difference in the amount of heat required to increase the temperature of a sample and reference is measured as a function of temperature. Both the sample and reference are maintained at nearly the same temperature throughout the experiment . The basic principle underlying this technique is that, when the sample undergoes a physical transformation such as phase transitions, more or less heat will need to flow to it than the reference to maintain both at the same temperature [97].

The DSC measurements were performed using a TA instrument (New Castle, Delaware) DSC 200 under nitrogen atmosphere with a sample purge flow 50 mL/min. 10 mg of the composites samples were used each time in a sealed aluminum pan. The samples were heated to 250°C at a rate of 10°C/min to eliminate the heat history. Then they were cooled below 0°C at a rate of 10°C/min and heated again at the same rate to the temperature 500°C.

2.3 IMPACT TEST METHOD

Drop a weight in a vertical direction, with a tube or rails to guide the falling weight during the free fall. With known height and weight, impact energy can be calculated. The main advantages of drop weight test are:

- It is applicable for molded samples, molded parts, etc.
- It is unidirectional with no preferential direction of failure. Failures originate at the weakest point in the sample and propagate from there.
- Samples do not have to shatter to be considered failures. Failure can be defined by deformation, crack initiation, or complete fracture, depending on the requirements.

These factors make falling weight testing a better simulation of functional impact exposures, and therefore closer to real-life conditions. It was originally developed for rigid plastics [2].

2.3.1 Drop Weight Apparatus

Drop-Weight apparatus locally made was used to impact the woven Kevlar laminates; this apparatus has the basic components in any drop weight technique devices (Fig. 2.5):

- Impactor (the punch weight about 30 kg).
- Clamping device (to fit the sample inside).
- Locking pin (to prevent sample from sliding during impact).
- Drop guide (detached from drop tower).
- Shock absorber (to reduce the vibration after each hit).
- Rolling Handle (to move the weight to any desired heights).

The device is appropriate to test pieces have 5 X 5 cm square dimensions, and 1–10 mm thick. The test piece will be supported on a hollow steel chamber with an inside dimension of 50 X 50 X 10mm. It may be clamped in position. The cylindrical steel striker has 25.4 mm diameter and 50 mm length, and is allowed to fall from a height of up to 1.3 m onto the specimen (equivalent to a maximum velocity of 5.1 m/s). This is about 380 J as the maximum capacity of this device.

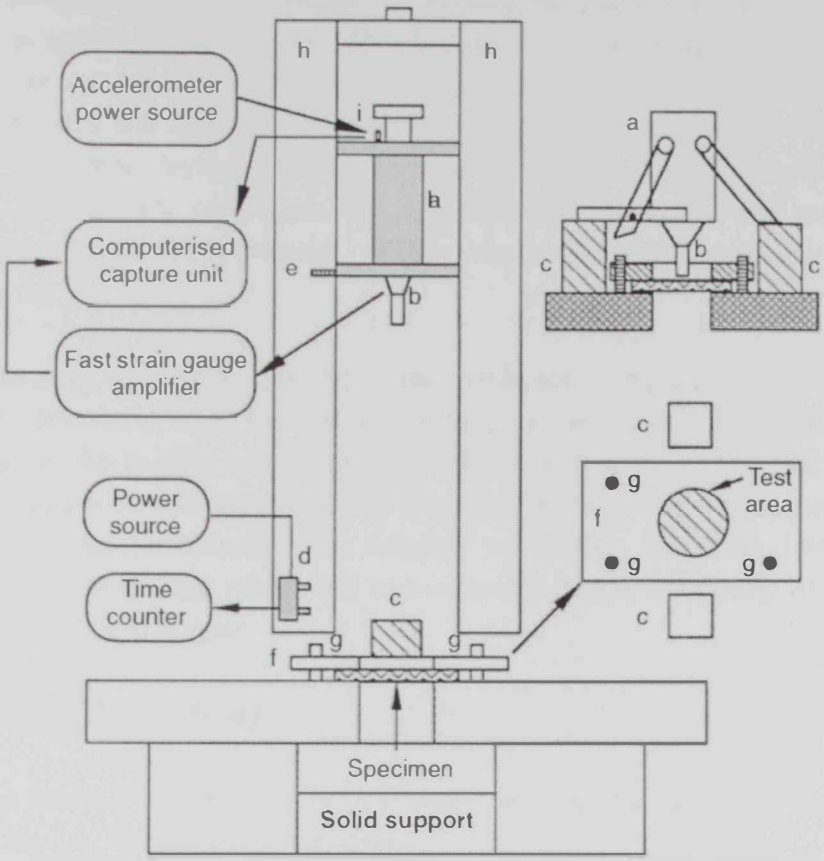

Fig. 2.5 An experimental setup for drop-weight impact tests.
(a) impactor (b) strain-gauged load cell (c) rebound catch block (d) photodiodes(e) flag (f) clamping device (g) locking pin (h) drop guide (i) accelerometer [2].

For a puncture test on a composite, a strike velocity of 4.4 m/s and a total striker mass of 5–20 kg (equivalent to energies of 48–193 J) are preferred [2]. Many variants of the dropped weight test are described in the literature, with specimens ranging in size from 127 X 127 mm square to 100 mm in diameter, and impactors with tip radii of 5–12.7 mm.

2.3.2 Experimental Setup

The experimental setup was created according to guidelines given in the ASTM-D 7136 [98], this test method determines the damage resistance of multidirectional polymer matrix composite laminated plates subjected to a drop-weight impact event. The composite material forms are limited to continuous-fiber reinforced polymer matrix composites. A flat, rectangular composite plate is subjected to an out-of-plane,

concentrated impact using a drop-weight device with a cylindrical impactor. The potential energy of the drop-weight, as defined by the mass and drop height of the impactor, is specified prior to test. The damage resistance is quantified in terms of the resulting size and type of damage in the specimen. The damage resistance properties generated by this test method are highly dependent upon several factors, which include specimen geometry, layup, impactor geometry, impactor mass, impact force, impact energy, and boundary conditions. Thus, results are generally not scalable to other configurations, and are particular to the combination of geometric and physical conditions tested.

The samples were simply supported inside the clamping device, locking pin was fastened to prevent sample from sliding during impact, the weight lifted manually by rolling handle, the guiding tower tubes were lubricated to insure minimum friction, then the height measured and recorded, the pin removed and the weight free fell over the specimen. Similar procedures were adopted by Hallett and Ruiz [99] to study the response of unidirectional reinforced carbon/epoxy beams consisting of alternate 0/90° plies under low speed impact.

2.3.3 Projectile (IMPACTOR)

The IMPACTOR has cylindrical shape with length equal 50 mm and 25.4 mm diameter, Fig 2.6. It was made from steel.

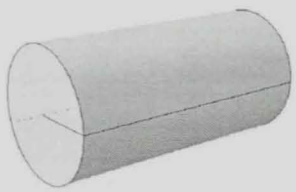

Fig. 2.6 The Impactor

2.3.4 Test Procedure

After samples were prepared, they were tested under a low speed impact, the weight was lifted manually by the rolling handle to the desired height, the sample was placed between the fixing plates (specimen chamber), then the locking screw was placed to prevent any lateral sliding, after that the weight was released to toward the specimen.

After the impact the weight was lifted again to release the impacted specimen, the locking screw was removed, and the sample was liberated.

These are the steps of each test trial, each test was followed by extensive visual investigation to capture any failure happened. The number of removed layers and the delamination between the woven Kevlar layers in the lateral direction was noticed and recorded.

2.3.5 Determination of the minimum energy for complete penetration

The control specimen was used to evaluate the minimum energy to completely penetrate the composite specimens. This amount of energy is very important because it will be a constant parameter during the entire research. The different composition composites were impacted with the same amount of energy.

Fourteen trials at fourteen identical samples each one composed of 15 woven Kevlar layers with fiber fraction equal 73%wt, the height was varied and the failure mode was noticed, complete penetration took place only at 85 cm and above heights. This is equivalent to 250J.

2.3.6 Calculation of Energy Absorption Values

All energy stored as potential energy in the striker before releasing the load according to the formula:

$$\text{Potential Energy (PE)} = (m * g * h)$$

Where m: mass.
g: acceleration of gravity.
h: the height.

$PE = 30\ kg\ X\ 9.81\ m/s^2\ X\ 0.85\ m = 250\ J.$

This energy is transformed to kinetic energy when the weight released according to the formula:

$$\text{Kinetic Energy (KE)} = \frac{1}{2}\ X\ m\ X\ V^2$$

Then, the velocity just before the impact will be

$V = \sqrt{2X9.81X0.85^2} = 4.08$ m/sec.

2.4 Summary

Samples composed of 15 woven Kevlar layers oriented in [0°/45°] directions were prepared manually using regular painting brush and consolidating metallic roller to distribute the matrix evenly between the Kevlar fibers. The specimens were compressed using hot pressing machine. The samples prepared in this study had 17 cm x 17 cm dimensions, the samples were cut to small 5 cm x 5 cm dimensions. Samples were tested using locally made drop weight apparatus.

A study on the mechanical and thermal properties of nano clay addition to vinylester resin was performed; five different percentages of nano clay in vinylester were prepared by hand mixing (0%, 2%, 4.3 %, 7% and 9.4%) different mechanical and thermal analysis were performed on these samples.

Chapter 3

RESULTS & DISCUSSION

CHAPTER 3

RESULTS & DISCUSSION

This chapter reports all experimental results in this research study, the drop weight impact results of all samples, the X-ray photography of the impacted Kevlar samples, three point bending, microhardness, nano indentation, TGA and DSC results of Nanoclay/Vinylester composite.

3.1 DROP-WEIGHT IMPACT TEST

An in-house designed Drop-Weight testing machine was used to study the impact resistance of different composite samples. A total of five different Kevlar composite samples were prepared namely control, Aluminum Oxide, Nanoclay, CNT and Silicon Carbide. All samples were constructed out of 15 woven Kevlar layers with the addition of above mentioned materials. The prepared samples were of 5cm X 5cm size with thickness varying between 3.10 – 5.65 mm. Table 3.1 shows the description of 10 samples with their corresponding fiber, matrix, weights and additive percentage. The following theme was used in a numbering the samples

Sample Type	Sample No.	Composition	Fiber Weight (g)	Matrix Weight (g)	Additive in wt % of Composite	Additive in wt % of Resin	Weight (g)
Control	DW 1	15 Kevlar layers + Vinylester	78	37	0.00	0.00	106.65
	DW 2	15 Kevlar layers + Vinylester	78	29	0.00	0.00	106.65
Alum. Oxide	DW 3	15 Kevlar layers + Vinylester + Al_2O_3	78	43	1.31	3.70	120.68
	DW 4	15 Kevlar layers + Vinylester + Al_2O_3	78	58	5.60	13.34	137.10
Nano Clay	DW 5	15 Kevlar layers + Vinylester + NC	78	59	4.30	10.00	137.4
	DW 6	15 Kevlar layers + Vinylester + NC	78	132	9.40	15.00	210.00
CNT	DW 7	15 Kevlar layers + Vinylester + CNT	78	36	0.32	1.00	114.4
	DW 8	15 Kevlar layers + Vinylester + CNT	78	52	0.80	2.00	130.45
Silicon Carbide	DW 9	15 Kevlar layers + Vinylester + SiC	78	31	0.82	2.86	109.17
	DW 10	15 Kevlar layers + Vinylester + SiC	78	45	4.15	11.43	122.45

Table 3.1 Coding system used to represent our Drop Weight tested samples.

DW 5 means that this sample composed of 15 Kevlar layers + Vinylester + NC 4.3 wt %. DW 3-2 (Fig. 3.1) means that this sample composed of 15 Kevlar layers + Vinylester + Al_2O_3 1.31 wt %, and represents the statistical trial number 2.

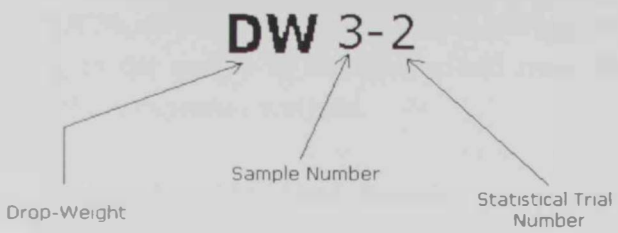

Fig. 3.1 Example on Coding System

The matrix mix were added in such a way to insure saturation of each Kevlar layer, the fiber matrix ratios were calculated after curing each composite in the hot press technique. Fig. 3.2 below shows the Matrix weight percentage in each composite. it can be seen from the figure that the resin amount needed to saturate the Kevlar layers was increased by increasing the percentage of additives; this was due to the decrease in viscosity of the matrix mix when the additive percentage increased.

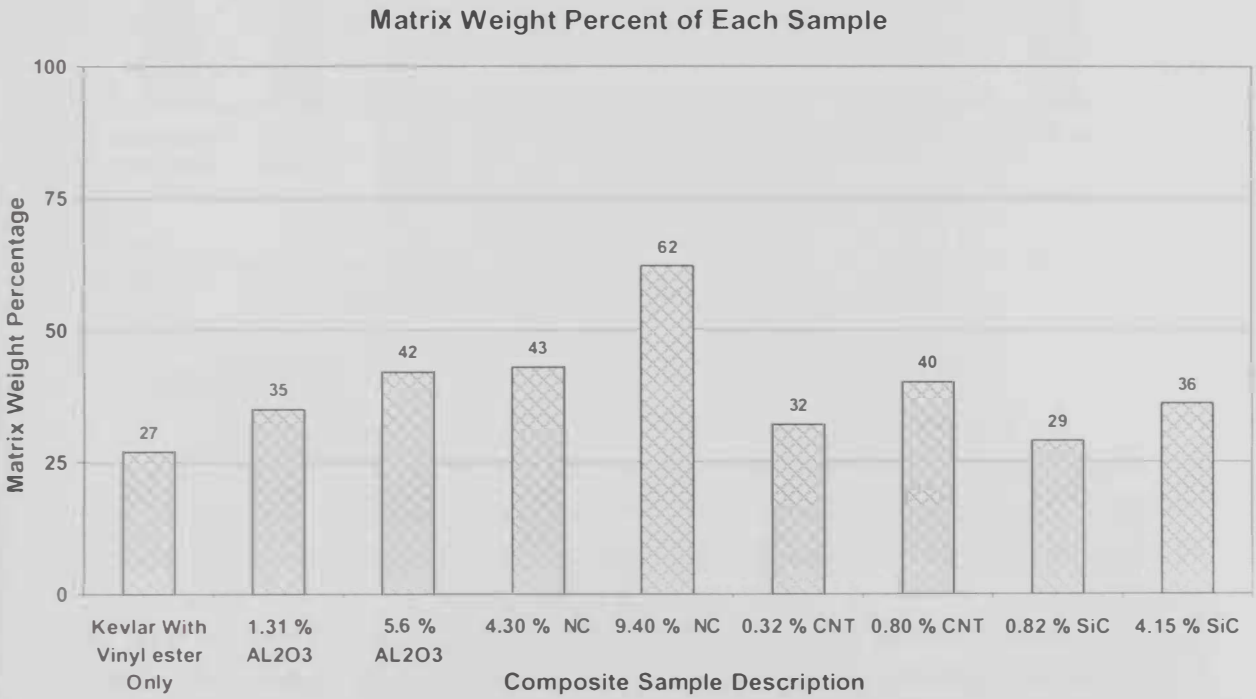

Fig. 3.2 Matrix Weight Percentage in Each Composite.

The change in fiber/matrix percentage in each sample reflected on each sample weight. The weight of the composite is very important as a design parameter, especially in aerospace application and other applications which need high strength to weight ratio materials. It can be noticed that the weight of the particles reinforced samples had increase in weight varying from 2 % in the composite contains 0.82 wt % SiC to 96 % in the composite contains 9.4 % of Nanoclay (Fig. 3.3). Although the additives weights were very low comparing to the weight of the Kevlar and resin, the change in matrix viscosity had an effect on the composites weights.

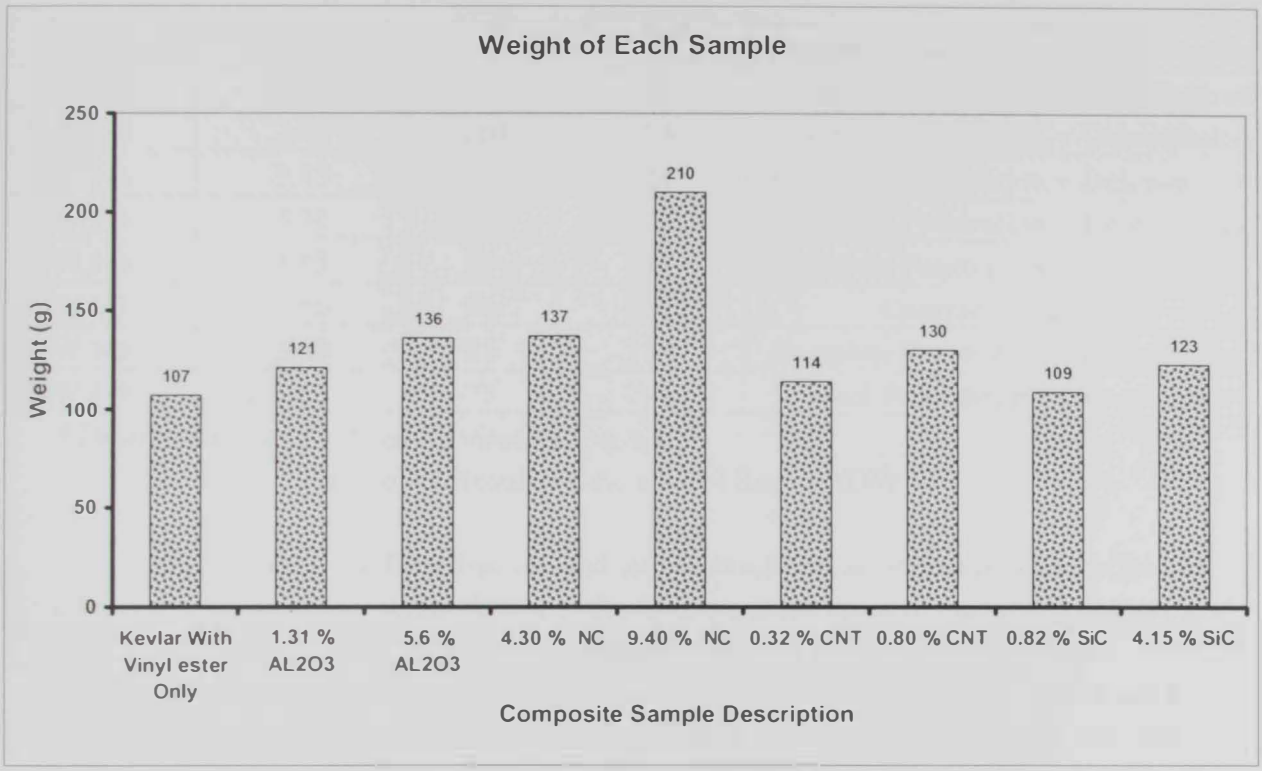

Fig. 3.3 Weight of Each Composite after Curing.

3.1.1 Control Samples

Samples from DW 1-1 to DW 1-9 were tested under different impact energies, the main focus was to investigate the impact response of the control sample and study their failure modes. This allowed us to notice any change in response when different types of additives introduced.

Nine samples were examined with different energy levels, the recorded results provided about the drop weight device capability and consistency. Nine samples were enough to predict the 15 Kevlar layer capability and impact resistance potential.

Beside the penetration resistance capability, the failure mechanism of the different control samples was studied and recorded in Table 3.2.

DW 1-1 to DW 1-9 showed considerable variation in thickness, this was due to the manual preparation process and inclination of one of the hot press machine plates, to eliminate this variation; the composite specimen was placed between two aluminum plates when pressed by the hot press machine.

Sample	Thickness (mm)	Height (cm)	Impact Energy(J)	Response
DW 1-1	3.25	115	338	Complete Penetration + Delamination *
DW 1-2	3.30	111	327	Complete Penetration + Delamination*
DW 1-3	3.40	110	324	Complete Penetration + Delamination*
DW 1-4	3.15	110	324	Complete Penetration + Delamination*
DW 1-5	3.30	104	306	Complete Penetration + Delamination*
DW 1-6	3.15	94	277	Complete Penetration + Delamination*
DW 1-7	3.50	94	277	Complete Penetration
DW 1-8	3.50	85	250	Complete Penetration + Delamination*
DW 1-9	3.30	75	221	Partial Penetration + Delamination*

* Delamination was noticed by visual inspection.

Table 3.2 Results of the control Sample (DW 1)

In addition to the fiber fracture and matrix cracking, delamination was noticed in all tested samples, delamination is one of the most common types of damage in laminated fiber reinforced composites due to there relatively weak interlaminar strength.

DW 2-1 to DW 2-5 samples were tested under different impact energies to predict the minimum energy required to completely penetrate the control sample. This will allow us to compare the energy absorption enhancement achieved when different types of additives introduced. Five samples were examined with different energy levels, the recorded results were able to define the complete penetration threshold, and the minimum energy was 250 J. This was an extremely important step in this research because all the followed tests were done at the same amount of energy. The energy was a fixed parameter, to examine what are the modifications that will happen when we add different material to the composite matrix. DW 2-1 to DW 2-5 showed homogeneity in thickness, this was due to the placement of the composite between two aluminum plates when compressed by the hot press machine. The results are summarized in Table 3.3.

Sample	Thickness (mm)	Height (cm)	Impact Energy(J)	Response
DW 2-1	3.10	89	262	Complete Penetration + Delamination *
DW 2-2	3.10	87	256	Complete Penetration + Delamination*
DW 2-3	3.10	86	253	Complete Penetration + Delamination*
DW 2-4	3.10	85	250	Complete Penetration + Delamination*
DW 2-5	3.05	83	244	Partial Penetration (two plies remain) + Delamination*

* Delamination was noticed by visual inspection.

Table 3.3 Results of the control Samples (DW 2)

The delamination and fiber fracture modes in sample DW 2 were similar to the control sample DW 1.

3.1.2 Aluminum Oxide reinforced Samples

The set of first alumina samples (DW 3) contained 1.31 wt % of Al_2O_3, all samples had 3.55 mm thickness, this percentage was low, so no increase in the penetration resistance noticed, the impactor was able to penetrate the composite samples all three trials. The visual inspection of the impacted samples didn't show any evidence of presence of any delamination through the composite thickness, see Table 3.4.

Sample	Thickness (mm)	Height (cm)	Impact Energy(J)	Response
DW 3-1	3.55	85	250	Complete Penetration + No Delamination *
DW 3-2	3.55	85	250	Complete Penetration + No Delamination*
DW 3-3	3.55	85	250	Complete Penetration + No Delamination*

* Delamination was noticed by visual inspection.

Table 3.4 Results of the Aluminum Oxide (1.31 wt %) Samples (DW 3)

The second set of alumina samples (DW 4) contained 5.60 wt % of Al_2O_3, this percentage contributed to the impact resistance of the samples, the impactor was able to partially penetrate the composite samples in all three trials. The visual inspections of the impacted samples showed high tendency of samples to delaminate, See Table 3.5

Sample	Thickness (mm)	Height (cm)	Impact Energy(J)	Response
DW 2-1	3.10	89	262	Complete Penetration + Delamination *
DW 2-2	3.10	87	256	Complete Penetration + Delamination*
DW 2-3	3.10	86	253	Complete Penetration + Delamination*
DW 2-4	3.10	85	250	Complete Penetration + Delamination*
DW 2-5	3.05	83	244	Partial Penetration (two plies remain) + Delamination*

* Delamination was noticed by visual inspection.

Table 3.3 Results of the control Samples (DW 2)

The delamination and fiber fracture modes in sample DW 2 were similar to the control sample DW 1.

3.1.2 Aluminum Oxide reinforced Samples

The set of first alumina samples (DW 3) contained 1.31 wt % of Al_2O_3, all samples had 3.55 mm thickness, this percentage was low, so no increase in the penetration resistance noticed, the impactor was able to penetrate the composite samples all three trials. The visual inspection of the impacted samples didn't show any evidence of presence of any delamination through the composite thickness, see Table 3.4.

Sample	Thickness (mm)	Height (cm)	Impact Energy(J)	Response
DW 3-1	3.55	85	250	Complete Penetration + No Delamination *
DW 3-2	3.55	85	250	Complete Penetration + No Delamination*
DW 3-3	3.55	85	250	Complete Penetration + No Delamination*

* Delamination was noticed by visual inspection.

Table 3.4 Results of the Aluminum Oxide (1.31 wt %) Samples (DW 3)

The second set of alumina samples (DW 4) contained 5.60 wt % of Al_2O_3, this percentage contributed to the impact resistance of the samples, the impactor was able to partially penetrate the composite samples in all three trials. The visual inspections of the impacted samples showed high tendency of samples to delaminate, See Table 3.5

Sample	Thickness (mm)	Height (cm)	Impact Energy(J)	Response
DW 4-1	4.00	85	250	Partial Penetration (7 plies removed) + Delamination at different places.
DW 4-2	4.00	85	250	Partial Penetration (7 plies removed) + Delamination at different places*.
DW 4-3	4.00	85	250	Partial Penetration (7 plies removed) + Delamination at different places*.
DW 4-4	4.00	85	250	Partial Penetration (6 plies removed) + Delamination at different places*.

* Delamination was noticed by visual inspection.

Table 3.5 Results of the Aluminum Oxide (5.60 wt %) Samples (DW 4)

3.1.3 Nano Clay reinforced Samples

The first set Nano Clay of samples (DW 5) contained 4.30 wt % of NC, this percentage was enough to increase the penetration resistance of the composite; the impactor was able to partially penetrate the composite samples in all trials. The visual inspection of the impacted samples didn't show any evidence of delamination, Table 3.6.

Sample	Thickness (mm)	Height (cm)	Impact Energy(J)	Response
DW 5-1	4.50	85	250	Partial Penetration (5 plies removed) + No Delamination*.
DW 5-2	4.55	85	250	Partial Penetration (5 plies removed) + No Delamination*.
DW 5-3	4.65	85	250	Partial Penetration (5 plies removed) + No Delamination*.

* Delamination was noticed by visual inspection.

Table 3.6 Results of the Nano Clay (4.30 wt %) Samples (DW 5)

The second Nano Clay reinforced composites set of samples (DW 6) contained 9.40 wt % of NC, this percentage enhanced the impact resistance of the samples in noticeable way; the impactor was not able to penetrate the composite samples in all four trials. The visual inspections of the impacted samples showed high tendency of samples to delaminate and sowed almost complete delamination in some samples, Table 3.7

Sample	Thickness (mm)	Height (cm)	Impact Energy(J)	Response
DW 6-1	5.65	85	250	No Penetration (2 plies removed only) + Almost complete delamination at the mid of thickness*.
DW 6-2	5.25	85	250	No Penetration (2 plies removed only) + Almost complete delamination at the mid of thickness*.
DW 6-3	5.25	85	250	No Penetration (2 plies removed only) + Almost complete delamination at the mid of thickness*.
DW 6-4	5.65	85	250	No Penetration (2 plies removed only) + Almost complete delamination at the mid of thickness*.

* Delamination was noticed by visual inspection.

Table 3.7 Results of the Nano Clay (9.40 wt %) Samples (DW 6)

3.1.4 Carbon Nanotubes reinforced Samples

The first set of MWCNT's sample (DW 7) contained 0.32 wt % of CNT's, this percentage was not able to increase the penetration resistance of the composite; the impactor was able to penetrate the composite samples in all three trials. The visual inspection of the impacted samples didn't show any evidence of presence of any delamination, Table 3.8.

Sample	Thickness (mm)	Height (cm)	Impact Energy(J)	Response
DW 7-1	4.20	85	250	Complete Penetration + No Delamination*
DW 7-2	4.20	85	250	Complete Penetration + No Delamination*
DW 7-3	4.20	85	250	Complete Penetration + No Delamination*

* Delamination was noticed by visual inspection.

Table 3.8 Results of the CNT's (0.32 wt %) Samples (DW 7)

The second set of MWCNT's samples (DW 8) contained 0.80 wt % of CNT's, this percentage enhanced the impact resistance of the samples in an insufficient way, the samples showed resistance to the impactor, but the impactor was still able to penetrate the

composite samples in the four trials. The visual inspection of the impacted samples didn't show any evidence of presence of any delamination, Table 3.9.

Sample	Thickness (mm)	Height (cm)	Impact Energy(J)	Response
DW 8-1	4.45	85	250	Penetration of the 15 layers at half of the circumference of the circle+ No delamination*.
DW 8-2	4.45	85	250	Penetration of the 15 layers at half of the circumference of the circle+ No delamination*.
DW 8-3	4.45	85	250	Penetration of the 15 layers at half of the circumference of the circle+ No delamination*.
DW 8-4	4.55	85	250	Penetration of the 15 layers at half of the circumference of the circle+ No delamination*.

* Delamination was noticed by visual inspection.

Table 3.9 Results of the CNT's (0.80 wt %) Samples (DW 8)

3.1.5 Silicon Carbide reinforced Samples

The first set of SiC samples (DW 9) contained 0.82 wt % of SiC, this percentage was not able to increase the penetration resistance of the composite; the impactor was able to penetrate the composite samples in the three statistical trials. The visual inspection of the impacted samples didn't show any evidence of presence of any delamination, Table 3.10.

Sample	Thickness (mm)	Height (cm)	Impact Energy(J)	Response
DW 9-1	4.00	85	250	Complete Penetration + No Delamination*
DW 9-2	4.00	85	250	Complete Penetration + No Delamination*
DW 9-3	4.00	85	250	Complete Penetration + No Delamination*

* Delamination was noticed by visual inspection.

Table 3.10 Results of the SiC (0.82 wt %) Samples (DW 9)

The second set of SiC samples (DW 10) contained 4.15 wt % of SiC, this percentage enhanced the impact resistance of the samples in a noticeable way; the impactor was able to partially penetrate the composite samples in the four statistical trials. The visual inspection of the impacted samples didn't show any evidence of presence of any delamination, Table 3.11

Sample	Thickness (mm)	Height (cm)	Impact Energy(J)	Response
DW 10-1	4.20	85	250	Partial Penetration (5 plies removed) + No Delamination*.
DW 10-2	4.20	85	250	Partial Penetration (5 plies removed) + No Delamination*.
DW 10-3	4.20	85	250	Partial Penetration (5 plies removed) + No Delamination*.
DW 10-4	4.20	85	250	Partial Penetration (5 plies removed) + No Delamination*.
DW 10-5	4.20	85	250	Partial Penetration (5 plies removed) + No Delamination*.

* Delamination was noticed by visual inspection.

Table 3.11 Results of the SiC (4.15 wt %) Samples (DW 10)

Figure 3.4 shows the impact results of all different samples under low speed impact. The Aluminum oxide composites with 1.31 wt % did not enhance the Kevlar composite resistance, but it changed the failure mode by enhancing the lateral direction, so no delamination was noticed by visual inspection. Samples containing 5.6 % of Aluminum oxide increased the impact resistance of the Kevlar composite so the impactor couldn't completely penetrate the Kevlar layers, but this was at the expense of the delamination resistance achieved by the low percentage of Aluminum oxide.

Nanoclay reinforced composite samples were the best additive. Samples with 4.3 wt % were able to resist the impactor so only five out of fifteen layers removed with no delamination noticed. While samples with 9.4 wt % of nanoclay resisted the impactor in such a way that only 2 layers were removed, this great response of energy absorption was on the expense of the delamination resistance showed in the composites that contains 4.3% of nanoclay.

Carbon nanotubes reinforced composites weren't able to resist the impactor penetration. This could be due to the random distribution and low percentage of the CNT's reinforced samples.

The silicon carbide composites with 0.82 wt % weren't able to enhance the Kevlar composite resistance, but it changed the failure mode by enhancing the lateral direction, so no delamination noticed by visual inspection. Samples with 4.15 % of Silicon Carbide increased the impact resistance of the Kevlar composite so the impactor couldn't penetrate more than one third of the Kevlar layers and at the same time no delamination

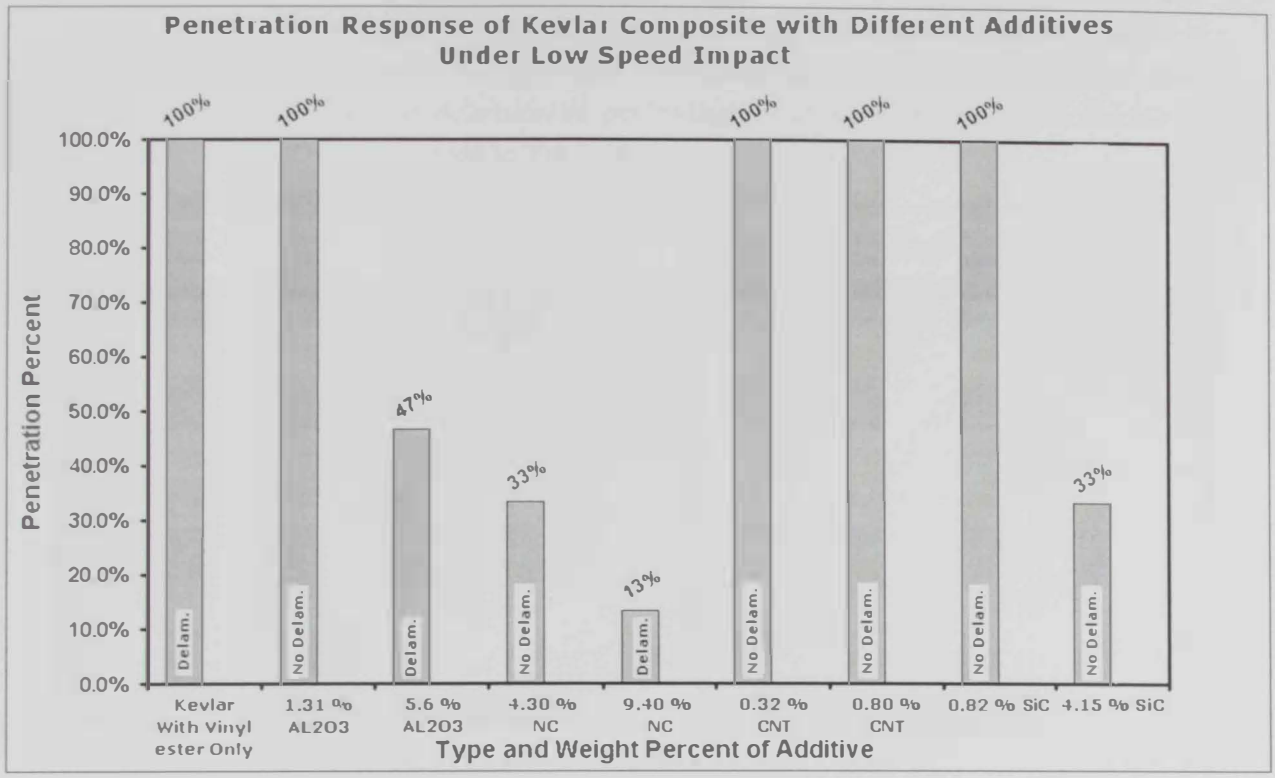

was noticed by visual inspection.

Fig. 3.4 Penetration Response of Kevlar Composite with Different Additives under Low Speed Impact

3.2 X-Ray Results

X-ray diffraction has been utilized to characterize the changes in the internal structure of the different Kevlar laminated composites after impact. X-Ray relies on the differential absorption coefficient being directly related to material density and a function of the atomic number or scattering of X-ray photons as they pass through a material.

Front and side views were taken for each type of Kevlar composites, the X-ray films then were exposed to strong illumination source to reveal the image details, then photos were captured using 10 mega pixels digital camera.

The photos in figures Fig. 3.5 to Fig. 3.13 show variation in light intensity; this was due to the delaminated areas. The ability of X-ray to penetrate empty places (delaminated) is higher than it is ability in solid regions (non-delaminated). The bright areas represent the delaminated areas while the dark areas represent the remained bonded areas. We can notice considerable mach between the front and side view for each sample.

Image processing software were used to modify the contrast and brightness of each photo, this allowed us to easily predict the boarder line around the delaminated areas (Fig. 3.5 to Fig 3.13). The delaminated percentage of composite areas were calculated and the results were summarized in Fig 3.14.

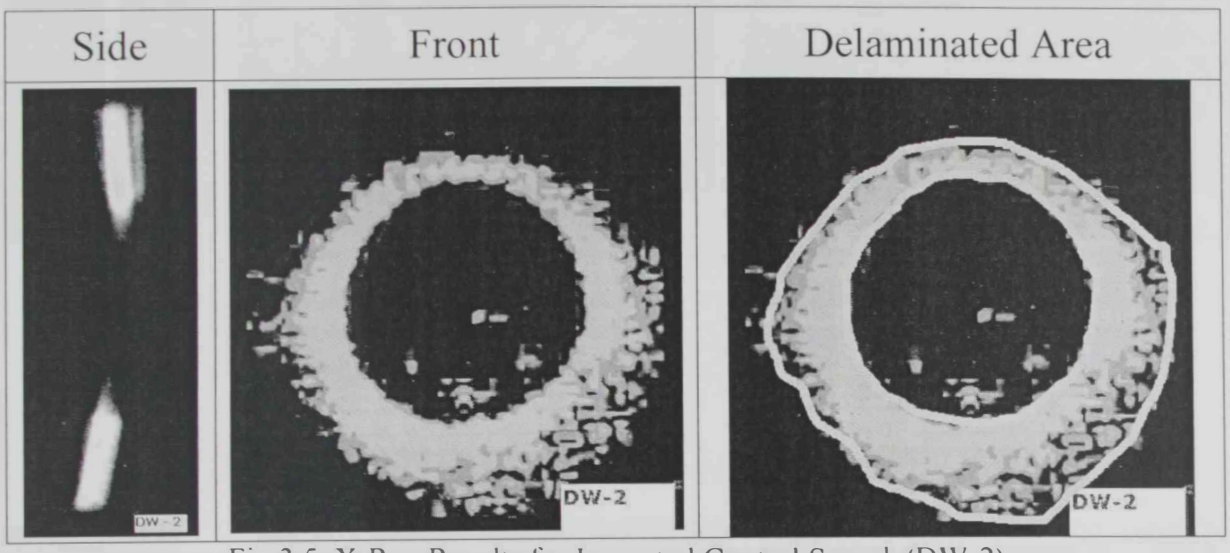

Fig 3.5 X-Ray Results for Impacted Control Sample(DW-2)

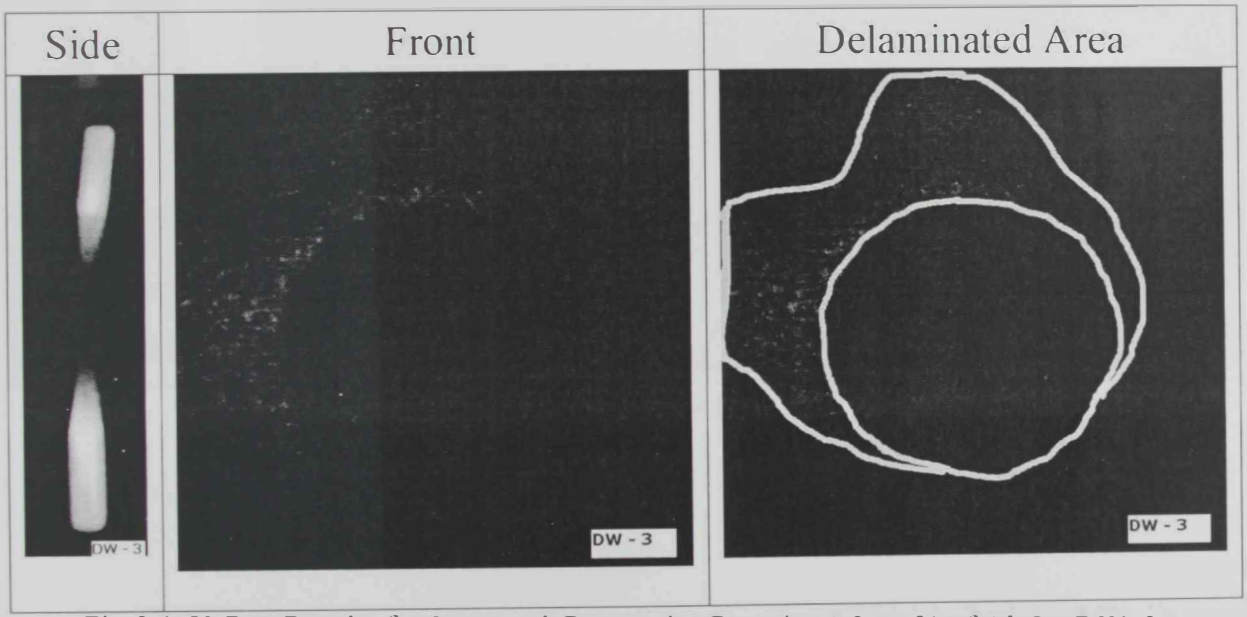

Fig 3.6 X-Ray Results for Impacted Composite Contains 1.3 wt % of Al_2O_3 (DW–3)

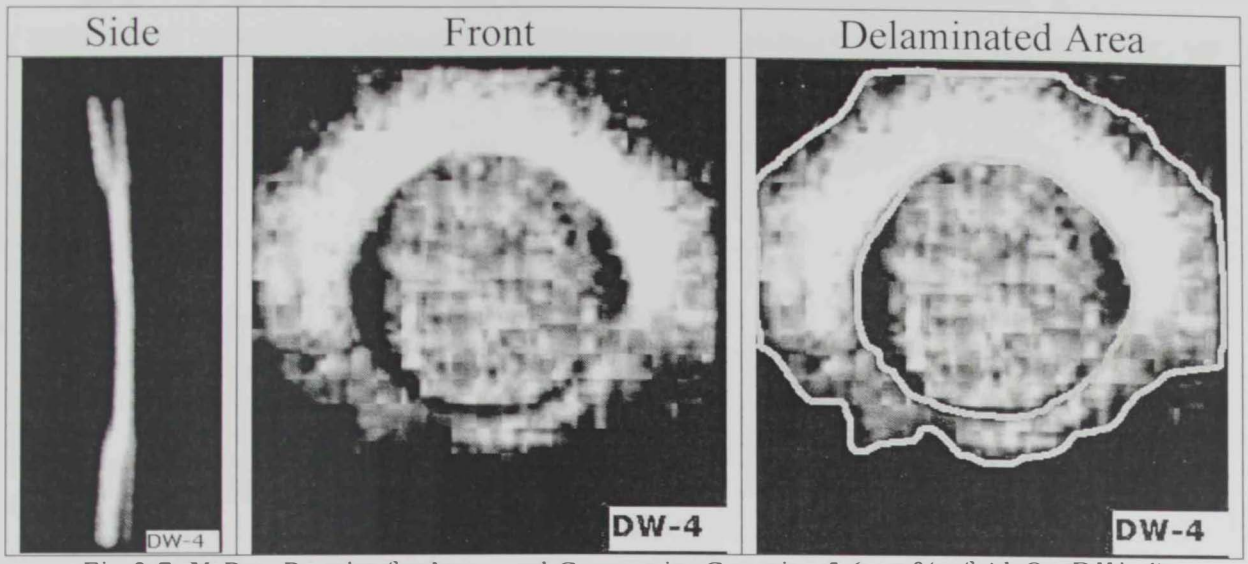

Fig 3.7 X-Ray Results for Impacted Composite Contains 5.6 wt % of Al_2O_3 (DW–4)

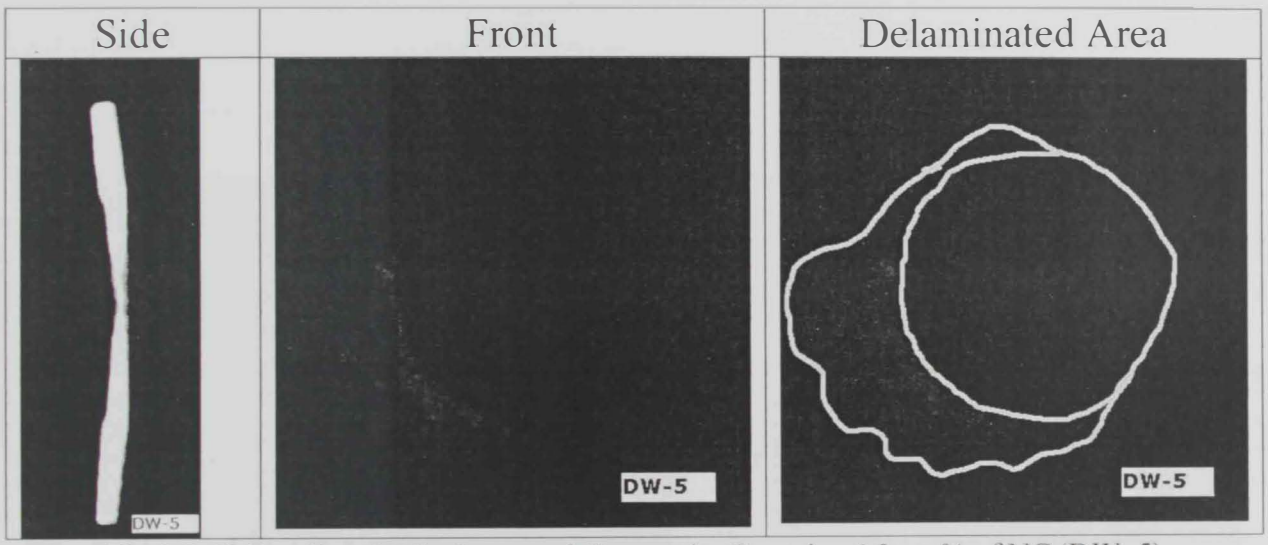

Fig 3.8 X-Ray Results for Impacted Composite Contains 4.3 wt % of NC (DW–5)

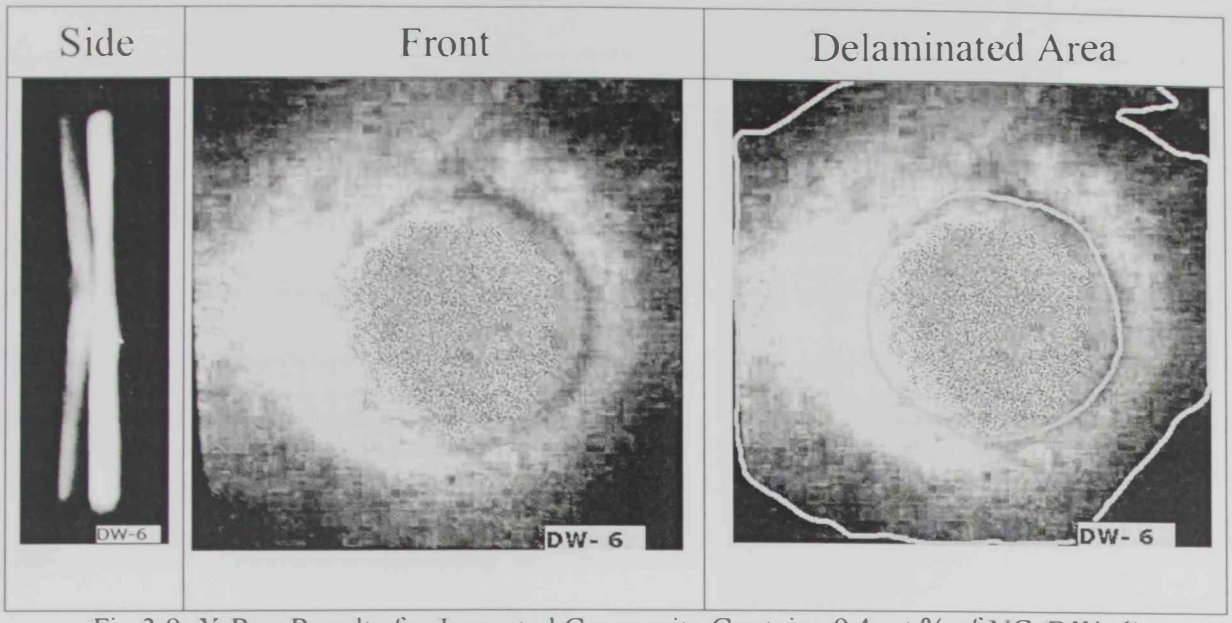

Fig 3.9 X-Ray Results for Impacted Composite Contains 9.4 wt % of NC (DW–6)

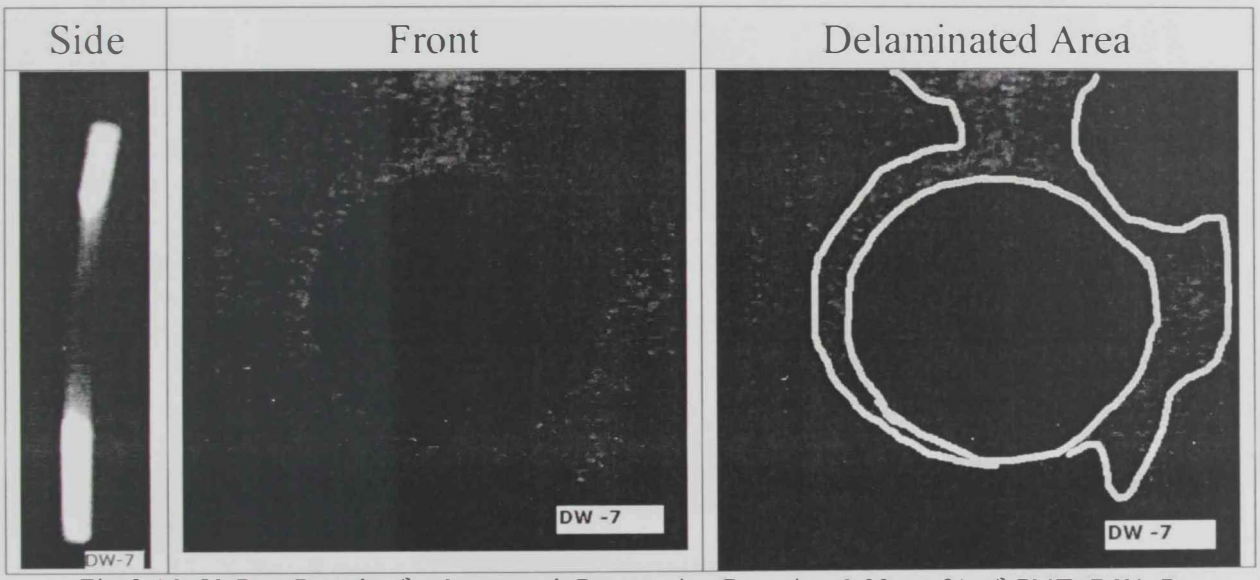

Fig 3.10 X-Ray Results for Impacted Composite Contains 0.32 wt % of CNT (DW–7)

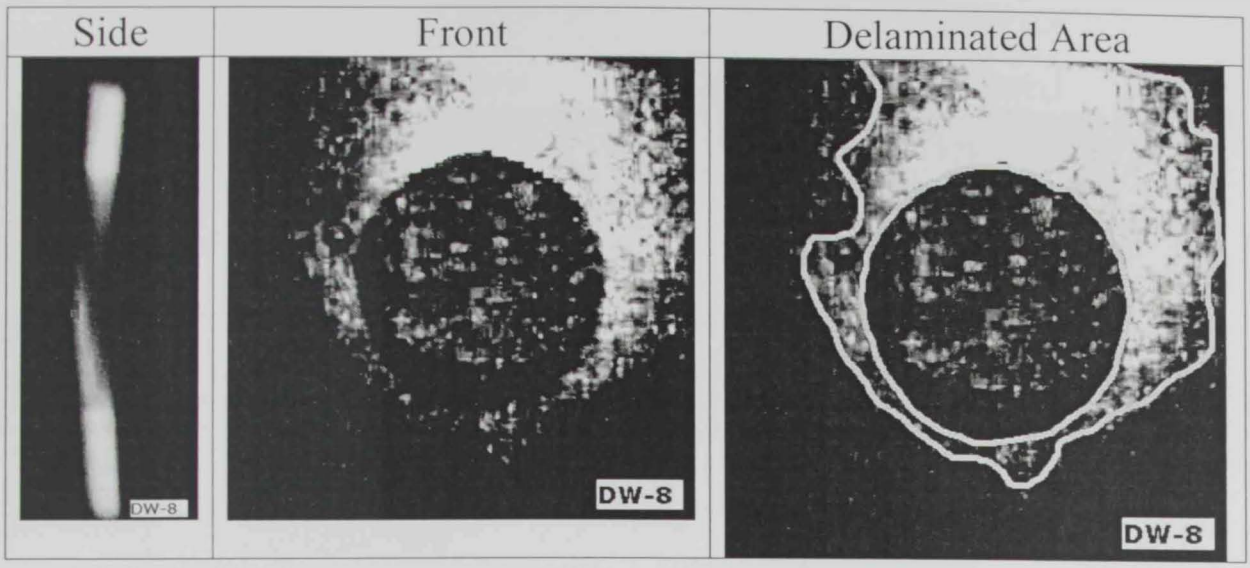

Fig 3.11 X-Ray Results for Impacted Composite Contains 0.80 wt % of CNT (DW–8)

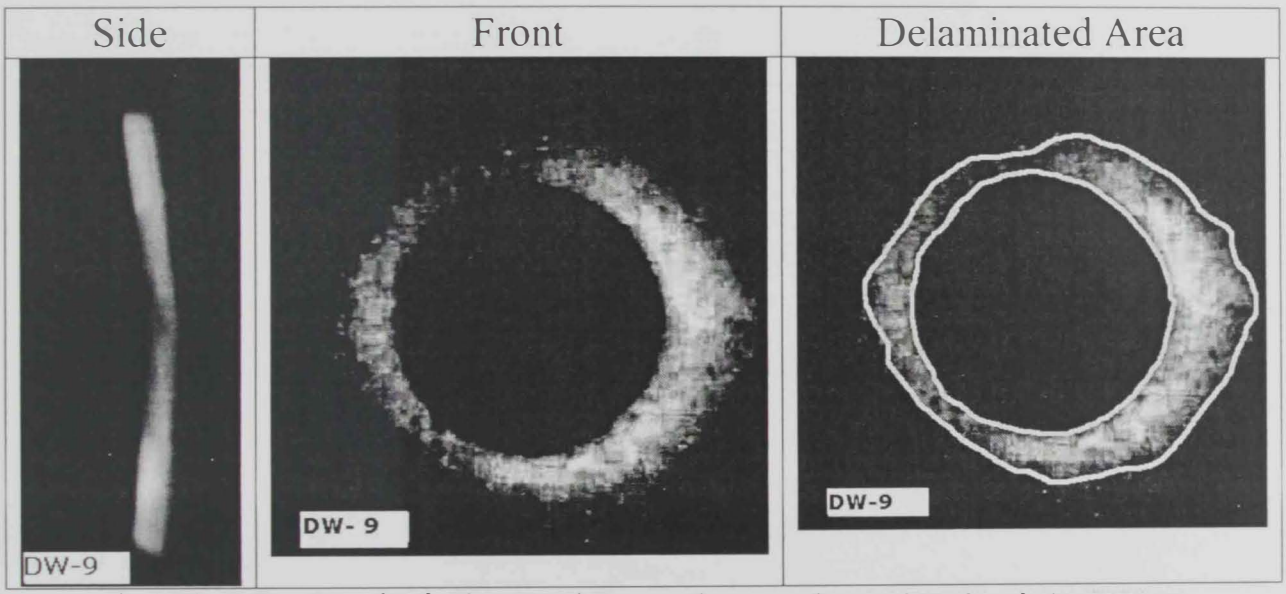

Fig 3.12 X-Ray Results for Impacted Composite Contains 0.82 wt % of SiC (DW–9)

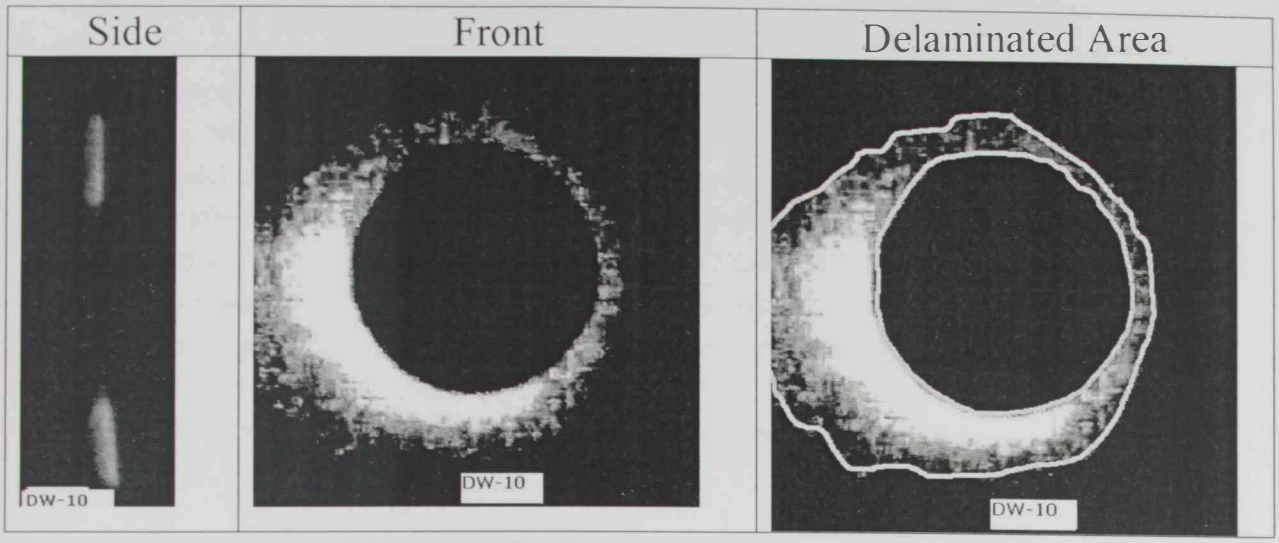

Fig 3.13 X-Ray Results for Impacted Composite Contains 4.25 wt % of SiC (DW–10)

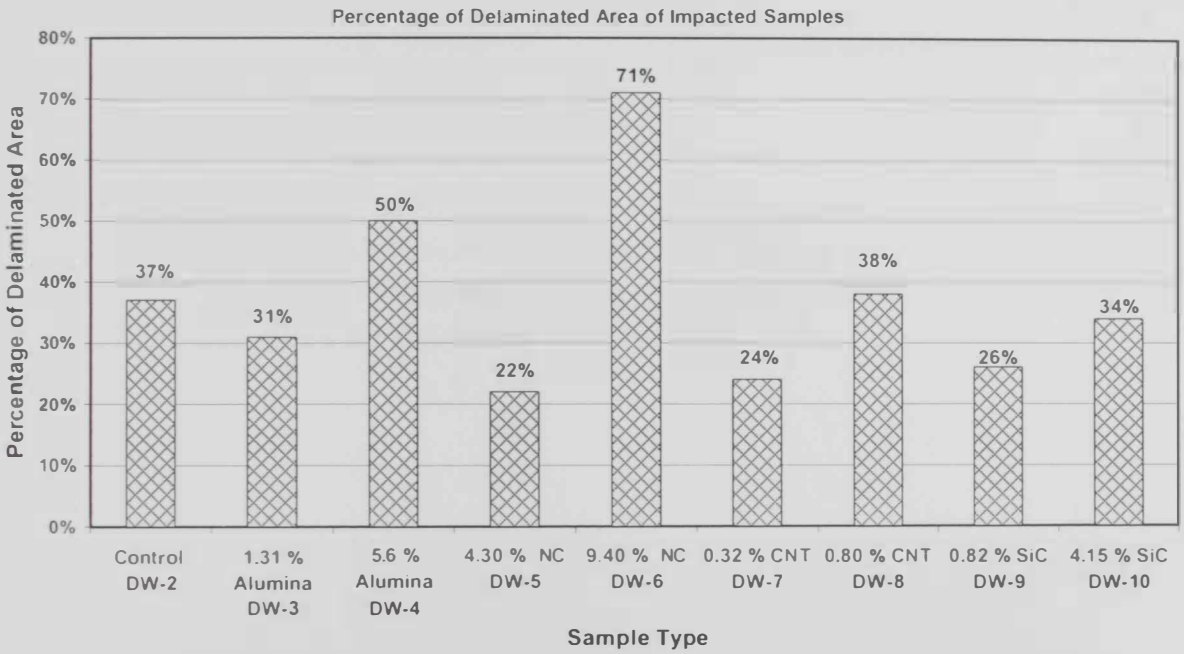

Fig 3.14 Percentage of Delaminated Area of Each Composite (From X-Ray Images).

The control sample show high tendency to delaminate,37% of the sample area was delaminated, the delamination of the control sample started at the circular impacted disk circumference and extended to one of the sample corners. Reinforcement with 1.3 wt% of Alumina didn't show any evidence of delamination by visual inspection, but from the X-ray results we can see decrease in delaminated area to 31%, while enhancement with high percentage of alumina (5.6 wt%) increased the delaminated area to 50% of the total area. Nanoclay with 4.3 wt% played an effective rule in delamination resistance, the delaminated area reduced to 22%. The increase in nanoclay percentage to 9.4 wt % contrary affect the results and almost complete delamination happened, the X-ray results showed that 71% of the total area was deboned. Multi wall carbon nanotubes with 0.32 wt% decreased the delaminated area to 24% while 0.8 wt% didn't change the delaminated percentage neither delaminated places in the control sample. Silicon carbide particles with 0.82 wt % enhanced the delamination resistance to 26% instead of 37% in the control sample, while 4.15 wt % from the same material resulted 34% delamination percentage.

The results revealed enhancement in delamination resistance in all additives at low percentages of additives, while the high percentage aggravated the delamination in all types of additives. The nanoclay with low percentage (4.3 wt%) had shown the best results in delamination resistance.

3.3 Three Point Bending Results of Nanoclay/vinylester composites

3.3.1 Samples Numbering Code

Table 3.12 shows a list NanoClay/ Vinylester samples (NC/VE) that were used in the three point bending test. A three point Bending (TPB) tests were performed for five different percentages of NC/Vinylester samples, two samples for each percentage were casted, Table 3.12 shows the dimensions of each sample.

	Specimen#	Width(mm)	Thickness(mm)	Span(mm)
0% NC	NC/VE 1	16.37	4.4	70
	NC/VE 2	15.61	4.22	67
2% NC	NC/VE 3	14.94	4.32	69
	NC/VE 4	16.28	3.92	66
4.3% NC	NC/VE 5	15.32	4.75	76
	NC/VE 6	16.29	4.63	74
7% NC	NC/VE 7	16.17	4.53	72
	NC/VE 8	16.13	4.65	74
9.4% NC	NC/VE 9	15.18	4.67	74
	NC/VE 10	16.26	5.33	82

Table 3.12 Coding system used to represent our TPB tested samples.

3.3.2 Load Deflection Curves for All Samples

3.3.2.1 Control Sample (0 wt % of NC)

The first set of samples (NC/VE 1 & NC/VE 2) was very important because they represent the control sample which contains vinylester only. The slope of the Load-Deflection curve was approximated by drawing the best fit linear relation, Fig. 3.15 and Fig 3.16. The flexure modulus then was calculated according to the ASTM D790 standard [89]. The calculated flexure modulus was 2.52 GPa & 2.17 GPa for samples NC/VE 1 and NC/VE 2 respectively.

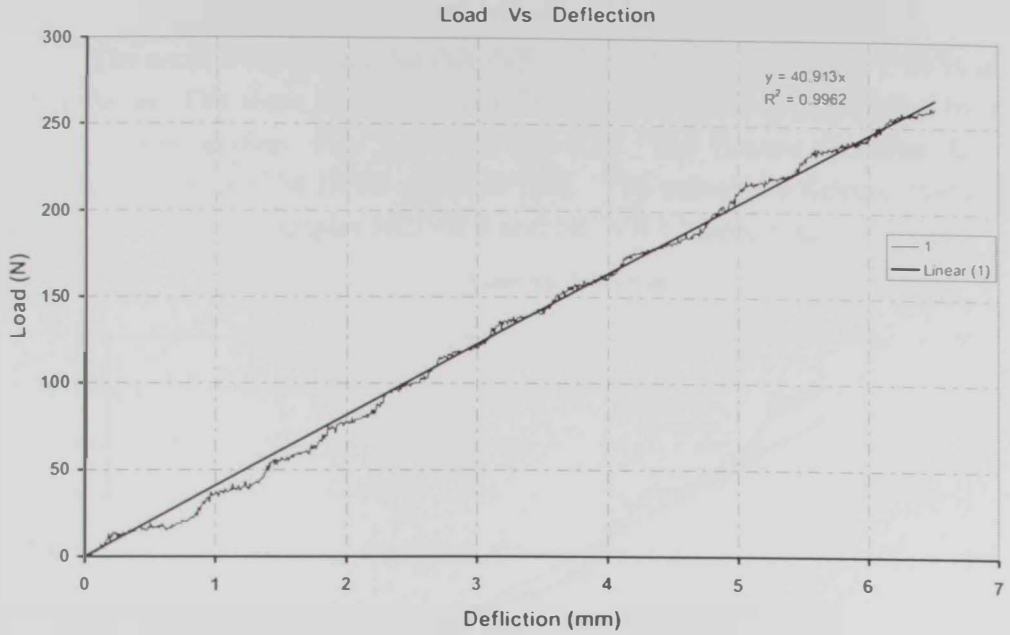

Fig. 3.15 Load – Deflection curve of NC/VE 1

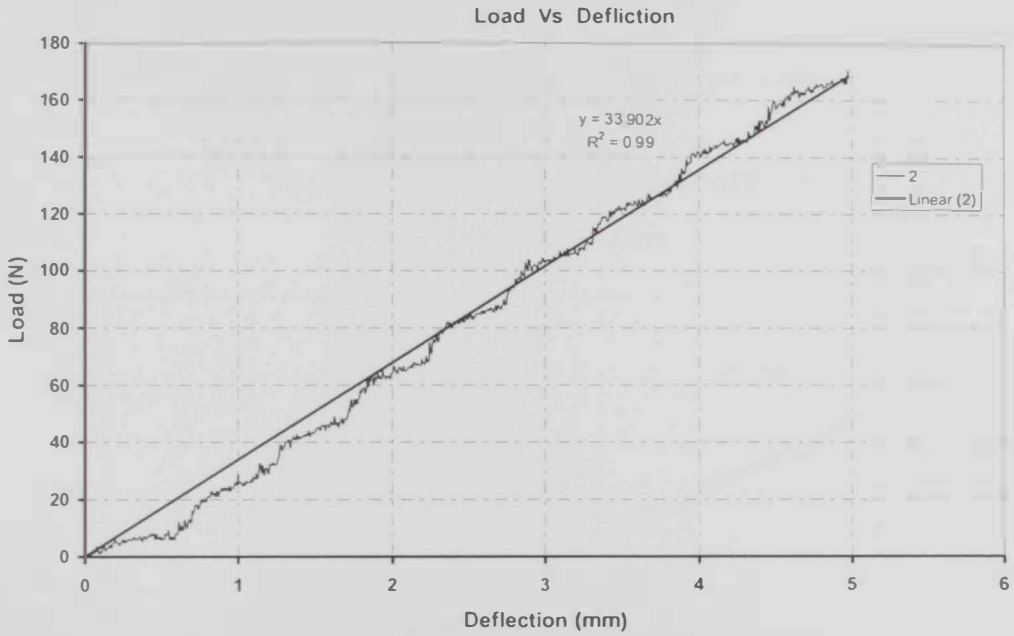

Fig. 3.16 Load – Deflection curve of NC/VE 2

3.3.2.2 Samples with (2 wt % of NC)

The second set of samples (NC/VE 3 & NC/VE 4) represents 2 wt % of NanoClay in Vinylester. The slope of the Load-Deflection curve was approximated by drawing the best fit linear relation, Fig. 3.17 and Fig 3.18. The flexure modulus then calculated according to the ASTM D790 standard [89]. The calculated flexure modulus was 2.46 GPa & 2.70 GPa for samples NC/VE 3 and NC/VE 4 respectively.

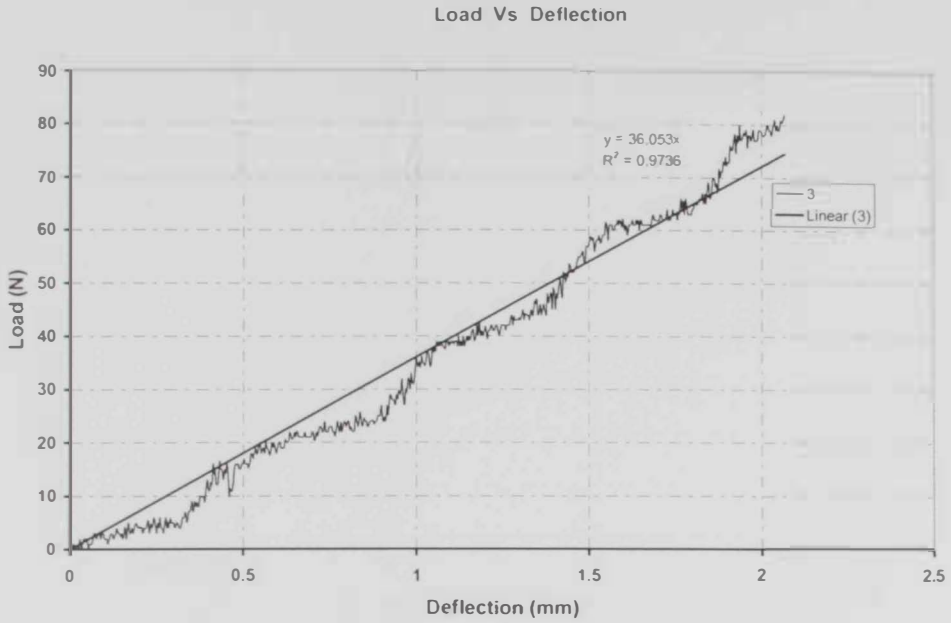

Fig. 3.17 Load – Deflection curve of NC/VE 3

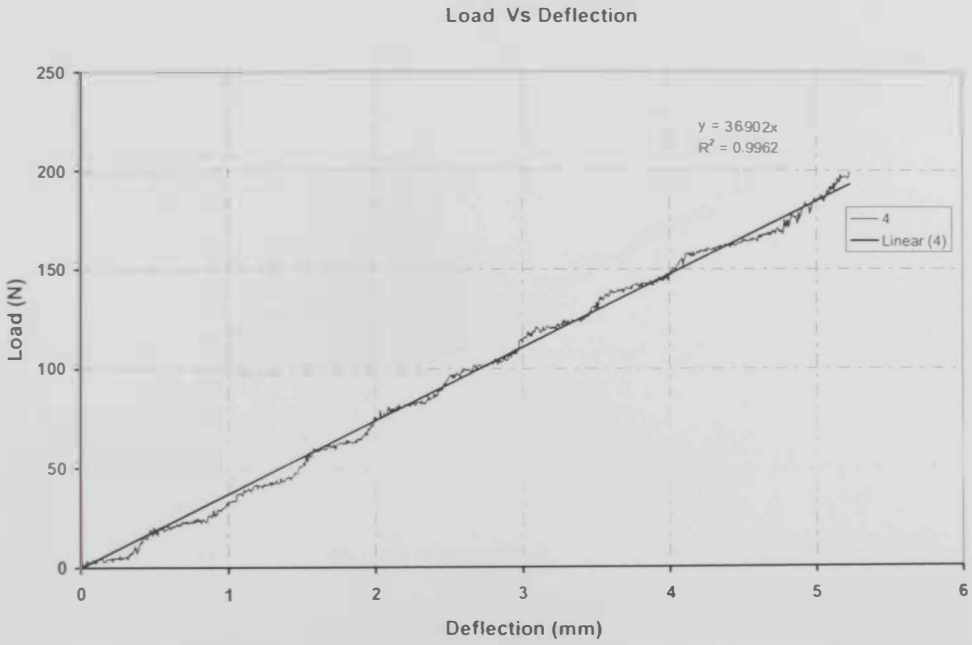

Fig. 3.18 Load – Deflection curve of NC/VE 4

3.3.2.3 Samples with (4.3 wt % of NC)

The third set of samples (NC/VE 5 & NC/VE 6) represents 4.3 wt % of NanoClay in Vinylester. The slope of the Load-Deflection curve was approximated by drawing the best fit linear relation, Fig. 3.19 and Fig 3.20. The flexure modulus then calculated according to the ASTM D790 standard [89]. The calculated flexure modulus was 2.60 GPa & 2.29 GPa for samples NC/VE 5 and NC/VE 6 respectively.

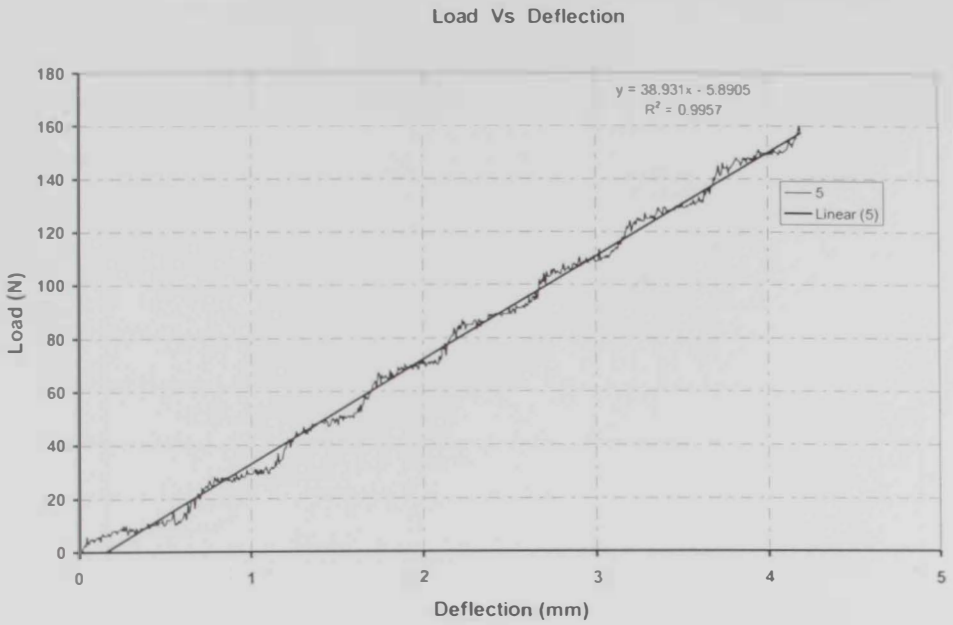

Fig. 3.19 Load – Deflection curve of NC/VE 5

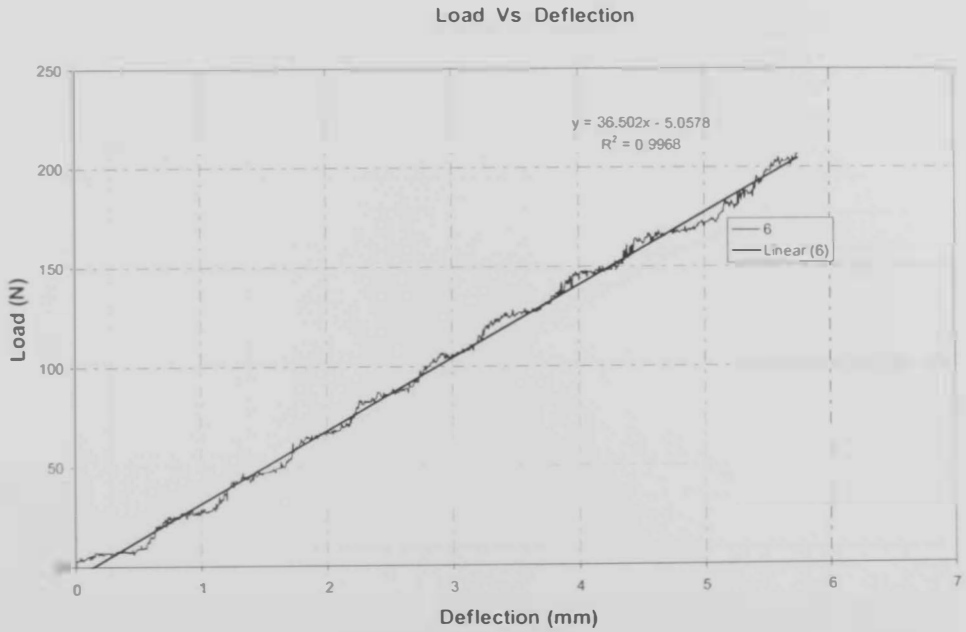

Fig. 3.20 Load – Deflection curve of NC/VE 6

3.3.2.4 Samples with (7.0 wt % of NC)

The fourth set of samples (NC/VE 7 & NC/VE 8) represents 7.0 wt % of Nanoclay in Vinylester. The slope of the Load-Deflection curve was approximated by drawing the best fit linear relation, Fig. Fig. 3.21 and Fig 3.22. The flexure modulus then calculated according to the ASTM D790 standard [89]. The calculated flexure modulus was 2.25 GPa & 2.42 GPa for samples NC/VE 7 and NC/VE 8 respectively.

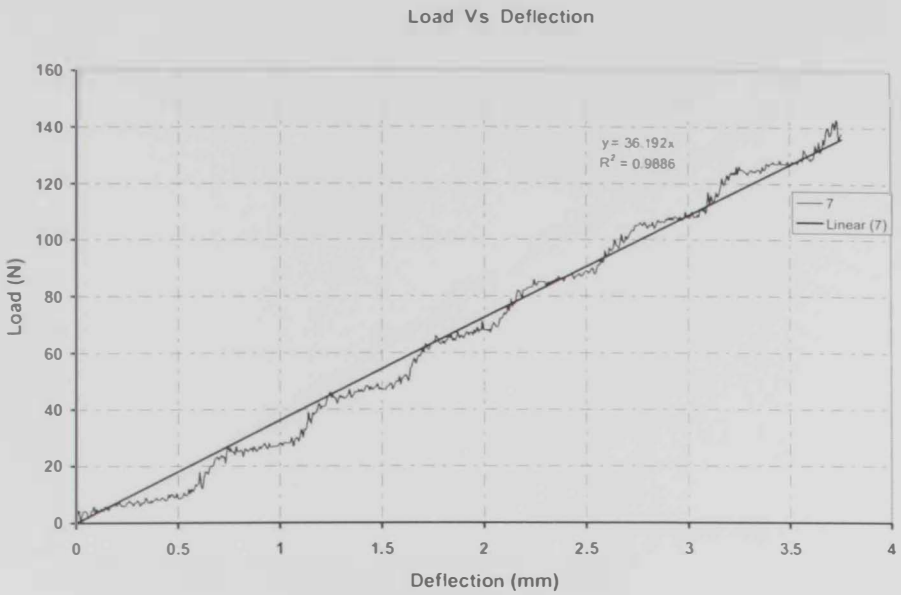

Fig. 3.21 Load – Deflection curve of NC/VE 7

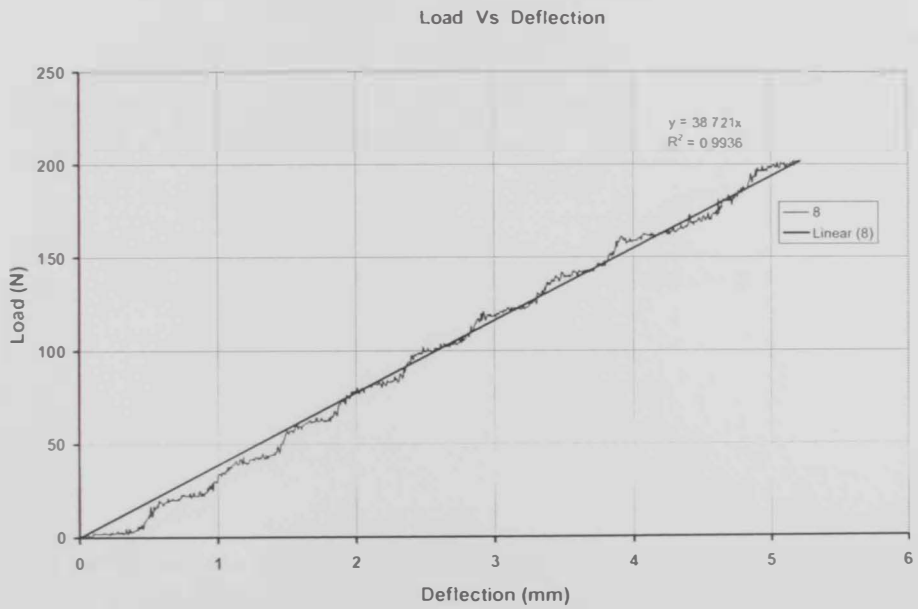

Fig. 3.22 Load – Deflection curve of NC/VE 8

3.3.2.5 Samples with (9.4 wt % of NC)

The last set of samples (NC/VE 9 & NC/VE 10) represents 9.40 wt % of NanoClay in Vinylester. The slope of the Load-Deflection curve was approximated by drawing the best fit linear relation, Fig. 3.23 and Fig 3.24. The flexure modulus then calculated according to the ASTM D790 standard [89]. The calculated flexure modulus was 2.23 GPa & 2.04 GPa for samples NC/VE 9 and NC/VE 10 respectively.

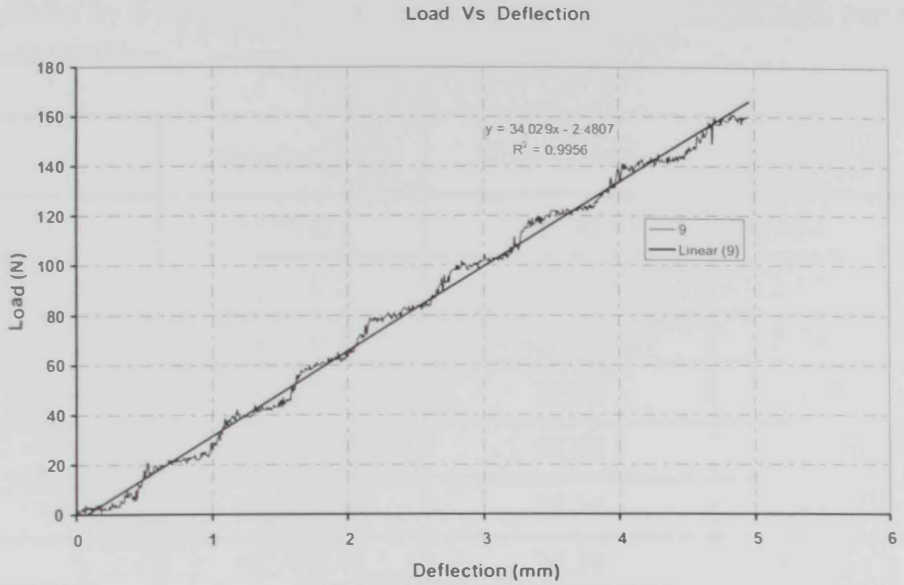

Fig. 3.23 Load – Deflection curve of NC/VE 9

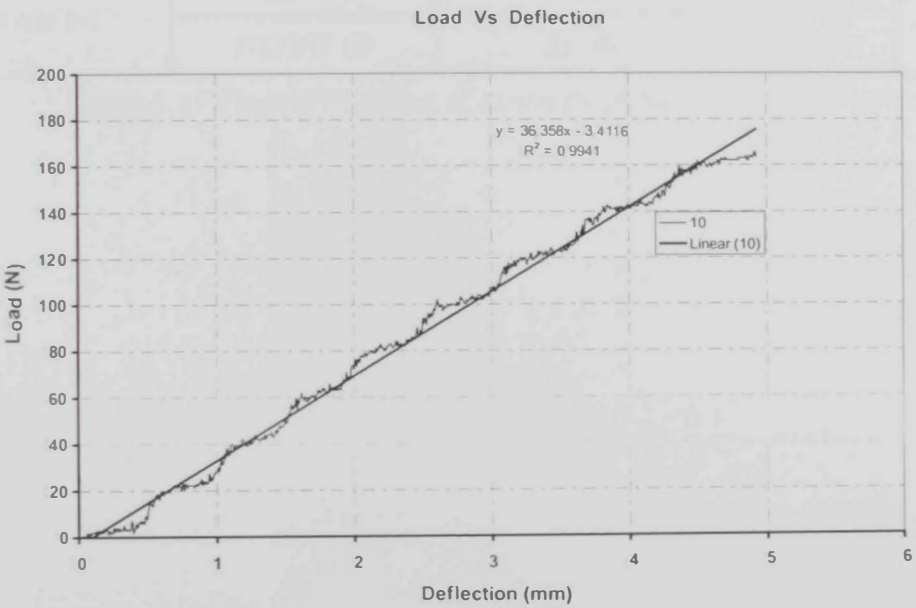

Fig. 3.24 Load – Deflection curve of NC/VE 10

Table 3.13 summarizes all the results of the Nanoclay/Vinelester results, the average of each set of groups was found, the results showed considerable changes in the stiffness of the nanoclay reinforced samples, the 2 % of NC increased the modulus of elasticity by 10 % from 2.34 GPa to 2.58 GPa. The 4.3 % of NC were able to increase the stiffness of the NC/ Vinylester composite by 7.5 % from 2.34 GPa to 2.44 GPa. We can notice that the stiffness don't increase with the increase in the Nanoclay weight percentage, the modulus of elasticity of the samples reinforced with 7 % almost had the same flexure modulus of the control samples. The stiffness of the composites with 9.4 % was reduced by 9 %. Fig. 3.25 describes the effect of Nanoclay weight percentage on the composite stiffness.

	Specimen #	Slope (N/mm)	E (GPa)	E_{avg} (GPa)
0% NC	NC/VE 1	40.91	2.52	2.34
	NC/VE 2	33.90	2.17	
2% NC	NC/VE 3	36.05	2.46	2.58
	NC/VE 4	36.90	2.70	
4.3% NC	NC/VE 5	38.93	2.60	2.44
	NC/VE 6	36.50	2.29	
7% NC	NC/VE 7	36.19	2.25	2.33
	NC/VE 8	38.72	2.42	
9.4% NC	NC/VE 9	34.03	2.23	2.13
	NC/VE 10	36.36	2.04	

Table 3.13 Flexure Modulus of elasticity of NanoClay/ Vinylester Samples.

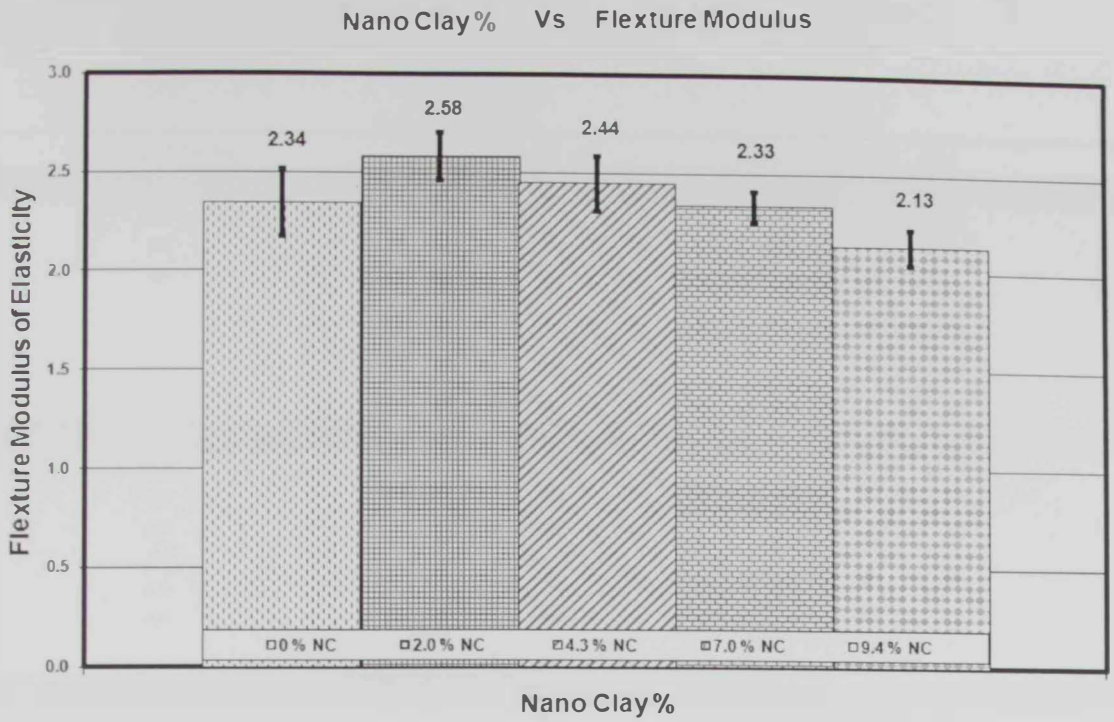

Fig. 3.25 Effect of Nano clay percentage on the Flexture Modulus of Elasticity of Nanoclay/ Vinylester composites.

3.4 Micro Hardness Results of Nanoclay/Vinylester composites.

The Micro Hardness Tests were performed for the different Nanoclay/ Vinylester composite samples, the Vickers micro hardness test results are summarized in the table below.

Table 3.14 summarizes all the results of the Nanoclay/Vinel ester composite, the average of each set of measurements was calculated, the results showed considerable changes in the hardness of the nanoclay reinforced samples, the 2 % of NC increased the Vickers hardness number by 265 % from 16.34 HV to 59.7 HV. The 4.3 % of NC were able to increase the hardness of the NC/ Vinylester composite by 6.4 % from 16.34 HV to 17.39 HV. It can be noticed that the hardness doesn't increase with the increased Nanoclay weight percentage, the Vickers hardness of the samples reinforced with 7 % decreased by 6.5 % from 16.34 HV to 15.27 HV. The hardness of the NC/VE composites with 9.4 % was reduced by 33 %. Fig. 3.26 describes the effect of Nanoclay weight percentage on the composite hardness.

Diagonal (μ m)	Load (g)	HV
0 % NC-VE		
49	25	19.31
56	25	14.78
53	25	16.50
56	25	14.78
58	25	13.78
56	25	14.78
	AVERAGE	**16.34**
2 % NC-VE		
35.6	50	73.16
40	50	57.95
49	100	77.23
59	100	53.27
61	100	49.84
63	100	46.72
	AVERAGE	**59.70**
4.3 % NC-VE		
56.5	25	14.52
56.5	25	14.52
46.5	25	21.44
45.3	25	22.59
45	25	22.89
66.6	25	10.45
67	25	10.33
45.5	25	22.39
	AVERAGE	**17.39**
7 % NC-VE		
56.8	25	14.37
67	25	10.33
58.3	25	13.64
44	25	23.95
56	25	14.78
58	25	13.78
56.5	25	14.52
52.5	25	16.82
	AVERAGE	**15.27**
9.4 % NC-VE		
66	25	10.64
55.8	25	14.89
53.7	25	16.08
102	25	4.46
59.9	25	12.92
59.6	25	13.05
65	25	10.97
98	25	4.83
	AVERAGE	**10.98**

Table 3.14 Vickers Micro Hardness of NanoClay/ Vinylester Samples.

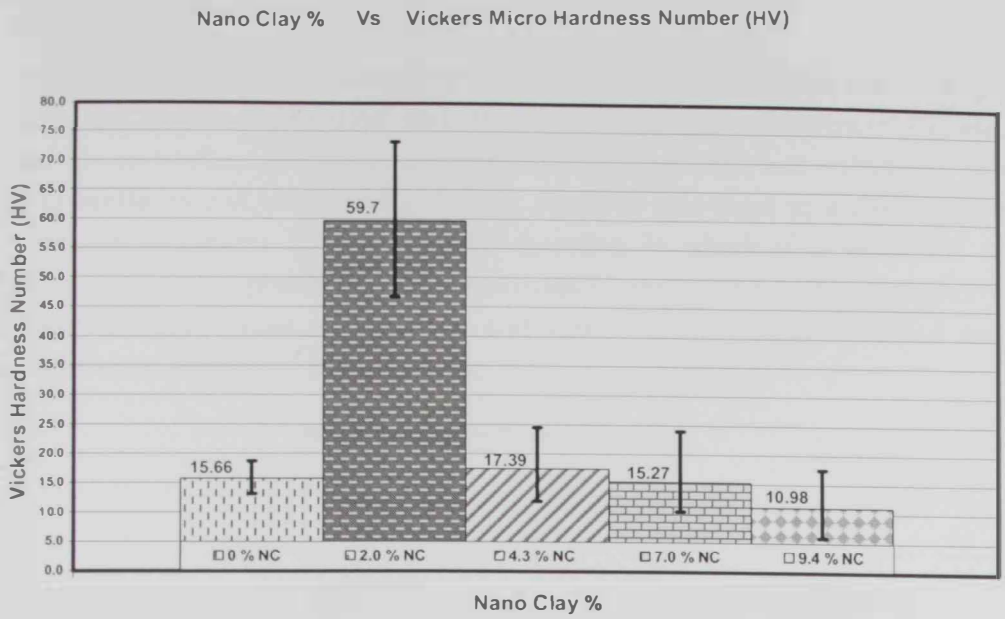

Fig. 3.26 Effect of Nano clay percentage on the Micro Hardness of Nanoclay/ Vinylester composites.

3.5 Nano Indentation Results of Nanoclay/ Vinylester composites.

A Micro Materials Ltd. naoindentation platform was used to measure the following mechanical properties: reduced modulus, elastic modulus and hardness. The results of the tests are shown in Table 3.15.

Sample	Reduced Modulus	Elastic Modulus	Hardness (GPa)	Hardness (HV)
NC-VE-0%	0.76	0.67	0.09	9.26
NC-VE-2%	7.17	6.33	0.54	55.12
NC-VE-4.3%	6.79	5.99	0.31	31.33
NC-VE-7%	7.07	6.24	0.40	40.32
NC-VE-9.4%	8.32	7.35	0.35	35.49

Table 3.15 The mechanical properties of Vinylester/Nanoclay nanocomposites deduced from nanoindentation

The values reported here represent an average of five cycles of loading and unloading curves. The elastic modulus which was obtained from the reduced modulus increased when the clay added to the vinylester which is not the same behavior of the elastic modulus obtained by the three point bend test (Fig. 3.27). Comparing the values of the elastic modulus of the same composite obtained by the two different methods

(Three point bending test and Indentation test) difference were observed with greater values obtained by the indentation test. Possible origins for differences reported by Dasari and his co-workers [100] are: different loading directions and differences in local and bulk crystallinity and crosslinking. Elastic modulus measured in a three point bend test for molded specimens differs from the direction in which it is measured during nanoindentation and the presence of nanoparticles is expected to affect polymer chain mobility and kinetics in their near vicinity and local chemistry at the interface and this will cause different properties from the bulk.

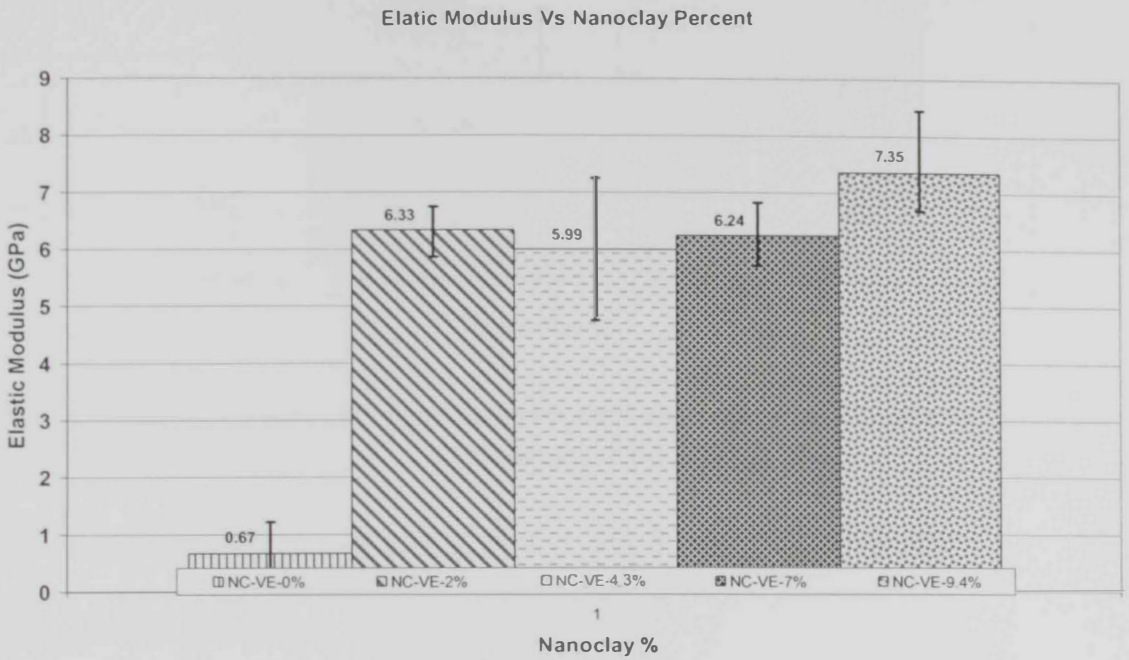

Fig. 3.27 Effect of Nano clay percentage on the Elastic Modulus of Elasticity of Nanoclay/ Vinylester composites deduced by nanoindentation.

Hardness, which quantifies the resistance of a material to plastic deformation, is shown in Figure 3.28 and it increased for nearly all the composites by the addition of the nanoclay. The nanohardness results reported from nanoindentation are close to the microhardness results. In both tests (Micro and Nano Hardness tests), a substantial increase in in hardness noticed at composites contains 2%. The results in both tests are very close to each other (55.12 HV nanohardness) and (59.7 HV microhardness).

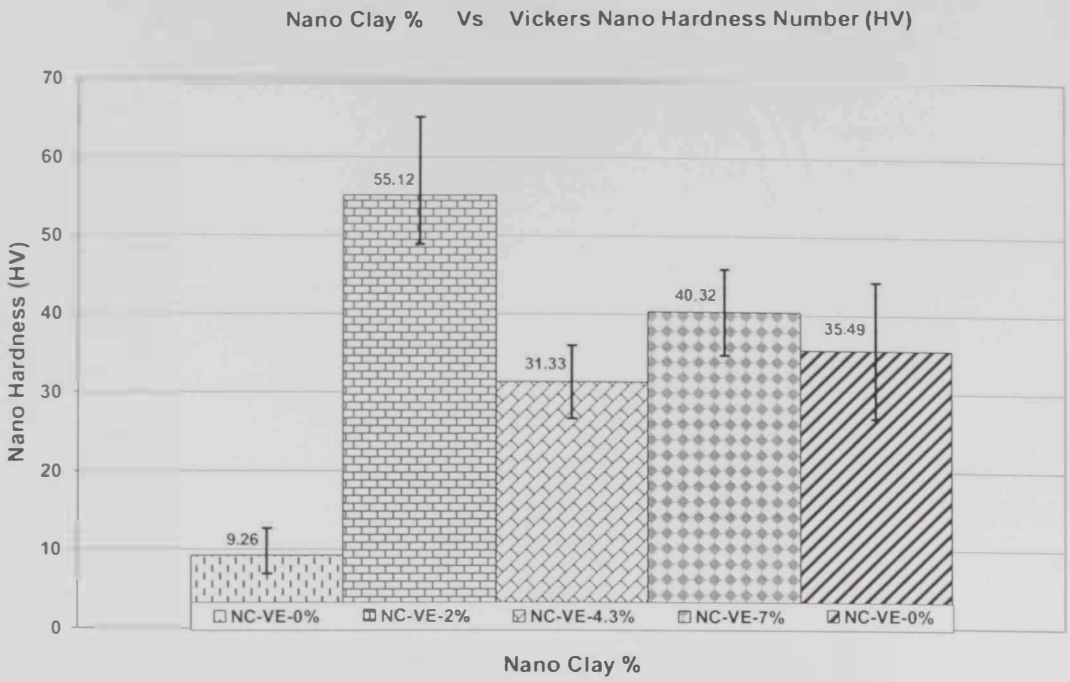

Fig. 3.28 Effect of Nano clay percentage on the Nano Hardness of Nanoclay/ Vinylester composites.

3.6 Thermal Analysis Results of Nanoclay/ Vinylester composites.

3.6.1 Thermal Gravimetric Analysis (TGA) Results

Figures 3.29 and 3.30 show the TGA results of all samples, the onset slope method used to evaluate the exact value of decomposition temperature. The Decomposition temperature of pure vinylester found to be 437°C, while 2% of nanoclay addition to the vinylester resin increase the decomposition temperature by 8°C to 445°C, almost each addition of nanoclay to the vinylester/nanoclay nanocomposite increased the decomposition temperature, addition of 4.3% of nanoclay raised the decomposition temperature by 23°C to 460°C. Addition of 7% and 9.4% increase the decomposition temperature to 468°C and 466°C respectively. The increase in the decomposition temperature is expected due to the cross linking effect of nanoclay.

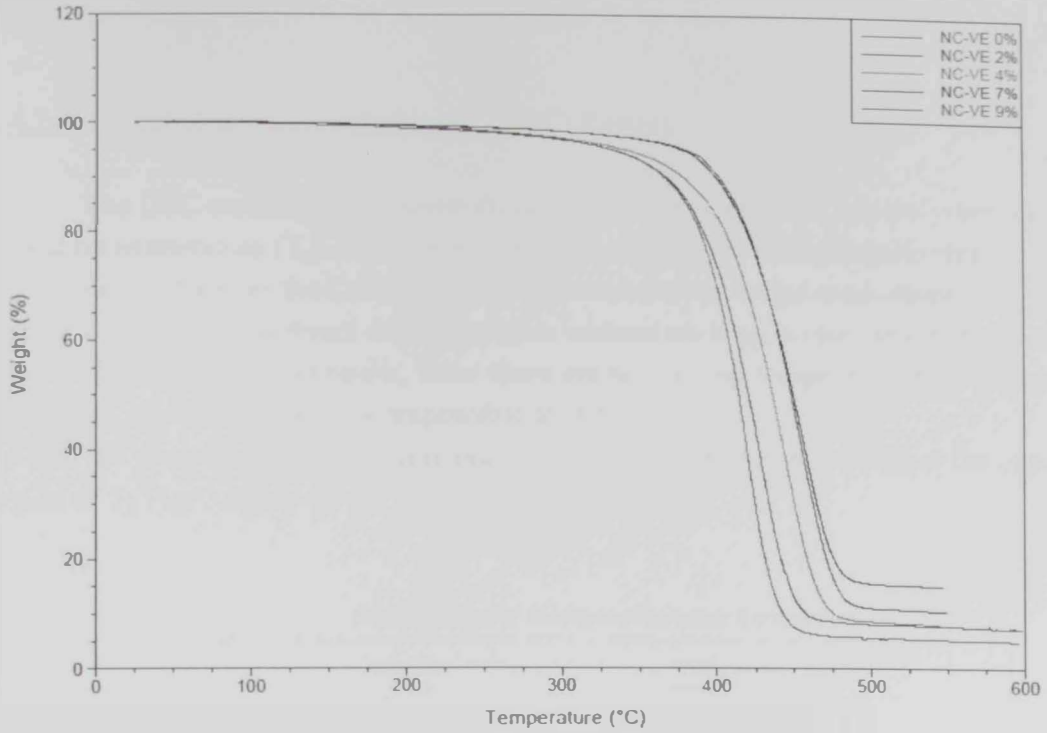

Fig. 3.29 TGA Results of NC-VE-All Results

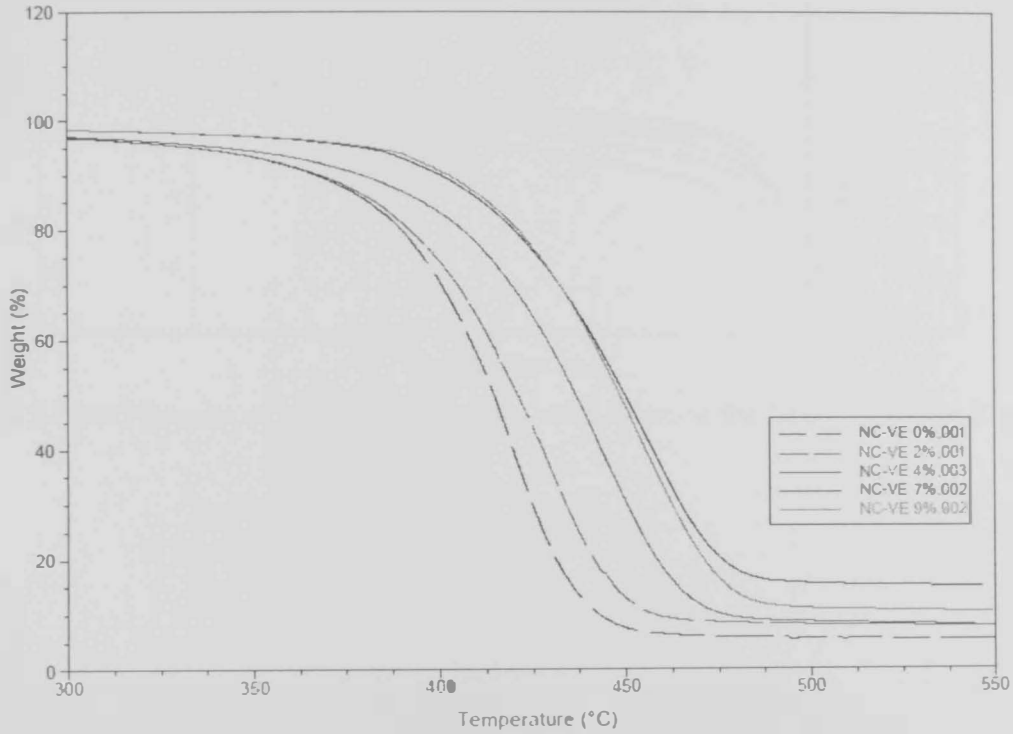

Fig. 3.30 TGA Results of NC-VE-All Results with Zoom at the Decomposition Region

3.6.2 Differential scanning calorimetry (DSC) Results

The DSC results usually show all the thermal properties of any polymer (Glass transition temperature (T_g), melting temperature, decomposition, crystallinity).

Fig.3.31 shows the DSC results of the nanocla/vinylester nanocomposites, the composite experienced direct decomposition without melting, so no melting temperature were defined for each composite, since there are no melting temperature for this type of composite, crystallinity will be impossible to define.

To find the glass transmission temperature, the results data were zoomed at the expected region of T_g Fig. 3.32).

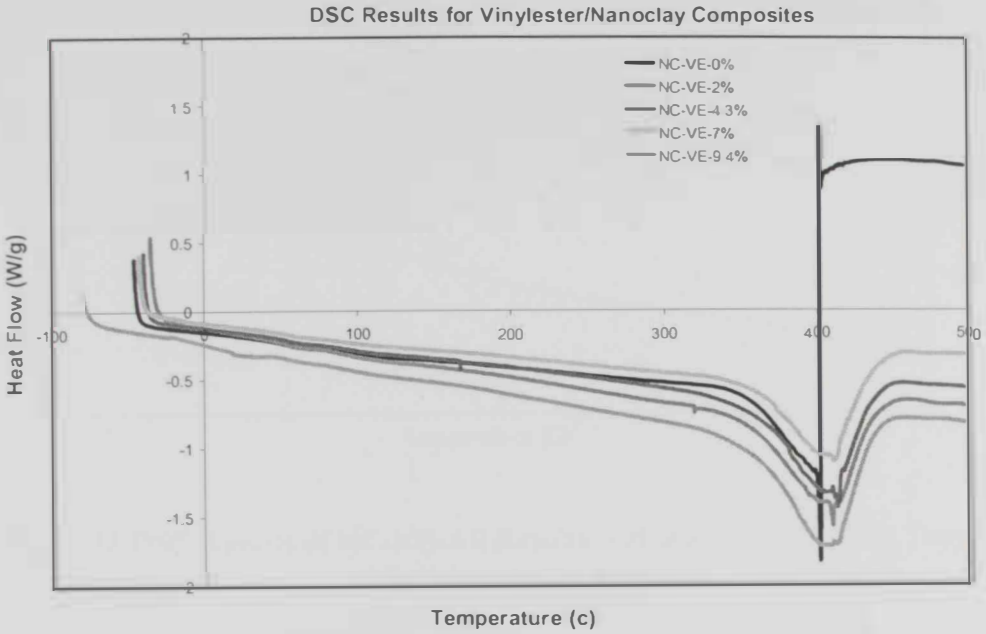

Fig. 3.31 DSC Results of NC-VE-All Results with Zoom at the Decomposition Region

The glass transition temperature for pure vinylester was 56.5°C, while addition of 2%, 4.3%, 7% and 9.4% change the glass transition temperature to 56.5°C, 53.8°C, 55.4°C and 56.8°C respectively. The results show very small variation in the glass transition temperature for all composites. Also we can notice broadening in the glass transition temperature, this is maybe indicate the cross linking effect of nanoclay.

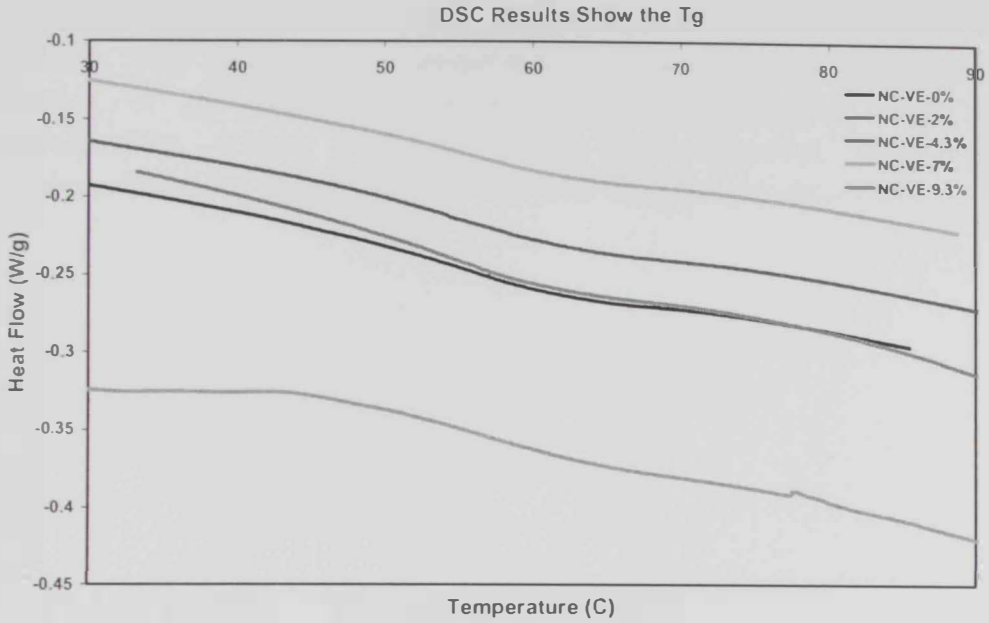

Fig. 3.32 DSC Results of NC-VE-All Results with Zoom at the Glass Transition Temperature (T_g) Region

3.7 Summary

Aluminum Oxide particles added to the matrix of Kevlar/ Vinylester composites in low percentage enhanced the interlaminar shear strength of the composite. With high percentage, it enhanced the composite energy absorption capacity but decreases the interlaminar shear strength. Nanoclay with 4.3 wt % was able to increase both the energy absorption of the Kevlar composite up to a very good level (one third of the composite were fractured only) and no delamination occurred. Nanoclay of 9.4 wt % improved the energy absorption capacity in excellent way but the composite showed tendency to delaminate during testing. Carbon nanotubes enhanced the interlaminar shear strength of the composite, but it didn't contribute to the energy absorption capacity. Silicon Carbide in low percentage enhanced the bonding between fiber and matrix phases, and with high percentage it enhanced the composite energy absorption capacity (one third of the

composite were fractured only), and against other types of additives the enhancement in energy resistance wasn't on the expense of the delamination resistance.

The Nanoclay addition to the Vinylester resulted a considerable change in the stiffness of the nanoclay reinforced samples, the best percentage was the 2 % of NC, it was able to increase the modulus of elasticity by 10 %. The Micro Hardness showed that the 2 % of NC was the best percentage and it increased the hardness of the vinylester by 265 %. The nanohardness response of the different nanoclay percents was similar to the microhardness results, the 2 % of nanoclay was the best percent to enhance the composite hardness. The Decomposition temperature of pure vinylester was increased by the addition of the nanoclay. The vinylester nanocomposites experienced direct decomposition without melting. The glass transition temperature of the vinylester/Nanoclay composite didn't affect by the nanoclay percentage.

Chapter 4

FINITE ELEMENT ANALYSIS

CHAPTER 4

FINITE ELEMENT ANALYSIS

The aim of this research study is to characterize the behavior of laminated woven Kevlar composites structures containing different additives under low-speed impact. In this chapter a presentation on the analysis of the structure using the nonlinear finite element method is presented. In such a FE-analysis it is possible to have better control over the varied parameters compared with experimental tests and consequently it is easier to draw conclusions. Furthermore, FE-analyses give the opportunity to study the structure more thoroughly because of the larger amount of results that can be analyzed. Hence, FE-analyses give the possibility to understand how a parameter affects the results. This means that the need for experiments can be greatly reduced by using the finite element method. However, the experiments are still needed to verify that the FE-analyses correspond to the actual behavior. Accordingly, when experiments and non-linear finite element analyses are used together they can become very powerful tool in gaining a better understanding of the dynamic response of composite samples.

The composite samples in this study were analyzed by using the finite element program ABAQUS/Explicit 6.8. The main topics of interest were the stress distribution in the composite samples; the ability of the impactor to penetrate the composite samples; and the expected failure mode in these samples. In order to study these phenomena a two-dimensional non-linear finite element model was established.

4.1 FINITE ELEMENT MODELING

4.1.1 Introduction to FEM

In the finite element method, a structure is broken down into many small simple blocks or elements. The behavior of an individual element can be described with a relatively simple set of equations. Just as the set of elements would be joined together to build the whole structure, the equations describing the behaviors of the individual elements are joined into an extremely large set of equations that describe the behavior of the whole structure. The computer can solve this large set of simultaneous equations. From the solution, the computer extracts the behavior of the individual elements. From this, it can get the stress and deflection of all the parts of the structure. The stresses are compared to allowed values of stress for the materials to be used, to see if the structure is strong enough [101].

4.1.2 FEM Software

Realistic finite element method (FEM) problems might consist of up to hundreds of thousands, and even several millions, of elements and nodes, and therefore they are usually solved in practice using commercially available software packages. There are currently a large number of commercial software packages available for solving a wide range of problems: solid and structural mechanics, heat and mass transfer, fluid mechanics, acoustics and multi-physics, which might be static, dynamic, linear and nonlinear. Most of these software packages use the finite element method, or are used in combination with other numerical methods. All these software packages are developed based on similar methodology, with many detailed and fine tuned techniques and schemes [102]. Table 4.1 lists some of the commercially available software packages that use the FEM, Finite Volume Method (FVM) and Boundary Element Method (BEM). The next section (4.1.3) introduces the use of ABAQUS, due to its strong capabilities in dealing with nonlinear problems.

Software package	**Method used**	**Application problem**
ABAQUS	**FEM (implicit, Explicit)**	**Structural analysis, acoustics, thermal analysis, etc.**
I-deas	FEM (implicit)	Structural analyses, acoustics, thermal analysis, etc..
LS-DYNA	FEM (explicit)	Structural dynamic, computational fluid dynamic, fluid- Structural interaction, etc.
Sysnoise	FEM\BEM	Acoustics (frequency domain)
NASTRAN	FEM (implicit)	Structural analysis, acoustics, thermal analysis, etc.
MARC	FEM (implicit)	Structural analysis, acoustics, thermal analysis, etc.
MSC-DYTRAN	FEM+FVM (explicit)	Structural dynamic, computational fluid dynamic, fluid- Structural interaction, etc.
ANSYS	FEM (implicit)	Structural analysis, acoustics, thermal analysis, multi-physics, etc.
ADINA DIANA	FEM (implicit)	Structural dynamic, computational fluid dynamic, fluid- Structural interaction, etc.

Table 4.1. Commercially available software packages [102].

4.1.3 ABAQUS Software

ABAQUS is a powerful finite element software package. It is used in many different engineering fields throughout the world. ABAQUS performs static and/or dynamic analysis and simulation on structures. It can deal with bodies with various loads, temperatures, contacts, impacts, and other environmental conditions. ABAQUS software has many different modules, our analysis carried out using ABAQUS/ Explicit finite element software (version 6.8). There are other modules in the ABAQUS finite element package, including ABAQUS/standard, ABAQUS/Implicit ABAQUS/CAE and ABAQUS/Viewer. ABAQUS/Explicit is mainly used for explicit dynamic analysis. ABAQUS/CAE is an interactive preprocessor that can be used to create finite element models and the associated input file for ABAQUS. ABAQUS/Viewer is a menu-driven interactive post-processor for viewing the results obtained from ABAQUS/Standard and ABAQUS/Explicit. In this research, however, the focus will be on the writing of the ABAQUS/Explicit input file, and ABAQUS/Explicit will from now on just be called ABAQUS.

4.2 ELEMENT TYPES

4.2.1 Kevlar Plates

The material properties in ABAQUS are defined as an embedded property for a proper "section", then the mechanical part will be assigned to this section. After this step, we can consider every geometrical part had been attached to it is material properties. Composite parts need to be assigned with proper section, ABAQUS library has specialized section to define "composite shells". This section is capable of defining the material property, the orientation, the thickness and the number of integration points of each layer. Shell section behavior is defined in terms of the response of the shell section to stretching, bending, shear, and torsion. Composite shell sections are composed of layers made of different materials in different orientations. 30-Layers were defined to capture the response of 15 woven Kevlar layers, the 30 layers arranged in [0/90/45/135] symmetrically to replace 15 woven layers arranged in [0/45] orientation, vinylester layers were defined between Kevlar layers [103]. Shell sections integrated during analysis allow the cross-sectional behavior to be calculated by numerical integration through the shell thickness, thus providing complete generality in material modeling. Any number of material points can be defined through the thickness, and the material response can vary from point to point. This type of shell section is generally used with nonlinear material behavior in the section.

4-node doubly curved general-purpose shell, reduced integration S4R element was used to model the two dimensional composite elements, this element capable of capturing the nonlinear response of the Kevlar material, Fig 4.1.

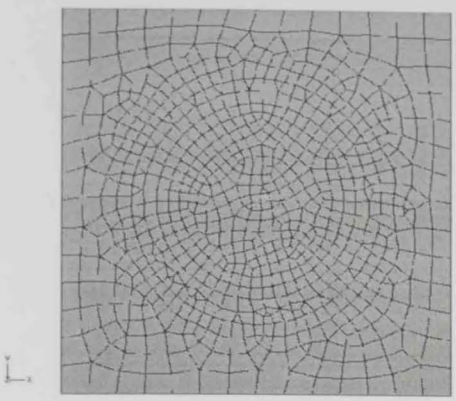

Fig. 4.1 Meshed Kevlar plate

4.2.2 Impactor.

The IMPACTOR didn't show any deformation during the experimental tests, because of this it is logical to model the impactor with rigid elements. Rigid elements can be used to define the surfaces of rigid bodies for contact. ABAQUS doesn't need to define material type or element type for rigid bodies, and we still can simulate a rigid projectile penetrating meshed area with nodes.

4.3 MATERIAL PROPERTIES

4.3.1 Kevlar

4.3.1.1 Composite Mechanical Properties:

Kevlar has orthotropic elastic properties [45], Linear elasticity in an orthotropic material is most easily defined in ABAQUS by giving the "engineering constants": the three moduli E_1, E_2, E_3; Poisson's ratios ν_{12}, ν_{13}, ν_{23}; and the shear moduli G_{12}, G_{13}, and G_{23} associated with the material's principal directions. These moduli define the elastic compliance according to

$$\begin{Bmatrix} \varepsilon_{11} \\ \varepsilon_{22} \\ \varepsilon_{33} \\ \gamma_{12} \\ \gamma_{13} \\ \gamma_{23} \end{Bmatrix} = \begin{bmatrix} 1/E_1 & -\nu_{21}/E_2 & -\nu_{31}/E_3 & 0 & 0 & 0 \\ -\nu_{12}/E_1 & 1/E_2 & -\nu_{32}/E_3 & 0 & 0 & 0 \\ -\nu_{13}/E_1 & -\nu_{23}/E_2 & 1/E_3 & 0 & 0 & 0 \\ 0 & 0 & 0 & 1/G_{12} & 0 & 0 \\ 0 & 0 & 0 & 0 & 1/G_{13} & 0 \\ 0 & 0 & 0 & 0 & 0 & 1/G_{23} \end{bmatrix} \begin{Bmatrix} \sigma_{11} \\ \sigma_{22} \\ \sigma_{33} \\ \sigma_{12} \\ \sigma_{13} \\ \sigma_{23} \end{Bmatrix}$$

The quantity ν_{ij} has the physical interpretation of the Poisson's ratio that characterizes the transverse strain in the *j*-direction, when the material is stressed in *i*-direction. In general, ν_{ij} is not equal to ν_{ji}: they are related by

$$\nu_{ij}/E_i = \nu_{ji}/E_j$$

The engineering constants can also be given as functions of temperature and other predefined fields, if necessary (ABAQUS).

The following mechanical properties were used for Kevlar 49:

E_1 = 129.6 GPa. E_2 = 2.49 GPa E_3 = 2.49 GPa ν_{12} = 0.35 GPa

ν_{13} = 0.35 GPa ν_{23} = 0.31 GPa G_{12} = 2.01 GPa G_{13} = 2.01 GPa

G_{23} = 2.01 GPa [104].

While fro vinylester they were E =2.34 GPa & υ = 0.33 [104].

4.3.1.2 Composite Failure Criteria:

4.3.1.2.1 Damage Initiation:

Damage initiation refers to the onset of degradation at a material point. In Abaqus the damage initiation criteria for fiber- reinforced composites are based on Hashin's theory (Hashin and Rotem [105] and Hashin [106]). These criteria consider four different damage initiation mechanisms: fiber tension, fiber compression, matrix tension, and matrix compression.

The initiation criteria have the following general forms:

Fiber tension: $(\hat{\sigma}_{11} \geq 0)$

$$F_F^T = \left(\frac{\hat{\sigma}_{11}}{X^T}\right)^2 + \alpha\left(\frac{\hat{T}_{12}}{S^L}\right)^2$$

Fiber compression $(\hat{\sigma}_{11} \angle 0)$

$$F_F^C = \left(\frac{\hat{\sigma}_{11}}{X^C}\right)^2.$$

Matrix tension $(\hat{\sigma}_{22} \geq 0)$:

$$F_M^T = \left(\frac{\hat{\sigma}_{22}}{Y^T}\right)^2 + \left(\frac{\hat{T}^{12}}{S^L}\right)^2$$

Matrix compression $(\hat{\sigma}_{22} < 0)$

$$F_M^C = \left(\frac{\hat{\sigma}_{22}}{2S^T}\right)^2 + \left[\left(\frac{Y^C}{2S^T}\right)^2 - 1\right]\frac{\hat{\sigma}_{22}}{Y_C} + \left(\frac{\hat{T}_{12}}{S^L}\right)^2$$

In the above equations

X^T Denotes the longitudinal tensile strength;

X^C Denotes the longitudinal compressive strength;

Y^T Denotes the transverse tensile strength;

Y^C Denotes the transverse compressive strength;

S^L Denotes the longitudinal shear strength;

S^T Denotes the transverse shear strength;

The following strength properties were defined for Kevlar fiber

X^T (Longitudinal tensile strength) = 3800 MPa.

X^C (Longitudinal compressive strength) = 3800 MPa.

Y^T (Transverse tensile strength) = 3200 MPa.

Y^C (Transverse compressive strength) = 3200 MPa.

S^{L} (Longitudinal shear strength) = 1700 MPa.

S^{T} (Transverse shear strength) =1700 MPa. [83]

α is a coefficient that determines the contribution of the shear stress to the fiber tensile initiation criterion; and

$\hat{\sigma}_{11}$, $\hat{\sigma}_{22}$, τ_{12} Are components of the effective stress tensor $\hat{\sigma}$, that is used to evaluate the initiation criteria and which is computed from:

$\hat{\sigma} = M\sigma$, Where σ is the nominal stress and M is the damage operator:

$$\mathbf{M} = \begin{bmatrix} \frac{1}{(1-d_f)} & 0 & 0 \\ 0 & \frac{1}{(1-d_m)} & 0 \\ 0 & 0 & \frac{1}{(1-d_s)} \end{bmatrix}$$

d_f , d_m , and d_s are internal (damage) variables that characterize fiber, matrix, and shear damage, which are derived from damage variables d_f^t , d_f^c, d_m^t, and d_m^c, corresponding to the four modes previously discussed, as follows:

$$d_f = \begin{cases} d_f^t & if \quad \hat{\sigma}_{11} \geq 0, \\ d_f^c & if \quad \hat{\sigma}_{11} < 0, \end{cases}$$

$$d_m = \begin{cases} d_m^t & if \quad \hat{\sigma}_{22} \geq 0, \\ d_m^c & if \quad \hat{\sigma}_{22} < 0, \end{cases}$$

$$d_s = 1 - \left(1-d_f^t\right)\left(1-d_f^c\right)\left(1-d_m^t\right)\left(1-d_m^c\right).$$

Prior to any damage initiation and evolution the damage operator, **M**, is equal to the identity matrix, so $\hat{\sigma} = \sigma$. Once damage initiation and evolution has occurred for at least one mode, the damage operator becomes significant in the criteria for damage initiation of other modes. The effective stress, $\hat{\sigma}$, is intended to represent the stress acting over the damaged area that effectively resists the internal forces.

An output variable is associated with each initiation criterion (fiber tension, fiber compression, matrix tension and matrix compression) to indicate whether the criterion has been met. A value of 1.0 or higher indicates that the initiation criterion has been met. If you define a damage initiation model without defining an associated evolution law, the initiation criteria will affect only output. Thus, we can use these criteria to evaluate the propensity of the material to undergo damage without modeling the damage process. In addition to the standard output identifiers available in ABAQUS, the following variables relate specifically to damage initiation at a material point in the fiber-reinforced composite damage model: Maximum value of the fiber tensile initiation criterion experienced during the analysis, the Maximum value of the fiber compressive initiation criterion experienced during the analysis, the Maximum value of the matrix tensile initiation criterion experienced during the analysis and the Maximum value of the matrix compressive initiation criterion experienced during the analysis. For the variables above that indicate whether an initiation criterion in a damage mode has been satisfied or not, a value that is less than 1.0 indicates that the criterion has not been satisfied, while a value of 1.0 or higher indicates that the criterion has been satisfied. If you define a damage evolution model, the maximum value of this variable does not exceed 1.0. However, if you do not define a damage evolution model, this variable can have values higher than 1.0, which indicates by how much the criterion has been exceeded [50].

The damage initiation criteria must be used with elements with a plane stress formulation, which include plane stress, shell, continuum shell, and membrane elements.

4.3.1.2.2 Damage Evaluation:

The damage evolution definition defines how the material degrades after one or more damage initiation criteria are met. Multiple forms of damage evolution may act on a material at the same time—one for each damage initiation criterion that was defined.

We can define damage evolution in term of Displacement or Energy:

- By Displacement damage evolution it is possible to define the damage as a function of the total or the plastic displacement after damage initiation.
- By Energy, evolution damage defined in terms of the energy required for failure (fracture energy) after the initiation of damage.

4.3.2 Impactor

Impactor was defined as a shell rigid part; rigid parts in ABAQUS can't be assigned sections, hence material properties. The rigid part only need to be assigned "Inertia", reference point picked, and mass defined to this reference point.

4.4 GEOMETRY

4.4.1 Kevlar Laminates Geometry:

Kevlar laminates were simulated in two dimensional model see Fig. 4.2. This model considered only the two lateral directions of the plates, the ABAQUS calculated the thickness of the sample be adding the thicknesses of all layers compose the composite sample.
The composite plate has the dimensions (50 mm x 50 mm x 3.1 mm), the thickness was divided evenly over the thirty layers of Kevlar laminates.

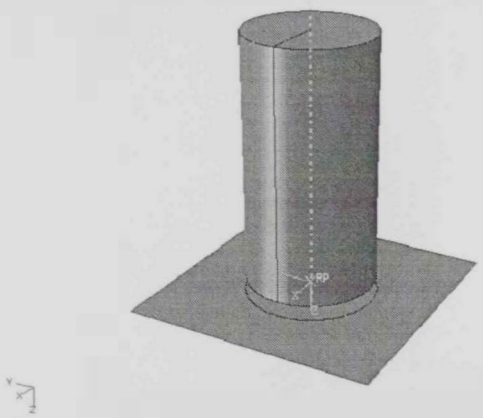

Fig. 4.2 The assembly of the Impactor and the projectile.

4.4.2 Impactor Geometry:

The dimensions of the Impactor were extracted, from the real measurements of the nose that was implemented in the drop-weight apparatus. It is cylindrical nose with 25.4 mm and length of 50 mm, see Fig 4.3.

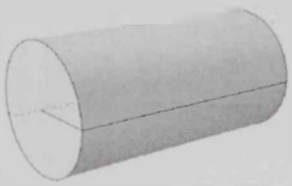

Fig. 4.3 The Impactor

4.5 LOADING AND BOUNDARY CONDITIONS

4.5.1 Boundary Conditions

The boundary conditions (BC's) are one of the main parameters that affect severely the results of any finite element model. The BC's must be close to the real case of any simulated problem. In our model the BC's mimic exactly the experimental procedures, the composite plate was simply supported, by means it is free to move in all directions except the direction of the impactor movement.
The impactor was constrained to move only in the Z-direction see fig 4.4. The constraint movement of the impactor was assigned to the impactor reference point.

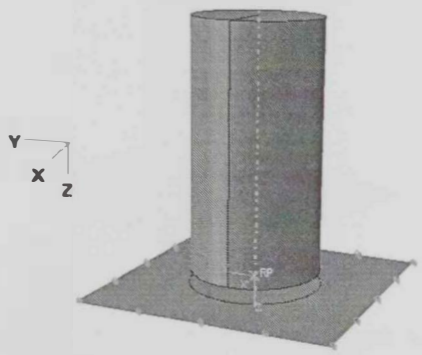

Fig. 4.4 The boundary Conditions of Our Mdel

4.5.2 Load

Load was applied as a contact pressure due to dynamic impact. the impactor hit the plate with a speed 4.1 m/sec. this is the same speed of the drop-weight just about to touch the Kevlar laminates. The solution will complete after 10 milliseconds.

4.5.3 Contact

Abaqus/Explicit provides two algorithms for modeling contact interactions; the general "automatic" contact algorithm allows very simple definitions of contact with very few restrictions on the types of surfaces involved. The contact pair algorithm which has more restrictions on the types of surfaces involved and often requires more careful definition of contact; however, it allows for some interaction behaviors that are not available with the general contact. The general contact and contact pairs algorithms in ABAQUS/Explicit differ by more than the user interface; in general they use completely separate implementations with many key differences in the designs of the numerical algorithms.

A surface-to-surface contact was defined in ABAQUS/Explicit as an alternative to general contact see Fig 4.5, because certain interaction behaviors can't be defined in Abaqus/Explicit by general contact.

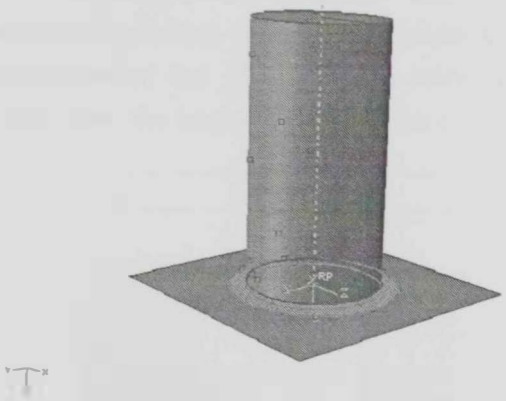

Fig. 4.5 Surface to Surface Contact Algorithm.

4.6 NONLINEAR FINITE ELEMENT ANALYSIS RESULTS

4.6.1 Control Sample

More than four hours were needed to the solution to converge, the results were able to till about the deformed shape, the different stress tensor components, the different strain tensor components, the different stress and strain failure criterion, displacements in all directions, velocity, acceleration, reaction forces, compression pressure and many other parameters.

The shear stress contours in the control sample at the final step was shown in Fig. 4.6. The values of stresses exceeded the interlaminar shear stress, and this means that the delamination between the Kevlar layers will take place during the penetration process.

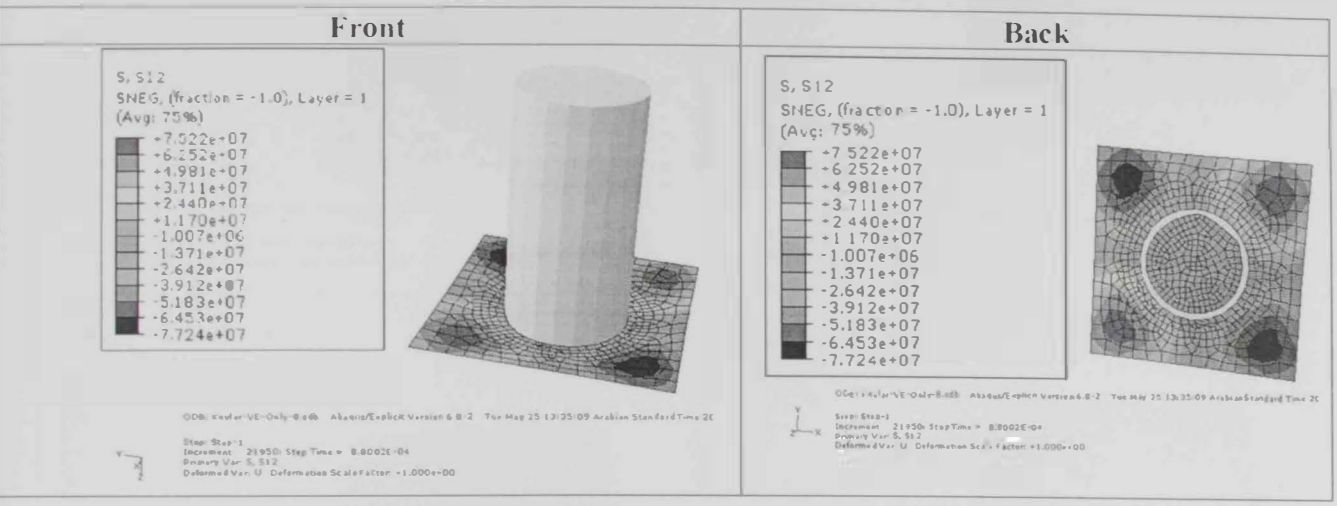

Fig. 4.6 Shear stress σ_{12} in the X-Y direction of the control sample.

Fig. 4.7 shows the Von Mises Stress distribution in the control sample at the final step. The stress level exceeded the fiber fracture strength at the circumference of the contact circle. This will allow the impactor to penetrate the Kevlar layers.

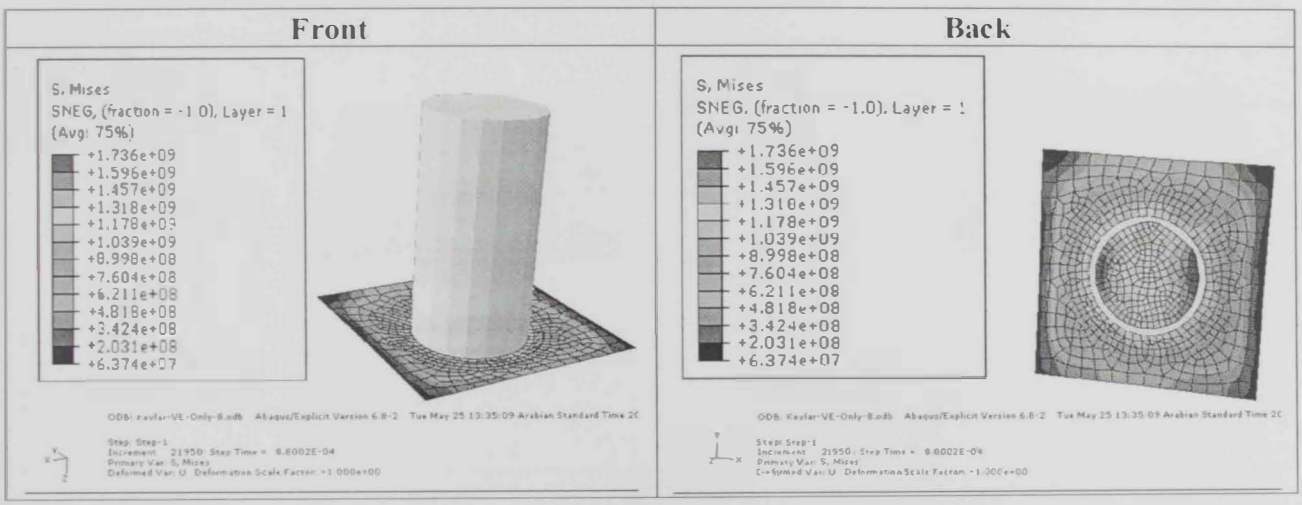

Fig. 4.7 Von mises stress failure criterion of the control sample.

Figure 4.8 describes the changes in stress distribution in the control sample during the impact. Eight stages of penetration were captured at different times. The von mises stresses shown indicate that there were fractured fibers during impact.

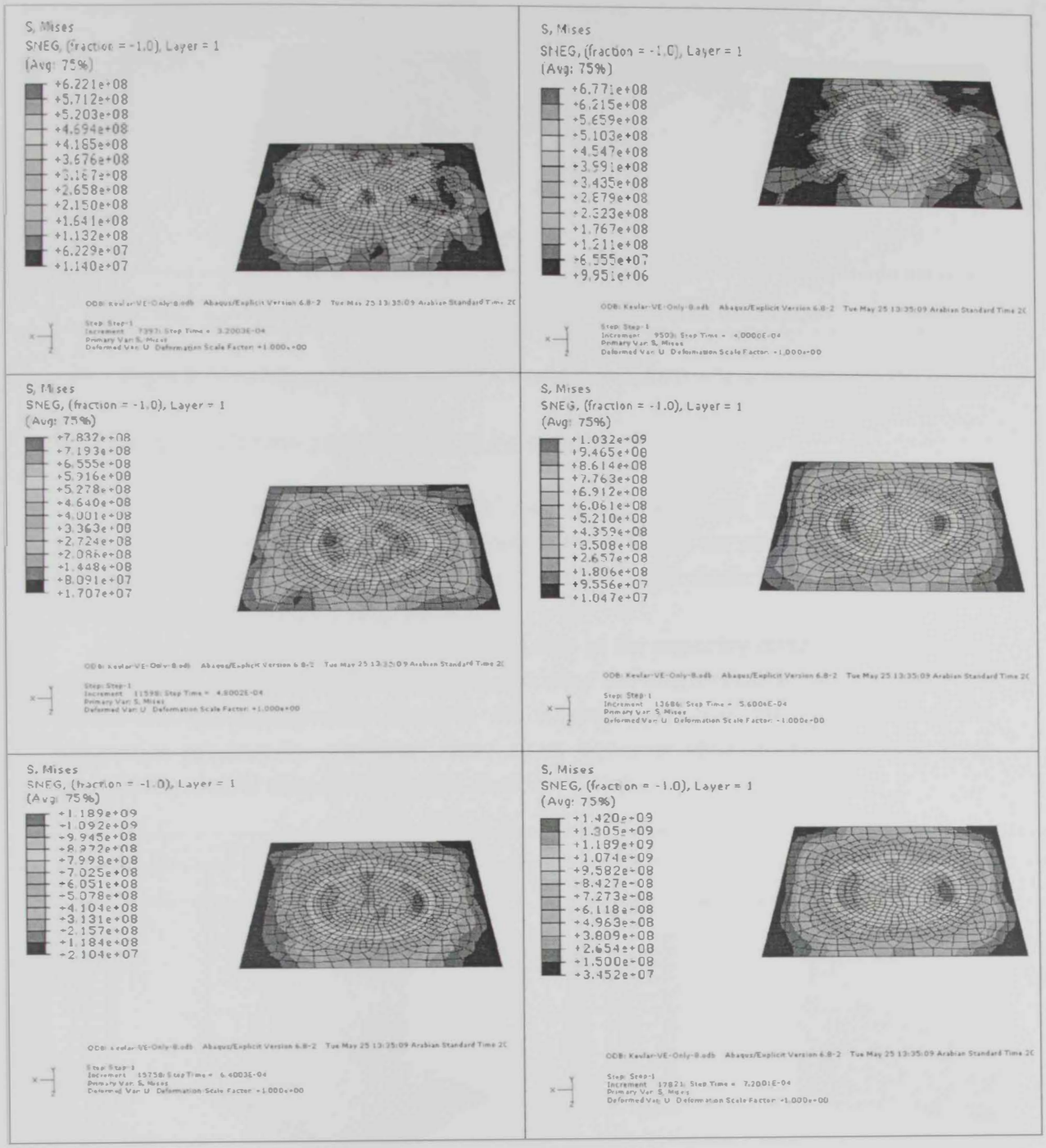
S, Mises
SNEG, (fraction = -1.0), Layer = 1
(Avg: 75%)
+6.221e+08
+5.712e+08
+5.203e+08
+4.694e+08
+4.185e+08
+3.676e+08
+3.167e+08
+2.658e+08
+2.150e+08
+1.641e+08
+1.132e+08
+6.229e+07
+1.140e+07
S, Mises
SNEG, (fraction = -1.0), Layer = 1
(Avg: 75%)
+6.771e+08
+6.215e+08
+5.659e+08
+5.103e+08
+4.547e+08
+3.991e+08
+3.435e+08
+2.879e+08
+2.323e+08
+1.767e+08
+1.211e+08
+6.555e+07
+9.951e+06
S, Mises
SNEG, (fraction = -1.0), Layer = 1
(Avg: 75%)
+7.832e+08
+7.193e+08
+6.555e+08
+5.916e+08
+5.278e+08
+4.640e+08
+4.001e+08
+3.363e+08
+2.724e+08
+2.086e+08
+1.448e+08
+8.091e+07
+1.707e+07
S, Mises
SNEG, (fraction = -1.0), Layer = 1
(Avg: 75%)
+1.032e+09
+9.465e+08
+8.614e+08
+7.763e+08
+6.912e+08
+6.061e+08
+5.210e+08
+4.359e+08
+3.508e+08
+2.657e+08
+1.806e+08
+9.556e+07
+1.047e+07
S, Mises
SNEG, (fraction = -1.0), Layer = 1
(Avg: 75%)
+1.189e+09
+1.092e+09
+9.945e+08
+8.972e+08
+7.998e+08
+7.025e+08
+6.051e+08
+5.078e+08
+4.104e+08
+3.131e+08
+2.157e+08
+1.184e+08
+2.104e+07
S, Mises
SNEG, (fraction = -1.0), Layer = 1
(Avg: 75%)
+1.420e+09
+1.305e+09
+1.189e+09
+1.074e+09
+9.582e+08
+8.427e+08
+7.273e+08
+6.118e+08
+4.963e+08
+3.809e+08
+2.654e+08
+1.500e+08
+3.452e+07

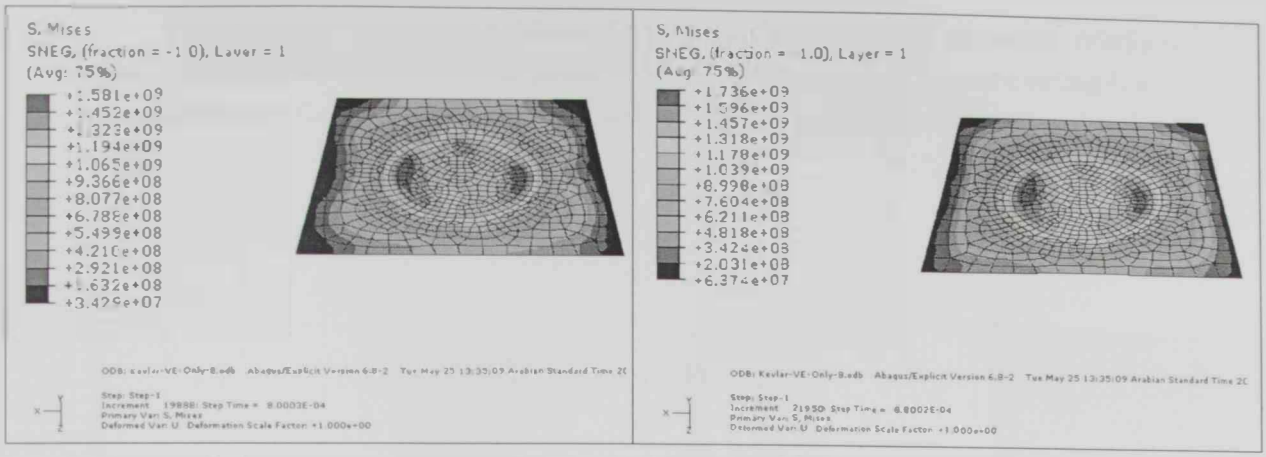

Fig 4.8 Von Mises Results for eight consecutive steps of the control sample.

4.2.2 Sample with nano particles (2 % of Nanoclay)

The only difference between the control sample model and this model is the mechanical properties of the composite matrix, the effect of the nanoclay on the bulk of the composite was modeled by modifying the modulus of elasticity of the matrix to be 2.58 GPa and the Poisson's ratio equal 0.33.

The shear stress contours at the final step in the nanoclay reinforced sample was shown in Fig. 4.9. The values of stresses exceeded the interlaminar shear stress, and this means that the delamination between the Kevlar layers will take place during the penetration process, the maximum shear stress was very close to the maximum shear stress in the control sample at the same time increment.

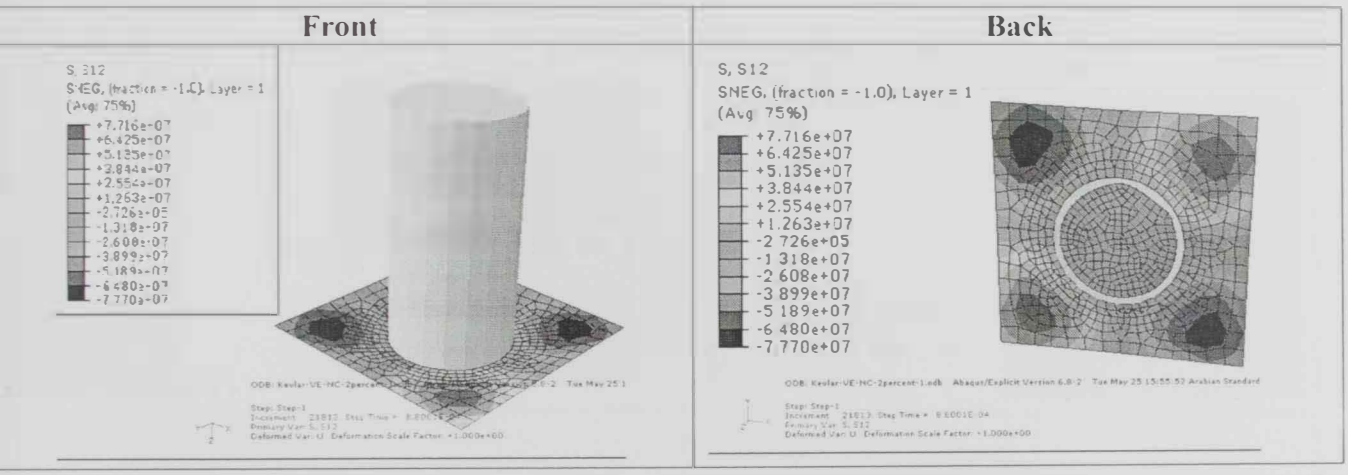

Fig. 4.9 Shear stress σ_{12} in the X-Y direction of nanoclay reinforced sample.

Fig. 4.10 shows the Von Mises Stress distribution in the nanoclay reinforced Kevlar sample at the final step. The stress level exceeded the fiber fracture strength at the circumference of the contact circle. This will allow the impactor to penetrate the Kevlar layers.

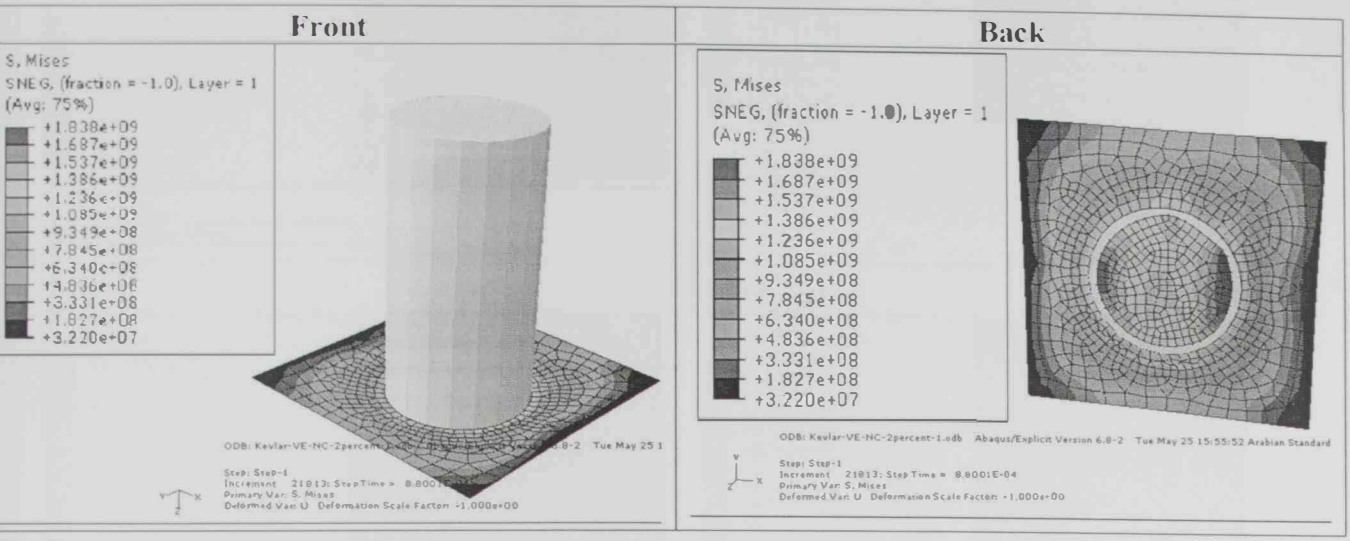

Fig. 4.10 Von mises stress failure criterion of nanoclay reinforced sample.

Figure 4.11 describes the changes in stress distribution in the nanoclay reinforced Kevlar layers during the impact. eight stages of penetration were captured at different times. The von mises stresses shown indicate that there were fractured fibers during impact. The sample failed at the same time increment with negligible change in the von mises stress distribution from the control sample.

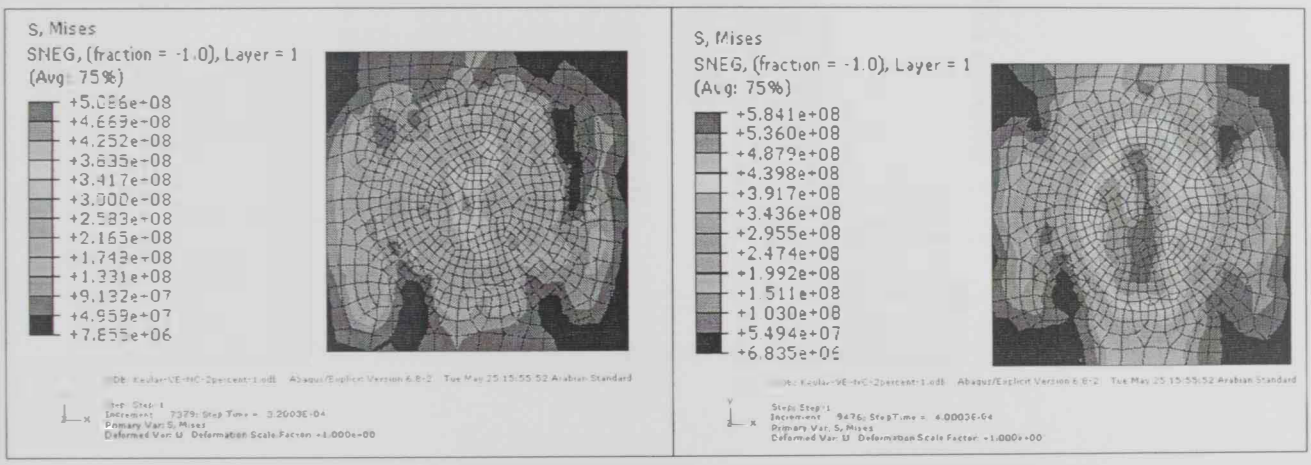

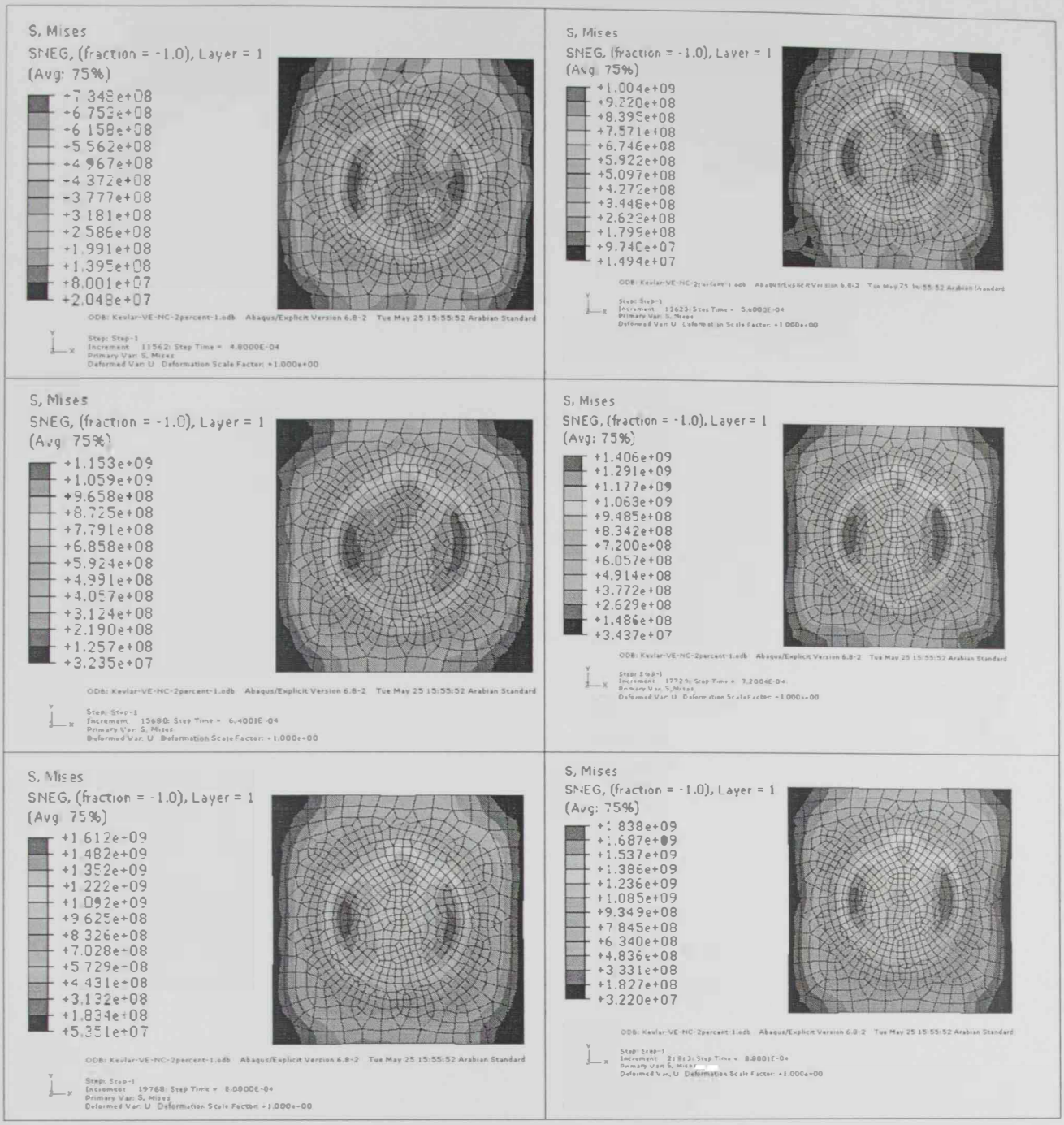

Fig 4.11 Von Mises Results for eight consecutive steps of nanoclay reinforced sample.

Chapter 5

CONCLUSIONS

CHAPTER 5

CONCLUSIONS

The effect of adding small amounts of various fillers on the impact resistance of Kevlar/ Vinylester composites have been studied in this work.

This research study identified methods to optimize the impact resistance of polymeric composites reinforced with laminated woven Kevlar layers. It was demonstrated that the amount of each different additive exerts significant influence over the energy absorption capability of polymer based composites. The factors contribute to the enhancement of the energy absorption and failure modes of composites were described, such as the percentage of each additive and the additive material used.

Aluminum Oxide particles (15 μm) added to the matrix of Kevlar/ Vinylester composites in low percentage (1.31 wt %) enhanced the bonding between fiber and matrix phases, hence the interlaminar strength of the composite. But it had no effect on the composite energy absorption capacity.
Aluminum Oxide particles (15 μm) added to the matrix of Kevlar/ Vinylester composites in high percentage (5.6 wt %) enhanced the composite energy absorption capacity (half of the thickness was fractured), but the interlaminar strength decreased, hence the composite had more tendency to delaminate.

Nano clay Montmorillonite clay, Nanomer I.34TCN contains 25-30 wt. % methyl dihydroxyethyl hydrogenated tallow ammonium were added in two different percentages to the vinylester to manufacture two different sets of samples. The first percentage was 4.30 % wt, and it was able to increase both the energy absorption of the Kevlar composite up to a very good level (one third of the composite were fractured only) and the interlaminar strength.
Nanoclay of 9.4 wt % improved the energy absorption capacity in excellent way (13 % of the composite thickness were fractured only), the composite showed tendency to delaminate during testing even during cutting and sample preparations.

Composites samples contained Carbon nanotubes consumed long time to prepare the samples, it needs to be mixed with methanol, also it needs sonication for better mixing with polymer. CNT's has magnetic properties that cause accumulation of CNT's if they used in high percentage, these accumulations works as stress concentration regions and it cause early failure in the nanocompsite. Also the density of CNT's is very

low, hence small weight percentage will represent considerable volume fraction of the composite.
CNT's with 0.32 wt % of the composite enhanced the interlaminar strength of the composite, but it didn't contribute to the energy absorption capacity. While 0.82 wt % of CNT's slightly improved the impact resistance of the Kevlar composite beside the improvement in the interlaminar strength.

Silicon Carbide particles (15 μm) added to the matrix of Kevlar/ Vinylester composites in low percentage (0.82 wt %) enhanced the bonding between fiber and matrix phases, hence the interlaminar strength of the composite. But it had no effect on the composite energy absorption capacity.
Silicon Carbide particles (15 μm) added to the matrix of Kevlar/ Vinylester composites in high percentage (4.15 wt %) enhanced the composite energy absorption capacity (one third of the composite were fractured only), and against other types of additives the enhancement in energy resistance wasn't on the expense of the delamination resistance, so that no delamination noticed.

The Nanoclay addition to the Vinylester resulted a considerable change in the stiffness of the nanoclay reinforced samples, the best percentage was the 2 % of NC, it was able to increase the modulus of elasticity by 10 %. The 4.3 % of NC were able to increase the stiffness of the NC/ Vinylester composite by 7.5 %. It has been found that the stiffness don't increase with the increase in the Nanoclay weight percentage, the flexure modulus of elasticity of the samples reinforced with 7 % almost had the same flexure modulus of the control samples. And the nanoclay if added in percentage more than 7 wt % will play negative role on the stiffness of the composites.

The Micro Hardness Tests were performed for the different Nanoclay/ Vinylester composites showed enormous changes in the hardness of the nanoclay reinforced samples at certain percentages, the 2 % of NC was the best percentage and it increased the hardness of the vinylester by 265 %. The 4.3 % of NC were able to increase the hardness of the NC/ Vinylester composite by 6.4 %. It was found that the hardness don't increase with the increase in the Nanoclay weight percentage, the hardness of the Nanoclay/Vinylester composites reduced when the nanoclay percentage increase to high weight percentage, for example; 7 % of nanoclay decrease the hardness by 6.5 %. The hardness of the nanoclay/vinylester nanocomposites with 9.4 % of nano clay was reduced by 33 %.

The nanohardness response of the different nanoclay percents was similar to the microhardness results, the 2 % of nanoclay was the best percent to enhance the composite hardness.

The nano indentation results showed higher elastic modulus than three point bending results, this was due to the different in local and bulk properties, the nano particles expected to affect polymer chain mobility and kinetics in their near vinicity.

The results from three point bending test, micro hardness test and nano indentation test are consistent, both showed that 2 wt % of nanoclay will give the stiffest and hard composite, this is logical because the hardness usually related to the strength of the material.

The enhancement in mechanical properties of the nanoclay composites didn't accompany considerable changes in the thermal properties. The Decomposition temperature of pure vinylester was increased by the addition of the nanoclay. The vinylester nanocomposites experienced direct decomposition without melting. The glass transition temperature of the vinylester/Nanoclay composite didn't affect by the nanoclay percentage, the results show small variation in the glass transition temperature for all composites.

Chapter 6

RECOMMENDATIONS

CHAPTER 6

RECOMMENDATIONS

It has been shown that the implementation of different filler materials on the matrix of a structural composite element is an effective method for improving the absorption of the impact energy of a projectile traveling at a low-speeds. In order to further substantiate this conclusion, the following recommendations are given.

- In this study, uniform additive distribution was attempted manual stirring. However, because of the small sizes of the different fillers and in some cases high volume fraction of fillers, it was difficult to get a uniform distribution of the additives. It would be beneficial to explore other mixing methods and configurations that enhance particles distribution. One type of approach would be to use mechanical mixer.

- Further tests considering more than one additive in the same composite maybe give optimum properties in term of impact resistance and interlamiar shear strength.

- Another area of study that merits further investigation is the effect of different sizes of the different additives. It is expected that improvements in energy absorption would be obtained by using a smaller particles size with the same weight percentage. Nano aluminum oxide and nano silicon carbide may be used as reinforcement to increase the matrix strength and the fiber/matrix bond.

- In this study, it has been observed that the carbon nanotubes addition in low percentages didn't affect the Kevlar composite impact resistance. However, this observation still needs to be proven by increase in the CNT's percentage or alignment of the carbon nanotubes to the direction of impact.

- Development to the drop weight apparatus used will armed our results with more parameters, electrical motor to left the weight, load cell to record the load during impact, data acquisition system to capture strain with time. This will help to plot the dynamic response of each composite under impact.

- High speed camera will add a lot to any future similar research, it will help comparing the finite element results with the experimental results.

- Studying the effect of carbon nanotubes, Aluminum oxide and silicon carbide on vinylester will contribute to this research; this will enable us to predict the best mixing ratio, and will tell us more about the fiber/matrix/filler interaction.

- Compression after impact test (CAI) may used to predict the residual compressive strength of a composite after low velocity impact damage. This will allow us to measure the composite damage tolerance. CAI testing is focused on characterizing the effect of impact damage by determining the reduction of compressive strength due to foreign object impacts on a composite structure.

- Unit cell finite element model to simulate the additives interaction inside the matrix will be helpful, then the response will be taken to simulate macro scale results depending on the representative volume element results.

- Composites most of the times don't give high consistency in results, to overcome this problem more and more samples need to be fabricated. This will cost money and will consume a lot of time.

- Helmets, goggles, and heavy-duty gloves are recommended when operating the drop weight tests.

- Finally, it would be interesting to test the same composites under ballistic (high speed) impact, the modes of failure and energy absorption expected to be different from those for low speed impact.

- CT Scan nondestructive test technique will give more clear and detailed photos than the X-ray technique, the use of CT scan will add to any future related research.

REFERENCES

1. W.D. Callister, "Materials Science and Engineering: An Introduction", New York, Wiley, 2007.
2. S.R. Reid and G. Zhou, "Impact behavior of fiber-reinforced composite materials and structures", Florida, CRC Press LLC, 2000.
3. R.J. Schwinghamer, "Shield Design for Protection against Hypervelocity Particles", NASA Tech Briefs, pp. 76-77, 1993.
4. Waters W and Scott B. "High velocity penetration of a Kevlar reinforced laminate". 22nd International SAMPE Technical Conference, Covina, California, p. 1078–1091, November, 1990.
5. Joseph H. Koo, "Polymer Nanocomposites Processing, Characterization, and Applications",USA, McGraw-Hill, 2006.
6. P.M. Ajayan, L.S. Schadler, P.V. Braun,"Nanocomposite Science and Technology", WILEY-VCH Verlag GmbH Co. KGaA, Weinheim, Germany, 2003.
7. K. Henkhaus and G. Ramirez, "Overview of Research on Composite Material Impact Behavior", 16th Engineering Mechanics Conference, University of Washington , Seattle, 2003.
8. Jeremy Gustin, Aaran Joneson, Mohammad Mahinfalah and James Stone "Low velocity impact of combination Kevlar/carbon fiber sandwich composites", Composite Structures ,pp. 396–406, 2005.
9. Zhu, W. Goldsmith and Dharan, "Penetration of laminated Kevlar by projectiles", International Journal of Solids and Structures, pp.399–420, 1992.
10. T. He, H.M. Wen, Y. Qin, "Finite element analysis to predict penetration and perforation of thick FRP laminates struck by projectiles", International Journal of Impact Engineering, pp.27–36, 2008.
11. H.E. Johnson , L.A. Louca , S. Mouring , A.S. Fallah "Modeling impact damage in marine composite panels", International Journal of Impact Engineering, volume 36, pp. 25–39, 2009.
12. D. Elder, R. Thomson, Minh Nguyen and Murray Scott "Review of delamination predictive methods for low speed impact of composite laminates", Composite Structures, pp. 677–683, 2004.
13. M. Hebert, C.E. Rousseau and A. Shukla "Shock loading and drop weight impact response of glass reinforced polymer composites". Composite Structures, pp. 199–208, 2008.
14. E. Sevkat, B. Liaw , F. Delale and B.B. Raju, "Drop-weight impact of plain-woven hybrid glass–graphite/toughened epoxy composites", Composites: Part A , pp.1090–1110, 2009.

15. E. Sevcat, B.M. Liaw, F. Delale "Experimental and Numerical Studies of S2-Glass Fiber/Toughened Epoxy Composite Beams Subject to Drop-Weight or Ballistic Impact" ASME International Mechanical Engineering Congress and Exposition IMECE2007, Seattle, Washington, USA, November 2007.
16. X. Xu, M.M. Thwe C. Shearwood and K. Liao, "Mechanical properties and interfacial characteristics of carbon-nanotube-reinforced epoxy thin films", Applied Physics Letters, Volume 81, pp. 2833-2835, 2002.
17. D. E. Resasco, W. E. Alvarez, F. Pompeo, L. Balzano, J. E. Herrera, B. Kitiyanan, and A. Borgna, "SWNT-Filled Thermoplastic and Elastomeric Composites Prepared by Miniemulsion Polymerization", Journal of Nanoparticle Research, Volume 4, pp.131-161, 2002.
18. B.C. Kim, S.W. Park and D.G. Lee, "Fracture toughness of the nano-particle reinforced epoxy composite", Journal of Composite Structures, pp. 69-77, 2008.
19. R. XU, V. BHAMIDIPATI, W.H. ZHONG, JIANG LI and C.M. LUKEHART, "Mechanical Property Characterization of a Polymeric Nanocomposite Reinforced by Graphitic Nanofibers with Reactive Linkers", Journal of Composite Materials, Vol. 38, 2004.
20. P. K. Jain, Y. R. Mahajan, G. Sundararajan, A. V. Okotrub, N. F. Yudanov and A. I. Romanenko, "Development of Carbon Nanotubes and Polymer Composites Therefrom", Carbon Science, Vol. 3, pp. 142-145, September 2002.
21. Mandar Kulkarni, David Carnahan, Kapil Kulkarni, Dong Qian, Jandro L. Abot "Elastic Response of a Carbon Nanotube Fiber Reinforced Polymeric Composite: A Numerical and Experimental Study", Composites: Part B, August 2009.
22. M. Pramanik, S. K. Srivastava, B. K. Samantaray and A. K. Bhowmick "EVA/Clay Nanocomposite by Solution Blending: Effect of Aluminosilicate Layers on Mechanical and Thermal Properties", Macromolecular Research, Volume 11, pp. 260-266, 2003.
23. S.T. Knauert,J. F. Douglas, Francis W. Starr "The Effect of Nanoparticle Shape on Polymer-Nanocomposite Rheology and Tensile Strength", Journal of Polymer Science: Part B: Polymer Physics, Volume 45, pp. 1882–1897,2007.
24. Yaohui Wang, Xu Zhang , Xianying Wu, Huixing Zhang, Xiaoji Zhang "Compositional, structural and mechanical characteristics of nc TiC/a-C:H nanocomposite films", Applied Surface Science, pp. 1801–1805, 2008.
25. K. Hbaieb, Q.X. Wang, Y.H.J. Chia, B. Cotterell "Modelling stiffness of polymer/clay nanocomposites", Polymer, Volume 48, pp. 901-909, 2007.
26. Q.H. Zeng, A.B. Yu, G.Q. Lu "Multiscale modeling and simulation of polymer nanocomposites", Progress in Polymer Science, Volume 33, pp. 191–269, 2008.
27. B.J.Ash, A.Eitan, L.S. Schadler, "Polymer Nanocomposites with Particle and Carbon Nanotube Fillers", Dekker Encyclopedia of Nanoscience and Nanotechnology, 2004.

28. Timmerman JF, Hayes B, Seferis JC. Nanoclay reinforcement effects on the cryogenic micro cracking of carbon fiber/epoxy composites. Compos Sci Technol 2002;62:1249–58.
29. Siddiqui NA, Woo RSC, Kim JK, Leung CCK, Munir A. Mode I interlamina fracture behavior and mechanical properties of CFRPs with nanoclay-filled epoxy matrix. Composites: Part A 2007;38:449–60.
30. Fukushima Y and Inagaki S, "Synthesis of an intercalated compound of montmorillonite and 6-polyamide", Journal of Inclusion Phenomena and Macrocyclic Chemistry,Volume 5. pp. 473, 1987.
31. Usuki A, Kojima Y, Kawasumi M, Okada A, Fukushima Y, Kurauchi T, et al. "Synthesis of nylon 6-clay hybrid", Journal of Material Research, Volume 8, pp.1179, 1993.
32. J.S. Shelley, PTM, and K.L. Devries, "Reinforcement and Environmental Degradation of Nylon-6/Clay Nanocomposites," *Polymer*, Volume 42, pp. 5849-5858, 2001.
33. A. Okada, T. Usuki, O. Kurauchi, Kamigaito, in: J.E. Mark, C.Y.-C. Lee, P.A. Branconi (Eds.), "Hybrid Organic-Inorganic Composites", ACS Symposium, pp. 55–65, 1995.
34. J. J. Luo, I. M. Daniel, "Characterization and Modeling of Mechanical Behavior of Polymer/Clay Nanocomposites," Composites Science and Technology, Vol. 63, pp. 1607-1616, 2003.
35. Y.T. Vu, J.E. Mark, L.H. Pham, M. Engelhardt, "Clay nanolayer reinforcement of cis-1,4-polyisoprene and epoxidized natural rubber", Journal of applied polymer science , Volume 82, pp. 1392–1403, 2001.
36. Y.-Q. Zhang, L.-H. Lee, H.-J. Jang, C.-W. Nah, "Preparing PP/clay nanocomposites using a swelling agent", Composite. Part B, Volume 35, pp. 133–138, 2004.
37. C.-R. Tseng, J.-Y. Wu, H.-Y. Lee, F.-C. Chang, "Preparation and Characterization of Polystyrene/Clay Nanocomposites by Free-Radical Polymerization", Journal of Applied Polymer Science, Volume 85, pp. 1370–1377, 2002.
38. M. Tortora, G. Gorrasi, V. Vittoria, G. Galli, S. Ritrovati, E. Chiellini, "Structural characterization and transport properties of organically modified montmorillonite/polyurethane nanocomposites", Polymer, Volume 43, pp.6147–6157, 2002.
39. K. Masenelli-Varlot, E. Reynaud, G. Vigier, J. Varlet, « Mechanical properties of clay-reinforced polyamide", Journal of Polymer Science, part B: Polym. Phys, Volume 40, pp. 272–283, 2002.

40. P. Uribe-Arocha, C. Mehler, J.E. Puskas, V. Altstat, "Effect of sample thickness on the mechanical properties of injection-molded polyamide-6 and polyamide-6 clay", Polymer, Volume 44, pp. 2441–2446, 2003.
41. T. Tzianetopoulou, M.C. Boyce. "Micromechanics of PS/PB/PS Triblock-Copolymer Films with Lamellar Morphology", Materials Research Society, Volume 788, pp. 601–607, 2003.
42. I. M. Daniel, H. Miyagawa, E. E. Gdoutos, and J. J. Luo, "Processing and Characterization of Epoxy/Clay Nanocomposites," Experimental Mechanics, Volume 43, No. 3, pp. 348-354, 2003.
43. Sheng, N., Boyce, M.C., Parks, D.M., Rutledge, G.C., Abes, J.J., Cohen, R.E., "Multiscale Micromechanical Modeling of Polymer/Clay Nanocomposites and the Effective Clay Particle", *Polymer*, Volume 45, pp. 487-506, 2004.
44. C. Aymonier, D. Bortzmeyer, R. Thomann, R. Mulhaupt, "Poly (Methylmethacrylate)/Palladium Nanocomposites: Synthesis and Characterization of the Morphological, Thermomechanical, and Thermal Properties" Chemistry of Materials, Volume 15, pp. 4874–4878, 2003.
45. Tseng, C. R. , Wu, J .-Y. , Lee, H. Y. Chang, F. C., "Preparation and Characterization of Polystyrene/clay Nanocomposites by Free Radical Polymerization," Journal of Applied Polymer Science , Volume 85, pp.1370-1377, 2002.
46. T.D. Fornes, P.J. Yoon, D.R. Paul, "Polymer matrix degradation and color formation in melt processed nylon 6/clay nanocomposites", Polymer, Volume 44, pp. 7545–7556, 2003.
47. Weiping L, Suong VH, Martin P. "Fracture toughness and water uptake of highperformance epoxy/nanoclay nanocomposites", Composite Science Technology, Volume 65, pp.2364–73, 2005.
48. Lei W, Ke W, Ling C, Yongwei Z, Chaobin H. "Preparation, morphology and thermal/mechanical properties of epoxy/nanoclay composite". Journal of Composite Part A, Volume 37,pp.1890–6, 2006.
49. Qi B, Zhang QX, Bannister M, Mai YW, "Investigation of the mechanical properties of DGEBA-based epoxy resin with nanoclay additives" Journal of Composite Structure, Volume 75, pp. 514–9, 2006.
50. Ho MW, Lam CK, Lau KT, Dickon HL, David H. "Mechanical properties of epoxy based composites using nanoclays". Journal of Composite Structures, Volume 75, pp.415–21, 2006.
51. Subramaniyan AK, Sun CT. "Toughening polymeric composites using nanoclay: crack tip scale effects on fracture toughness", Composite Part A, Volume 38, pp. 34–43, 2007.

52. Lingyu Sun, Ronald F. Gibson, Faramarz Gordaninejad, Jonghwan Suhr, "Energy absorption capability of nanocomposites: A review", Composites Science and Technology, Volume 69, pp. 2392–2409, 2009.
53. Editorial "Blast/impact on engineered (nano) composite materials", Composites: Part B, Volume40, pp. 413–415, 2009.
54. Babur Deliktas, George Z. Voyiadjis and Anthony N. Palazotto " Simulation of perforation and penetration in metal matrix composite materials using coupled viscoplastic damage model", Composites Part B: Volume 40, pp. 434-442, 2009.
55. A.M. Dongare, L.V. Zhigilei, A.M. Rajendran, B. LaMattina, "Interatomic potentials for atomic scale modeling of metal–matrix ceramic particle reinforced nanocomposites", Composites Part B, Volume 40, pp. 461-467 2009.
56. Rashid K. Abu Al-Rub, Sun-Myung Kim, "Predicting mesh-independent ballistic limits for heterogeneous targets by a nonlocal damage computational framework", Composites Part B, Volume 40, pp. 495-510, 2009.
57. Mahmoud M. Reda Taha, Arife B. Colak-Altunc, Marwan Al-Haik, "A multi-objective optimization approach for design of blast-resistant composite laminates using carbon nanotubes",Composites Part B, Volume 40, pp. 522-529,2009.
58. B. Sun, Y. Liu, B. Gu "A unit cell approach of finite element calculation of ballistic impact damage of 3-D orthogonal woven composite", Composites Part B, Volume 40, pp.552-560, 2009.
59. Md.A. Bhuiyan, M.V. Hosur, S. Jeelani, "Low-velocity impact response of sandwich composites with nanophased foam core and biaxial (±45°) braided face sheets" Composites Part B, Volume 40, pp. 561-571, 2009.
60. Al-Ostaz A., Pal G., Mantena P.R. and Cheng A.H-D "Molecular Dynamics Simulation of SWCNT Polymer Nanocomposite and its Constituents" Journal of Materials Science, Volume 43, pp.164-173, 2008.
61. Paul Akangah, Shivalingappa Lingaiah, Kunigal Shivakumar, "Effect of Nylon-66 nano-fiber interleaving on impact damage resistance of epoxy/carbon fiber composite laminates", Composite Structures, Volume 92, pp. 1432–1439, 2010.
62. Ahmad Almagableh, Swasti Gupta, P. Raju Mantena and Ahmed Al-Ostaz "Dynamic Mechanical Analysis of Graphite Platelets and Nanoclay Reinforced Vinylester, and MWCNT Reinforced Nylon 6,6 Nanocomposites" Proceedings of the 2008 SAMPE Fall Technical Conference, Memphis, TN, 2008.
63. Raju Mantena, Alexander H.D. Cheng and Ahmed Al-Ostaz, "Blast and Impact Resistant Composite Structures for Navy Ships," The2008 ONR Solid Mechanics Review at University of Maryland, Adelphi, MD, 2008.
64. Swasti Gupta, P. Raju Mantena and Ahmed Al-Ostaz "Effect of Strain Rates on Energy Absorption of Exfoliated Graphite Platelet and Cloisite Nanoclay Reinforced Vinylester Nanocomposites" Proceedings of the American Society for Composites 23rd Technical Conference, Memphis, TN, 2008.

65. J. W. SONG AND A. J. HSIEH, "Ballistic Impact Resistance of Monolithic, Hybrid and Nano Composites of PC and PMMA", Proceedings of the American Society for Composites 17th Technical Conference, Lafayette, IN, October, 2002.
66. Kosar Iqbal, Shafi-Ullah Khan, Arshad Munir, Jang-Kyo Kim, "Impact damage resistance of CFRP with nanoclay-filled epoxy matrix", Composites Science and Technology, Volume 69, pp. 1949–1957, 2009.
67. A.F. Avila, M.G.R. Carvalho, E.C. Dias, D.T.L. Cruz "Nano-structured sandwich composites response to low-velocity impact", Composite Structures, Volume 92, pp. 745–751, 2010.
68. Byung Chul Kim and Seong Jae Lee, "Silicate dispersion and rheological properties of high impact polystyrene/organoclay nanocomposites via in situ polymerization", Korea-Australia Rheology Journal, Vol. 20, No. 4, pp. 227-233, December 2008.
69. DuPont Company, "Technical Guide, Kevlar Aramid Fiber", Richmond,USA, 2010.
70. Martin Hollmann' "Composite Aircraft Design", Published by Martin Hollmann, California, USA, 1983.
71. Sanjay K. Mazumdar, "Composite Manufacturin, Materials, Product, and Process Engineering", CRC Press LLC, Florida, USA, 2002.
72. Cantwell W J, Curtis P T and Morton J, "Post impact fatigue performance of carbon fiber laminates with non woven and mixed woven layers", Composites, Volume 14, pp. 301–305, 1983.
73. Vedula M and Koczak M J., "Impact resistance of cross-plied polyphenylene sulfide composites", Journal of Thermoplastic Composite Materials, Volume 2, pp. 154–163, 1989.
74. ABAQUS, ABAQUS Manual Set, 2007, Simulia Inc., Providence, RI 02909-2499, USA.
75. P. J. F. Harris, Carbon Nanotubes and Related Structures, New Materials for the Twenty-First Century, Cambridge University Press, Cambridge, 1999.
76. K. Tanaka, T. Yamabe, and K. Fukui, "The Science and Technology of Carbon Nanotubes", Elsevier, Amsterdam, 1999.
77. R. Saito, G. Dresselhaus, and M. S. Dresselhaus, Physical Properties of Carbon Nanotubes, Imperial College Press, London, 1998.
78. M. S. Dresselhaus, G. Dresselhaus, and P. C. Eklund, "Science of Fullerenes and Carbon Nanotubes", Academic Press, San Diego, CA, 1996.
79. T. J. Pinnavaia and G. W. Beall, "Polymer-Clay Nanocomposites", John Wiley & Sons, New York,USA, 2000.
80. Gutowski, T.G., "A resin flow/fiber deformation model for composites", SAMPE Quarterly, 1985.

81. Springer, G.S., "Resin flow during the cure of fiber reinforced composites", Journal of Composite Materials, 16, September 1982.
82. Loos, A.C. and Springer, G.S., "Curing of epoxy matrix composites", Journal of Composite Materials, March 1983.
83. Gutowski, T.G., Morigaki, T., and Cai, Z., "The consolidation of laminate composites", Journal of Composite Materials, 21, 172, 1987.
84. HASMUKH A PATEL, RAJESH S SOMANI, HARI C BAJAJ* and RAKSH V JASRA, "Nanoclays for polymer nanocomposites, paints, inks, greases and cosmetics formulations, drug delivery vehicle and waste water treatment", Bulletin of Materials Science, Volume 29,, pp. 133–145, April 2006.
85. Park, C., Ounaies, Z., Watson, K.A., Crooks, R.E., Smith, J., Lowther, S.E.,Connell, J.W., Siochi, E.J., Harrison, J.S., Clair, T.L.S., "Dispersion of single wall carbon nanotubes by in situ polymerization under sonication", Chemical Physics Letters, pp. 303–308, 2002.
86. Michael J. O'Connell, "Carbon Nanotubes Properties and Applications", Taylor & Francis Group LLC, Florida, USA,2006.
87. Konig, W., Grass, P., Heintze, A., Okcu, F., and Schmitz-Juster, Cl.,"New developments in drilling and contouring composites containing Kevlar aramid fiber", Technical Symposium V, Design and Use of Kevlar Aramid fiber in Composite Structures, pp.95–103, 1984.
88. Abrate, S. and Walton, D.A., "Machining of composite materials I. Traditional methods", Composites Manufacturing, pp. 75, 1992.
89. ASTM international, "Flexural Properties of Unreinforced and Reinforced Plastics and Electrical Insulating Materials", American Society for Testing and Materials D 790, West Conshohocken, PA, 2000.
90. ASM international, ASM Handbook, "Mechanical Testing and Evaluation", Macro indentation Hardness Testing, Volume 8, American Society of Metals, 2000.
91. Surface Engineering Forum. (2010, Apr 29). Micro Hardness Test. Retrieved from Gordon England, website: http://www.gordonengland.co.uk/hardness/microhardness.htm.
92. ASTM international, "Standard Test Method for Micro indentation Hardness of Materials", American Society for Testing and Materials E 384, West Conshohocken, PA, 2000.
93. Oliver. W.C.; Pharr, G.M. "A new improved technique for determining hardness and elastic modulus using load and sensing indentation experiments", Journal of Materials Research, Volume 7, p.p. 1564-1582, 1992.
94. Shuman, D.J.; Costa, A.L.M., Andrade, "Calculating the elastic modulus from nanoindentation and microindentation reload curves", Materials Characterization, Volume 58, p.p 380-389, 2007.

95. W C Oliver, G M Pharr, "Measurement of hardness and elastic modulus by instrumented indentation: Advances in understanding and refinements to methodology",Journal of Materials Research, Volume: 19, p.p 3-20, 2004.
96. Q Series Manual, "TGA Thermogravimetric Analyzer", TA Instruments, Waters LLC, 2006.
97. Q Series Manual, "DSC Differential Scanning Calorimeter", TA Instruments, Waters LLC, 2007.
98. ASTM international, "Test Method for Measuring the Damage Resistance of a Fiber-Reinforced Polymer Matrix Composite to a Drop-Weight Impact Event", American Society for Testing and Materials D 7136, West Conshohocken, PA, 2000.
99. Hallett S R and Ruiz C, "Fracture of composite beams under impact", Proceeding 11th International Conference of Experimental Mechanics, Oxford, 1998.
100. Aravind Dasari, Zhong-Zhen Yu and Yiu-Wing Mai, "Fundamental aspects and recent progress on wear/scratch damage in polymer nanocomposites" Materials Science and Engineering, Volume 63, P.P 31-80 2009.
101. The Internet Journal of Dental Science. (2010, Apr 14). Finite element analysis, A Boon to Dental Research. Retrieved from ISPUB.com, website: http://www.ispub.com/journal/the_internet_journal_of_dental_science/volume_6_number_2_25/article/finite_element_analysis_a_boon_to_dental_research.html.
102. R. Liu, S. S. Quek, "The Finite Element Method: A Practical Course", Oxford, Elsevier Science Ltd., 2003.
103. Daniel Gay, Soung Hoa and Stephen Tsai, "Composite Materials, Design and Applications", France, Paris, CRC Press, 2003.
104. Schwartz, "Composite Materials Handbook", USA, New York, McGraw-Hill, 1984.
105. Hashin, Z., and A. Rotem, "A Fatigue Criterion for Fiber-Reinforced Materials," Journal of Composite Materials, vol. 7, pp. 448--464, 1973.
106. Hashin, Z., "Failure Criteria for Unidirectional Fiber Composites," Journal of Applied Mechanics, vol. 47, pp. 329–334, 1980.

جامعة الإمارات العربية المتحدة
UNITED ARAB EMIRATES UNIVERSITY

جامعة الامارات العربية المتحدة
عمادة الدراسات العليا

خصائص التصادم للمواد المركبة البوليمريه المعززة بمواد متناهية الدقة

رسالة مقدمة من

عمار محمد العمري

اشراف:

أ.د. يوسف الحايك
قسم الهندسة الميكانيكية
جامعة الامارات العربية المتحدة

د. سعود الدعجة
قسم الهندسة الميكانيكية
جامعة الامارات العربية المتحدة

رسالة مقدمة الى عمادة الدراسات العليا في جامعة الإمارات العربية المتحدة لاستكمال متطلبات الحصول على درجة الماجستير في الهندسة الميكانيكية

يونيو 2010 م

جامعة الإمارات العربية المتحدة
UNITED ARAB EMIRATES UNIVERSITY

جامعة الامارات العربية المتحدة
عمادة الدراسات العليا

خصائص التصادم للمواد المركبة البوليمريه المعززة بمواد متناهية الدقة

رسالة مقدمة من

عمار محمد العمري

اشراف:

أ.د. يوسف الحايك
قسم الهندسة الميكانيكية
جامعة الامارات العربية المتحدة

د. سعود الدعجة
قسم الهندسة الميكانيكية
جامعة الامارات العربية المتحدة

رسالة مقدمة الى عمادة الدراسات العليا في جامعة الإمارات العربية المتحدة لاستكمال متطلبات الحصول على درجة الماجستير في الهندسة الميكانيكية

يونيو 2010 م